NANYANG
TECHNOLOGICAL
UNIVERSITY
SINGAPORE

MULTI-SENSORS FOR REALIZATION OF HOME TELE-REHABILITATION

YEAN SEANGLIDET

SCHOOL OF COMPUTER SCIENCE AND ENGINEERING

2019

MULTI-SENSORS FOR REALIZATION OF HOME TELE-REHABILITATION

YEAN SEANGLIDET

SCHOOL OF COMPUTER SCIENCE AND ENGINEERING

A thesis submitted to Nanyang Technological University
in partial fulfillment of the requirement for the degree of
Doctor of Philosophy

2019

Statement of Originality

I hereby certify that the work embodied in this thesis is the result of original research, is free of plagiarised materials, and has not been submitted for a higher degree to any other University or Institution.

02-Feb-2020

.....

Date

.....

YEAN SEANGLIDET

Supervisor Declaration Statement

I have reviewed the content and presentation style of this thesis and declare it is free of plagiarism and of sufficient grammatical clarity to be examined. To the best of my knowledge, the research and writing are those of the candidate except as nowledged in the Author Attribution Statement. I confirm that the investigations were conducted in accord with the ethics policies and integrity standards of Nanyang Technological University and that the research data are presented honestly and without prejudice.

02-Feb-2020

.....

Date

.....

Assoc Prof Lee Bu Sung

Authorship Attribution Statement

This thesis contains material from 5 papers published in the following peer-reviewed journals and from papers accepted at conferences in which the candidate is listed as an author.

Chapter 3 is published as S. Yean, B.S. Lee, C.K Yeo, C.H. Vun, and H. L. Oh. Smartphone Orientation Estimation Algorithm Combining Kalman Filter with Gradient Descent. IEEE Journal of Biomedical and Health Informatics, 1421-1433 (2019), DOI:10.1109/JBHI.2017.2780879.

The contributions of the co-authors are as follows:

- Prof Lee and Prof Yeo provide the idea with guidance regarding the porject direction and edited the manuscript
- The candidate prepared the manuscript draft and analysed all of the plotted data.
- The candidate conducted all the experiments with volunteered participants.
- Prof Vun and Mr. Oh help me in discussion of the sensor characterics and synchronisation.

Chapter 4 is published as S. Yean, B.S. Lee, C.K. Yeo, and Z. Chen. Automatic Oscillation Detection and Correction of Fused Wearable Sensor Signals Using Machine Learning. 16th IEEE Wireless Telecommunication Symposium (WTS), 1-6 (2018), DOI:10.1109/WTS.2018.8363935.

The contributions of the co-authors are as follows:

- The candidate initiated the pilot study of oscillationd detection upon observing the post-fusion behavior.
- Prof Lee and Prof provide guidance for the project direction and editted the manuscript draft.
- the candidate prepared the manucript draft and concluded the anlaysis.
- Dr. Chen assisted in discussion of feature engineering of sensor signal.

Chapter 5 is published as S.L. Lim, S. Yean, B.S. Lee, and C.K. Yeo. Rehab-Partner: Motion Tracking Assistant Using a Novel Complementary Feedback Filter. IEEE Consumer Communications and Networking Conference (CCNC), 1-6 (2018), DOI:10.1109/CCNC.2018.8319277 as well as S. Yean, B.S.Lee, and C.K. Yeo. Lowerlimb-Rehabilitation at Home: A Survey on Exercise Assessment and Initial Study on Exercise State Identification toward Biofeedback. International Journal of Interdiscliplinary Telecommunications and Networking (IJITN), accepted (2019).

The contributions of the co-authors are as follows:

- Prof Lee and Prof Yeo provided guidance of the project direction and materials as well as edited the manuscript drafts.

- The candidate drafted the manuscripts and conducted experiments for exercise segmentation experiment.

- Mr. Lim implemented the RehabPartner application while the candidate contributedin the orientation estimate algorithm for the application. Both Mr. Lim and the candidate discussed on the features of RehabPartner feedback mechanism.

02-Feb-2020

Date

YEAN SEANGLIDET

I would like to dedicate this thesis to my mom and dad. I would not be where I am today without their investment in my education and trust in me.
To papa, who enthusiastically listens to my research progress everyday and constantly reminds me to write this thesis, this is for you.
To my husband, thank you for your support and unwavering confidence in me regardless of my best and worst days.

Acknowledgements

I would like to take this opportunity to acknowledge the people who have made my Ph.D. study at Nanyang Technological University (NTU) enriching and impactful to my future endeavour. My gratitude transcends these modest acknowledgements as without them, this thesis would not have been possible.

Firstly, I would like to express my utmost gratitude to my supervisors, Associate Professors Lee Bu Sung and Yeo Chai Kiat, for their guidance, knowledge of expertise, encouragement and research freedom to carry out the research in the area I am passionate about. Under their supervision, I have learnt to use my curiosity to ask the right questions in scientific research and have acquired the critical thinking necessary in conducting the research. Their feedbacks have always enabled me to look at the problem in different perspectives. Their comments and encouragement taught me be persistent, independent and organised, especially in time management. These experience are priceless for my future career and life.

Secondly, I would like to extend my gratitude to the Thesis Advisory Committee, Associate Professor Vun Nicholas and Associate Professor Chan Syin, who have given me many useful inputs as well as recommendations to extend my understanding with regards to Internet-Of-Things, embedded systems and motion tracking systems. I would like to thank Mr. Oh Hong Lye for his inputs on motion sensors, especially providing the TI SensorTag for my research. I would like to thank Associate Professor Zheng Jianmin who takes time from his busy schedule to advise me on the transformation of motion data to the visualization of 3D stick figure.

Moreover, I would like to thank Mr. Toh Leong Teck and Ms. Irene Goh, staff of Computer Networks and Communications Lab (CNCL) in the School of Computer

Science and Engineering (SCSE) at NTU, for their technical support. I would like to thank my seniors, Liu Yi, Pham Thi Ngoc Diep, Chen Zhaomin, Chen Weiling, Liu Jigang and Ahmed Amir; the FYP and URECA students, Lim Shao Loong, Chen Jin Ling, Hu Qingyao, Fan Ran and Wong En Teng. They have not only provided me with their valuable discussion for my studies and research, but also enriched my life at NTU.

Finally, I would like to express my gratitude to my mom, dad and husband for their unconditional love and support. To my late father, Yean Seang, my Ph.D. journey would not be so enjoyable without you who has always been interested in my findings. To my mom, Lam Mouly, who inspires me to choose the most adventurous path. To my husband, Taing Meng, who has been the shoulder to cry on and the strong support throughout my Ph.D. and thesis writing journey. I am grateful to makmings (aunts), uncles and cousin Narith for their care and who have always supported me. My gratitude also extends to my friends, Vichet Pisey, Nguon Phoungtepsonich, SreyLeap Hout, Ponnaka Phan, Sithsakal Oum, Foo Chery, Loh Alice, Ho Victor and Yang Junjie, for always encouraging me and bringing joy into my life. I hope to share my joy of completion with them.

Contents

List of Figures

List of Tables

List of Abbreviations

ABBREVIATIONS	FULL EXPRESSIONS
IMU	Inertial Measurement Unit
MEMS	Micro-Electro-Mechanical Systems
CFF	Complementary Feedback Filter
KFGD	Kalman Filter with Gradient Descent Method
MW	Madgwick's Algorithm
SVM	Support Vector Machines
LR	Logistic Regression
MLP	Multi-layer Perceptron
HMM	Hidden Markov Model
NN	Neural Network
KNN	K-Nearest-Neighbor
RF	Random Forest
NB	Naive Bayes
AF	Angle Frame or Angular Displacement
SF	Signal Frame or Wearable sensors' data

Abstract

Research in assistive healthcare, in particular home rehabilitation, has spawn huge potential owing to the recent advancement of internet-of-things technology and the wearable hardware, Inertial Measurement Unit (IMU) in wearable sensors and smartphones become affordable for community usage. However, using low cost IMU sensors or smartphones face certain challenges, such as accurate orientation estimation for lower-limb motion tracking, which is usually less of a problem in specialized motion tracking sensor devices. To address these issues, the candidate has made three main contributions: a new and better orientation estimation algorithm which combines quaternion-based Kalman filter with corrector estimates using gradient descent (KFGD), an auto-detector of post-filtered lower-limb orientation signal oscillation and the machine-learning based state identification of rehabilitation exercise.

Firstly, obtaining accurate orientation readings with noise-prone IMU and post-processing drift is a key challenge in motion tracking research. It is the result of accumulated errors over the integration of the gyroscope signal to calculate the angular displacement, in other words, the orientation of the limb, in the motion tracking application. Thus, the candidate proposes two sensor fusion algorithms: the complementary filter feedback (CFF) and the quaternion-based Kalman filter with corrector estimates using gradient descent (KFGD). The complementary filter feedback (CFF) focuses on the components' performance of high-pass filter (from angular velocity) and low-pass filter (from fusion of gravity and earth magnetic field). These components contribute to the estimated orientation while the proposed feedback loop can correct the drift. KFGD is later introduced to further improve the limitation of the low-pass filter and the fixed fusion threshold of the CFF. Gradient descent method and quaternion-based

Kalman Filter are chosen for their progressive features. The performance was evaluated on the case study of early stage rehabilitation exercises, namely, leg extension and sit-to-stand. The result shows that CFF is capable of fast motion tracking and confirms that the feedback loop is capable of correcting errors caused by integration of gyroscope data. KFGD outperforms the state-of-the-art Madgwick algorithm and is recommended for obtaining accurate orientation readings using motion sensors.

Secondly, upon observing the characteristics of the post-filtered orientation signals of the lower-limb, a noticeable artifact in the output signal that it would oscillate from positive to negative and vice versa. To address the oscillations in the signals of both motion capture and inertial measurement sensors, the candidate applied machine learning algorithms and compared them with the rule-based approach. Machine learning methods, such as Logistic Regression, Support Vector Machine and Multilayer perceptron, were adopted in order to automatically detect the oscillation. The results showed that machine learning methods are able to learn the oscillation patterns in wearable sensor data and identify the tendency of fluctuation thereby allowing the errors to be filtered out more efficiently than rule-based method.

Lastly, in order to realize meaningful home rehabilitation, there is a need for informative feedback or intervention in parallel with the exercise monitoring. The study aims to use the collected data and the understanding of wearable signal to simulate the high-level observations by the physiotherapist towards the patients and provide informative feedback during exercising at home. Therefore, the candidate proposes the study on machine-learning based state identification of rehabilitation exercise by using wearable sensors on the lower limbs. The informative feedback and quality assessment could be obtained by selectively segmenting the exercise into four states: rest, raise, hold and drop. The segmentation potentially increases the frequency of detection resulting in almost real-time feedback. In addition, identifying the abnormal sequences

against the correct pattern in the respective state results in more specific and informative feedback. In this work, the candidate analyses the impact and derives valuable insights of the extracted sensor signals in relation to the predicted. As a result, the predictive model yields up to 95.89% (SVM) and 94.04% (SVM) accuracy for binary and multi-label pattern recognition respectively. The experiment and recommended framework show the efficiency and potential of using signal data as features in motion-based exercise pattern recognition.

The work presented in this thesis demonstrates the realization of home rehabilitation from the hardware-level to the simulation of user intervention. The methodologies exploit the affordable hardware to correctly track the limb motion while the motion signal prediction model and analysis boost the potential of intervention strategy for the user's home exercise feedback.

Chapter 1

Introduction

In this chapter, the background of rehabilitation and assistive technology is presented. Based on the challenges of rehabilitation, the motivation and scope of the research are discussed. Lastly, the key contributions of the thesis are listed.

1.1 Background and Motivation

In the fast-pace of today's technology, Internet of Things (IoT), the network of physical objects such as sensors, software and network connectivity have greatly facilitated these objects to communicate and exchange data. This has sparked a new interest in many research disciplines. Wearable device is now one of the primary focus of IoT deployment with its flexibility and connectivity [20]. Wearable sensors are often compacted and are used in all sorts of scenarios ranging from emergencies, medical monitoring to the affordable fitness monitors on our wrists.

Meanwhile, health-care system has advanced by integrating the available technologies [21, 22]. The patient-doctor experience has never been the same with the intro-

duction of assistive technologies [1] such as remote health monitoring and emergency notification system. The innovation enables health specialists to not only keep track of their patients' wellbeing in a scalable and manageable manner but also to understand their daily life environments that contribute to the recovery.

Assistive technology has positive impacts especially on citizens with disability and senior citizens. The monitoring provides insight on whether the treatment has been executed properly while the assistive wearable sensor could encourage users to move and regain their mobility. Rehabilitation (or physiotherapist) is a perfect candidate for the application of assistive technology. Rehabilitation describes the procedures to regain physical strength and mobility, which often involves a series of repeated exercises over a period of time. Thus, wearable devices with specialized physical rehabilitation aims to boost performance in curing impairment and improving mobility, functionality and quality of life. In other words, wearable sensor takes the role of assisting clinical diagnosis and prognosis by assisting and reminding patients when they exercise at home and reporting their performance to the doctors.

The continuous attention provided by such system benefits doctors so that they could provide care and monitoring to more than one patient at the same time. Moreover, while the customized set of exercises is taught to the patient, wearable device can ultimately be sophisticated enough to automatically help direct patient to the correct movement at home to avoid unintentional injuries. Exercises which are done incorrectly could lead to pain or worsen the existing condition.

Therefore, wearable technology for human motion tracking and assistance has become a popular research topic to assist in the clinical field for physiotherapists for more accurate prognoses, providing various solutions for therapeutic rehabilitation in

[1] An umbrella term which includes assistive, adaptive and rehabilitative devices for people with disabilities and also includes the process used in selecting, locating and using them

everyday environment for better patient-hospital administration experience.

1.1.1 The Global Demand for Home Rehabilitation

World Health Organization (WHO) stated that 110 million to 189 million of people above 15 years old are suffering from disability causing them to live with extreme hardship in terms of movement and mobility [23]. The number of people affected is expected to continue to rise because of chronic diseases and ageing population. Losing physical mobility happens to many people who are suffering from heart and lung diseases, Parkinson's diseases, stroke, paralysis, sport injuries, accidents, repetitive strain injury and old age conditions such as arthritis, osteoporosis and hip and joint replacements [24, 25].

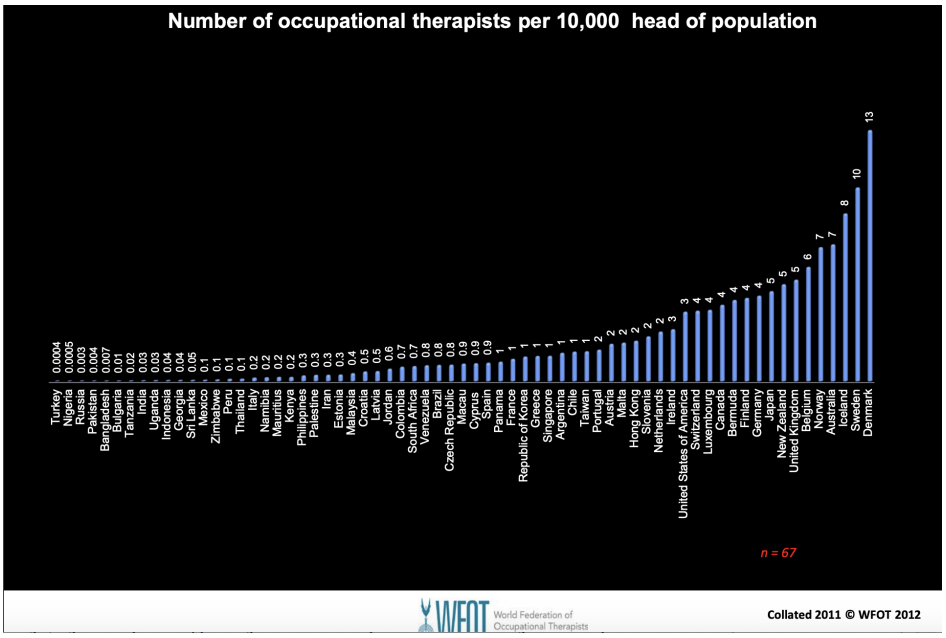

Figure 1.1: Number of Occupational Therapists [1]

The World Health Organisation (WHO) reported in the global atlas of health workforce that the world is in dire need of physiotherapists (Figure 1.1). WHO stated that there are at most 20.5 (Finland) per 10 000 population in selected countries [1,26]. The

unmet rehabilitation need results in deterioration in health, increases dependency on others for assistance and decreases the quality of life. Home rehabilitation is a means to alleviate this problem. However, monitoring and supervision are essential since if a patient does the physiotherapeutic exercises incorrectly, recovery may be slowed down or worsened; the injury may be exacerbated due to placing unnecessary pressure on the joint or injury.

Furthermore, in developed countries like Singapore, ageing population is a major concern. The elderly over 65 years old in Singapore is estimated to increase from 8.9% in 2014 to 18.7% in 2030. With the shortage of clinical manpower, there has been a drive towards integrating IT technologies with societal needs under a general umbrella of e-Health is a specific group called, "Tele-rehabilitation" [22,27–29]. Moreover, injuries on the lower limb of the body are reported to comprise up to 38% of all serious injuries [30]. That is why it is crucial to focus this research on assistive healthcare in lower-limb motion tracking given that these are the most common body segments which need rehabilitation after surgeries.

1.1.2 The Motion Tracking System for the Community

With unavoidable frailty, assistive technology could provide autonomous monitoring and care. While the system is highly needed to reduce the care hours and help with recovery, the demand is relatively low, especially in the mid and low-income community.

The reason for the low demand in the community is due to the mismatch of the available devices to the needs of the community. WHO survey questionare listed six domains of assessment of the merits of assistive technologies: Availability, Accessibilty, Acceptability, Adaptability, Affordability and Quality [31].

The motion tracking system is categorised into three groups, namely, the visual

system, robotic exoskeleton and non-visual system. The visual motion tracking system uses the camera to track the movements while producing location coordinates, posture and traverse line, etc. Multiple cameras are commonly used in the physical therapist centre and the research lab for high accuracy [32]. However, the system is either costly or requires customized space and setup for community usage. Recent researches have introduced cost-effective cameras, albeit it is debatable that sufficient space is mandatory to avoid obstructed vision.

The robotic exoskeleton is designed to support the movement of the limb to improve the physical activity. The robotic exoskeleton is used to alleviate the severity of existing health consequences [33]. Since it is created for a specific application, the disadvantage of exoskeleton is inflexible to set up and difficult to use without assistance at home. For home rehabilitation where the patients are trying to gradually regain their mobility, it is impractical due to its prohibitive cost and laborious setup.

Non-visual motion tracking system uses compact and sensor-based devices to sense the user's movement. In particular, inertial motion capture systems, embedded with Accelerometer, Gyroscope and Magnetometer, are deployed in clinical, laboratory and commercial [17, 34, 35] environments.

With the rise of IoT technology, the inertial measurement unit (IMU) sensor becomes more affordable and prevalent. IMU sensor is most suited for community usage due to its inexpensive price, flexibility and ease of customization. The limitation of cost-effective sensor is the noise of the integrated sensors of the IMU. It causes the orientation estimate of the motion tracker to drift from the desired accuracy. Thus, there has been numerous scientific studies to minimise and correct the noise by fusing the signals of the integrated sensors.

1.1.3 Realization of Home Rehabilitation for Physiotherapist and Patients

The goal of home rehabilitation is to address the issue of inadequate number of physiotherapists and caregivers for the ageing population. The assistive technology, such as cost-effective motion tracking at home, would enable the physiotherapist to track the performance of their patients while they are doing the exercise at home. It means digital supervision of physiotherapy exercises is a feasible and scalable solution by enhancing the motion tracking system with feedback-oriented feature.

While enabling assistive technology maximizes the accessibility and affordability of home rehabilitation, especially at the community level, there is a need for exercise monitoring and biofeedback in the home or community setting with motion tracking technology. If patients fail to execute the correct motion or improper placement of the lower limbs while exercising, it would slow down their recovery or place unnecessary pressure on the joints concerned [36]. One consequential example of incorrect exercise is Dynamic Knee Valgus (DKV) [37] which is a result of putting undue pressure on the knee joint by twisting it inwards. It could escalate to Anterior Cruciate Ligament (ACL) rupture. Hence, the automated feedback system is crucial to guide the patient at home to do the exercise correctly.

1.2 Research Objectives and Scope

In this thesis, the candidate explores the motion tracking device and techniques in order to enable efficient home exercise monitoring. Hence, fewer visits to the clinic is required by enabling the clinician to look after a larger number of patients remotely and closely. In addition to home exercise monitoring, the high-level observation of patients

performance while exercising is deemed crucial. It involves the design combination of wearable sensors with machine learning algorithm to automate the feedback to guide patients during their exercise at home. Therefore, the main objectives are to enable the use of home-friendly, affordable and accurate devices to measure up to clinical measurements as well as to provide at-home monitoring and intervention.

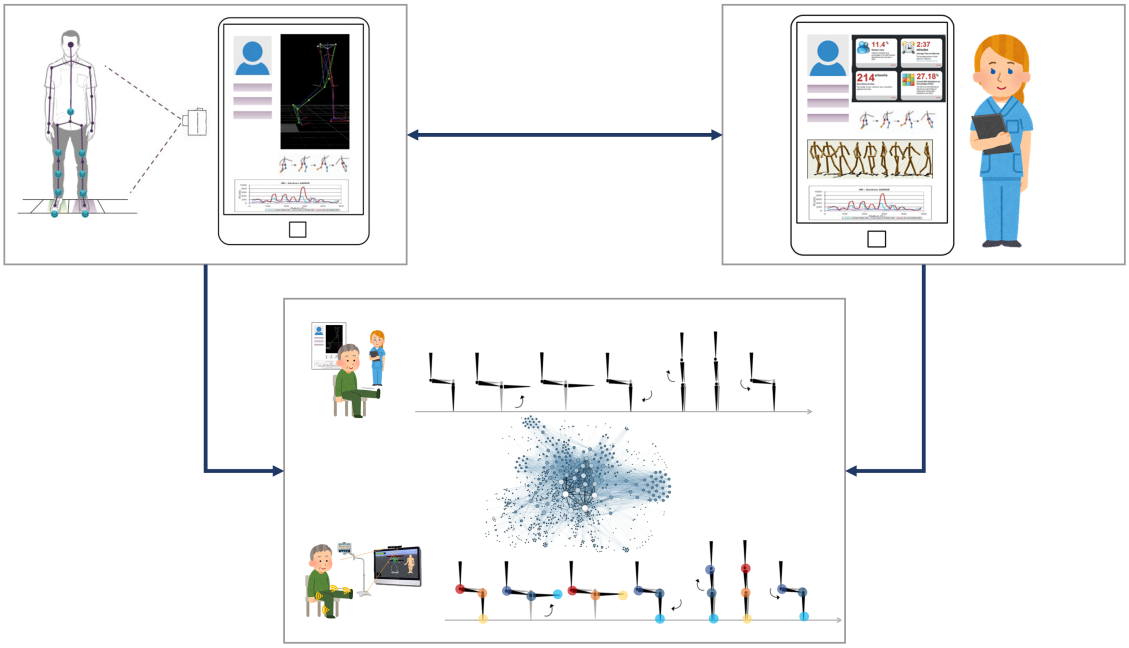

Figure 1.2: The Exploration of Wearable Sensors for Home Rehabilitation

- The first objective aims to choose the wearable device that is suitable for community and home usage. Motion tracking technology has its base on various systems such as mechanical, electromagnetic, acousitci, optical, and inertial systems [38]. Among all, wearable device emerges as the most suitable low-cost motion sensors unlike robotic system which could cater to only a few designed movements. In recent years, wearable device come in different sizes, functionalities, prices and customizability. In particular, the sensors could be compact or embedded in the smartphone.

- The second objective is to obtain clean and reliable estimates from affordable sensors, which could be mapped to existing clinical parameters and human-readable data for the physiotherapist. In an ideal circumstance, the orientation estimate is obtained by the integration of angular velocity, which results in angular displacement (orientation estimate). The joint estimates monitored in the ambulatory care and rehabilitation center are the combination of orientation estimates and the proportion of the body segment. Despite the compactness and mobility characteristics of wearable devices, such sensor data is reported to be noisy compared to the commercially available sensors. The noise is further accumulated by the integration process resulting in significant signal drift. Existing research involves fusing the sensor component data such as gyroscope, accelerometer and magnetometer in order to cancel the drift. Therefore, an objective of this research is to propose a robust sensor fusion algorithm and noise-cancellation method for the affordable sensors to measure up to the commercial devices in terms of the orientation estimate.

- The third objective is to address the interpretation and usability of the sensor signal in observing the quality of exercise and provide guidance feedback while the patient is exercising at home. As mentioned earlier, patients are taught exercise sets while being monitored by physiotherapists at the rehabilitation centre. According to Flanagan's research, patients have high tendency to reach for the end-point movement, when they are asked to redo a full motion of exercise [39]. Hence, this behavior may lead to ineffective result or injuries while patients are not monitored at home. Hence home-base exercise monitoring system contributes greatly to the tele-rehabilitation of the patients and allows specialists to keep track of more patients at one time.

1.3 Methodology

This thesis demonstrates methodologies and applications in sensor fusion and exercise state pattern recognition using the motion sensor. The research methodologies adopted in this work are as follows:

- Firstly, comprehensive literature reviews are conducted on previous research work on assistive technology for home rehabilitation. The challenges are identified from previous research work such as the limitation of ambulatory monitoring system, sensor fusion algorithm and the exercise assessment.
- Secondly, the candidate proposes signal processing algorithms for the fusion of motion sensors, such as gyroscope, accelerometer and magnetometer. The evaluation case study is based on early stage rehabilitation exercises.
- Thirdly, the candidate combines signal processing with machine-learning to the post filtered signal oscillation observed from the fusion output.
- Lastly, the candidate applies data mining and machine learning techniques to predict the state of the exercise. A framework is proposed as the intermediate step to bridge the gap between the motion data and the provision of informative feedback in home rehabilitation. Feature engineering method is applied to determine the correlation as well as derive insight from the signal to the predicted state.

1.4 Major Contributions

The following contributions are made to address the motion sensor fusion and pattern recognition mentioned in Sections 1.1 and 1.2.

1.4.1 Sensors Integration

The candidate proposes solutions to exploit signal processing techniques to fuse the smartphone sensor data and calibration techniques to configure the sensor settings and correct for the errors to obtain more accurate orientation estimation from the smartphone sensors. Details of the contributions are as follows:

- The candidate proposes a lightweight method, complementary Filter + Feedback (CFF), which initiates a feedback loop from the orientation estimate to the gyroscope data integration using complementary Filter (CF) to reduce the error due to gyroscope data integration or drift. It is an efficient modification to [40]. It uses Euler representation directly thereby reducing the computation complexity compared to [40].

- The placement of different sensors on the body segments is recommended to address the problem of Gimbal lock. There are many studies which report the placement of sensors according to the default Euler hierarchy. However, there is no study which recommends the orientation of the sensors and their placement so as to reduce signal fluctuation after converting from quaternion. The recommended placement of sensors has been shown to be well suited for all the lower limb rehabilitation exercises as well as for the hip joint range of motion [41].

- The candidate proposes a new and better orientation estimation algorithm which combines quaternion-based kalman filter with corrector estimates using gradient descent (KFGD). KFGD yields good results and outperforms the prominent Madgwick (MW) algorithm for low-cost sensors such as smartphones. It is well suited for slow and controlled range of motion. These exercises are commonly adopted during early stage rehabilitation and physical activities for the elderly.

1.4.2 Post Signal Processing and Data Analytics

A supervised osscillation detection and correction technique is introduced. An extensive study on angular interpretation based on raw inputs such as Accelerometer, Magnetometer and Gyroscope has been carried out. The contributions include:

- The candidate explores the application of a classification solution to correctly filter the oscillating outliers that appear in the post-fusion motion data from the wearable sensors (i.e. accelerometer, magnetometer and gyroscope).

- The candidate adopts the classification methods such as Support Vector Machine (SVM), Logistic Regression (LR) and Multilayer Perceptron (MLP) to find the most suitable detection model. The collected data are based on the use case of Sit-Stand and Leg Extension.

- A study has been performed on the significant features to be derived from the sensor data and the suitable classifier for the model. Thereafter, the candidate evaluates the efficiency of the detection model in eliminating the oscillations.

1.4.3 Feedback Mechanism Development

The exercise segmentation framework to bridge the gap from motion tracking to quality exercise and informative feedback is proposed to monitor the exercise in the granularity of segments to identify incorrect movement. Details of the contributions are as follows:

- The candidate proposes the segmentation of the rehabilitation exercise, performs feature engineering on the arrays of sensor signals (i.e. signal frame) and applies machine learning algorithms to identify incorrect movement for each state.

- The candidate evaluates the performance of the proposed signal frame as input features for machine learning against the angle frame [42]. The candidate analyses the various features derived from the extracted data and their impact on the accuracy of the predicted exercise state.

- The candidate proposes an intelligent framework with immediate feedback on the correctness of each state for lower limb exercise.

1.5 Thesis Organization

The rest of the thesis is organized as follows:

- **Chapter 2** The background of rehabilitation exercise is presented by connecting kinematic analysis of human movement in home environment to the clinical parameters. The motion tracking system is discussed for the most efficient solution in home environment. Characteristics of motion tracking sensor signals, such as Accelerometer, Gyroscope and Magnetometer, are introduced with the sensor fusion techniques. Realising home rehabilitation, review of assistive application, in particular, exercise assessment is conducted to compare and contrast the existing techniques.

- **Chapter 3** In order to provide a motion tracking system suitable for the community, low-cost sensors are being used. This chapter presents the background studies and challenges fusing the noise-prone sensor signals. Two fusion algorithms are proposed to obtain the clean reading for orientation estimate. The evaluation is done with the off-the-shell XSENS Awinda and against the prominent Madgwick algorithm. A placement of sensors is suggested while conducting

the case study of early-stage rehabilitation exercise, Sit-to-Stand and Leg Extension.

- **Chapter 4** This chapter focuses on correcting the oscillation observed in the post filtered signal. A novel oscillation detection model is proposed combine with sensor fusion technique. The selection and performance of the detection models are evaluated against the manually corrected signal.

- **Chapter 5** In order to realise home rehabilitation, a pilot movement application, RehabPartner, is developed to provide feedback to patients who may over twist their leg during exercise. Realising the challenge in obtaining continuous qualitative feedback, an intermediate exercise segmentation is proposed. The feature insights for each segmentation are extracted from the evaluation.

- **Chapter 6** This chapter concludes the thesis and also includes the possible future directions with regards to cost-effective home rehabilitation.

Chapter 2

Literature Review

This chapter provides the literature survey of the motion tracking system and intervention techniques for the realization of home rehabilitation. To begin with, the basis of rehabilitation exercise is elaborated with regards to the kinematic analysis of human movement in both clinical and home environment. Henceforth, the motion tracking system and signal fusion techniques are discussed in terms of their mutual and exclusive characteristics. The goal of choosing the cost-effective tracker for home and community usage has introduced the challenges in the wearable sensors' signal fusion leading to the proposed sensor fusion technique and signal-correction method. Various automatic intervention and assistive applications during home exercise are reviewed and they are being compared and contrasted.

The challenges presented in this chapter have inspired the candidate to carry out the research detailed in this thesis.

2.1 Rehabilitation Technologies: Clinical and Home Treatment

Injuries can affect our movements and can occur at all ages. They include sport injuries, chronic diseases, repetitive strain injury and old-age common conditions. Controlled movements and motion anlaysis are keys to regain physical strength, range of motions and muscle strength. These procedures are part of the physical rehabilitation, or physiotherapy. While clinical physiotherapist makes the diagnosis and customized treatments, the prognosis often rely on the visual assessment of the experienced experts.

Addressing the problem of the increasing number of people needing physiotherapy and the limited number of therapists, there has been a drive to combine the technologies with societal needs under a general umbrella of e-Heath, known as "Tele-rehabilitation" [43]. Baskett et al. [44] and Cavallo et al. [45] conducted group studies trying to introduce patient to the idea that rehabilitation is not just during official therapy sessions. Their study suggested at-home rehabilitation and the outcome showed that at-home rehabilitation has about the same effectiveness as supervised rehabilitation.

Many doors have opened for home rehabilitation system due to the routine nature of physiotherapy, need of specialists and availability of low-cost available sensors. A significant amount of research has been conducted to outsource home-suited system requirements, nature of tracking sensors, resourceful placement of sensors, recommendation of user feedback, etc. At-Home rehabilitation emphasizes on extending existing technology, especially wearable sensors, to meet clinical assessment report. Clinical assessment report is a method for physiotherapist to interpret, verify and analyse patients' performance. Thus, the report needs to conform to clinical norm.

2.1.1 Gait Analysis: The Clinical Perspective

In order to use unsupervised rehabilitaiton system at home efficiently, it is essential to bridge the engineering perspective and human motion tracking to clinical norm. The terms like "Gait Rehabilitation" and "Analysis" are widely used in clinical norm and to analyse the parameters observed [46, 47].

Gait rehabilitation refers to the process of learning how to walk normally. It often for patients who are suffering or sustaining from an injury or disability [48]. During the check-up, in order to find how much the patient has recovered, one of the strategy used by the physiotherapist to assess the patient is called "Gait Analysis". Precisely, Gait Analysis is described as the systematic study of human motion in order to obtain measurements such as body movements, mechanics and muscle activities. Specialist uses their visual judgement and expertise to make prognosis. As a result, a customized treatment is formed based on the posture-related problem of their patients. Subsequently, Gait Analysis is adopted by researchers as a systematic way to evaluate and as key parameter to verify their novel techniques [49].

Weijun T. presented Gait Analysis methods into 3 categories: Gait Kinematics, Gait Kinetics, and Electromyogram (EMG) [3]. Figure 2.1 briefly describes the usage and techniques of each category. Gait Kinematic refers to the tracking of movement of major joints and components of the lower limb. It uses various sensors to collect the Gait[1] data. Gait Kinetic studies the forces and movements that result in movement of human body segments. In clinical use, Gait Kinetic analysed the signal from force sensors in shoes or force plate. Lastly, Electromyogram (EMG) are components to track muscle conditions and usually produce the most complex signal.

[1] a person's manner of walking.

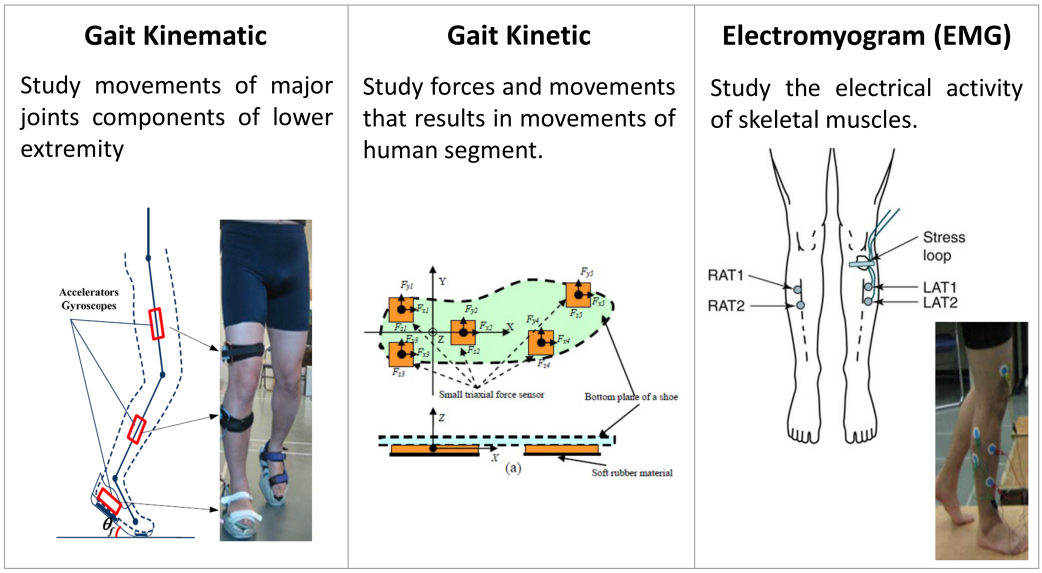

Figure 2.1: Gait Analysis Methods [2, 3]

2.1.2 Coordinate Anatomical Plane

Studying the motion and joint movements (Osteokinematics) of the human body requires a representation of coordinates in the Anatomical Plane. Lynn S. L. [50] denotes 3D rotation in anatomical plane coordination as shown in Figures 2.2 and 2.3.

Joint movements are identified in a wide variety and complexity of body parts and rotation in Kinesology[2]. However, since only lower limb is concerned, it is assumed that joint movement refers to 3 terminologies: Flexion/Extension, Abduction/Adduction, and Internal/External rotation. For bending movement of one bone to another, Flexion is decreasing motion in joint angle and Extension is increasing motion. For movement with the midline of body as reference, Abduction is the joint angle of moving away from midline and Adduction is vice versa. If the forepart of the body is rotating inwards, it is called Internal rotation; on the contrary, External rotation refers to rotating outwards.

[2]the study of movement

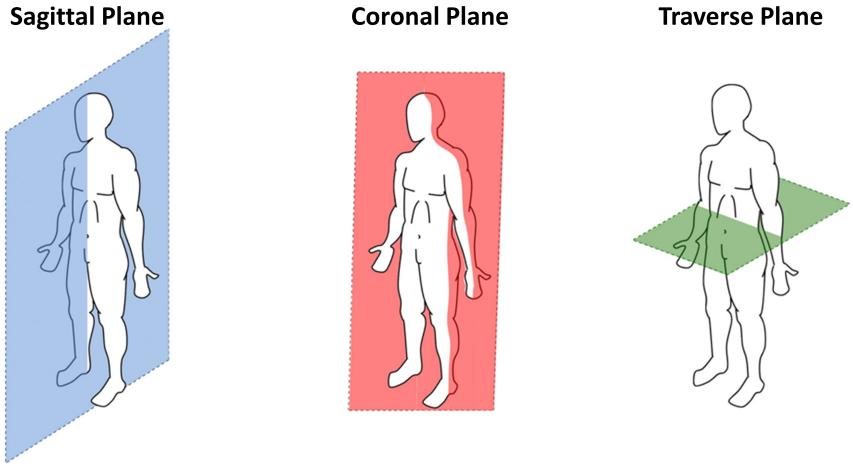

Figure 2.2: Body Coordinate Plane [4]

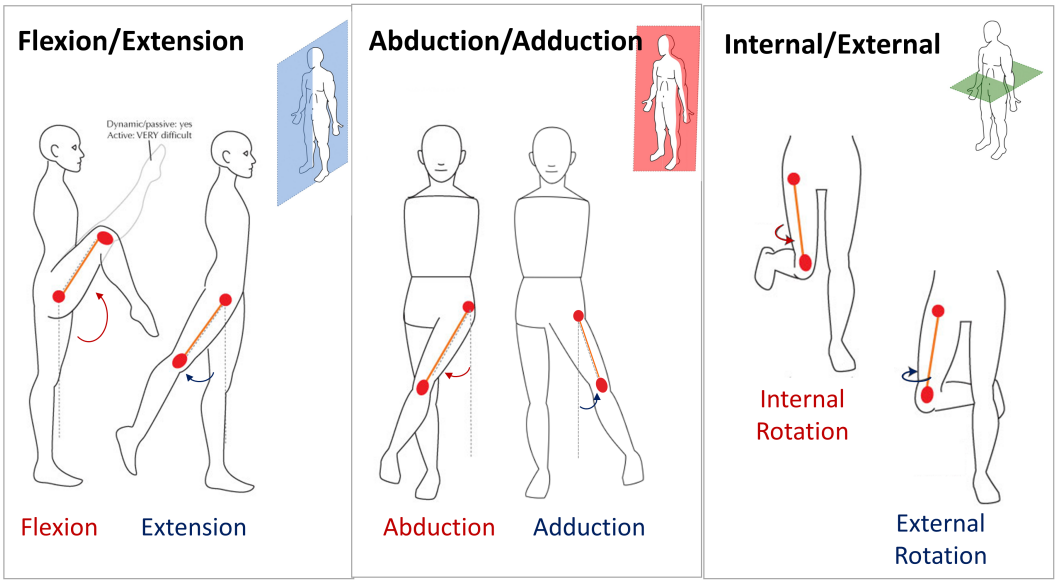

Figure 2.3: Body-Segment Rotation Terminology [5]

2.1.3 Addressing Limitation of Gait Analysis in Rehabilitation Exercise

Although Gait analysis acts as the baseline for rehabilitation assessment, limitation of Gait analysis lies upon the fact that it only monitors and assesses a patient's walking behavior. On the other hand, rehabilitation exercises go beyond walking [51] (Figure 2.4). Hence, tracking rotation, body-segment and joint rotation, is more applicable as they provide the desired angles under any form of exercises. In addition, it can be extended to Gait Kinematic for Gait Analysis.

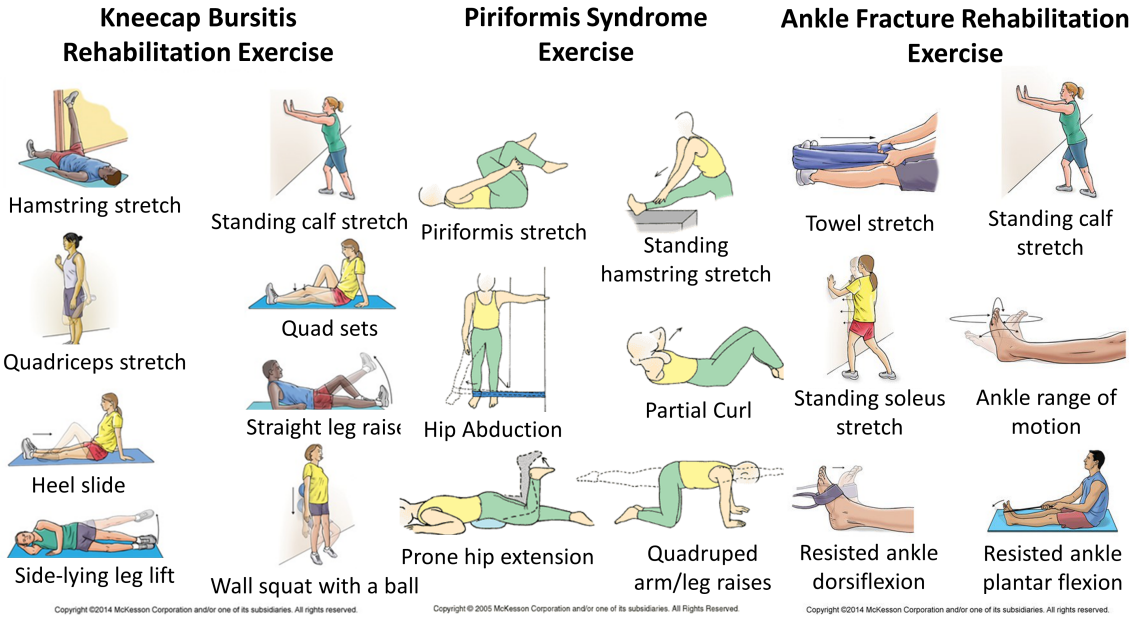

Figure 2.4: Various Rehabilitation Exercises [6–8]

Among the 3 main joint movements, Internal/External rotation has great potential beyond Gait Analysis, yet gets the least attention. Peng-Fei Y. [52] demonstrated mechanical relationship of bone and muscle by studying the load on bone. The experiment specifically investigated the peak tibia and torsional deformation angle during Gait. In other words, Internal/External rotation of the shank (Tibia) and thigh (Fe-

mur) plays an important role in this experiment to obtain Tibia-Torsional deformation angle. For research that is concentrated solely on Gait Kinematics, they figuratively targets Flexion/Extension in Sagittal plane causing loss of crucial information like rotation in Coronal plane (Internal/External rotation) [53, 54].

Therefore, in this thesis, the candidate focuses on the rotation in the coordinate anatomical plane for rehabilitation exercise motion tracking.

2.1.4 Introduction to Tele-Rehabilitation Technology

While physiotherapy aims to cure impairment and improve mobility, functionality and quality of life, tele-rehabilitation (Figure 2.5) is known as tools that enable specialists to engage with patients who are doing exercises at home with the help of technology. Tele-rehabilitation is believed to be an effective solution to overcome personal and community barriers regarding cost, travel time, shortage of clinical manpower and enable patient's interaction with their physiotherapists from home.

Video conferencing was the first tele-rehabilitation solution for the physiotherapist to oversee the performance of patients remotely. It was introduced by Tousignant et al. [55] aiming to reduce patient travel time and cost to the hospital. Although the patient is present remotely, a physiotherapist is required to give direction and oversee rehab[3] exercises using video camera and communicate in real-time.

Videoconferencing presents several limitations. In particular, the therapist can only attend to one patient at a time. In an ageing society, it cannot address the problem of therapist manpower shortage [56]. Moreover, the doctors could not ensure that their remote patients would not fall during the session. Hence, additional manpower is thus needed [57]. Lastly, video camera cannot see 3 dimensional movements when only 2

[3]rehabilitation

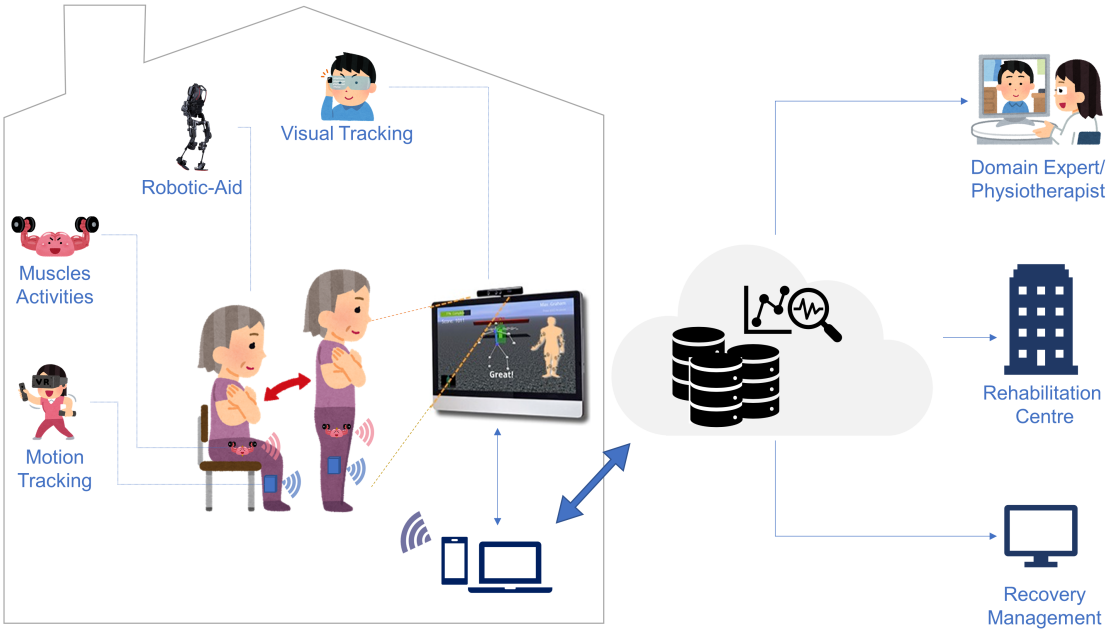

Figure 2.5: Tele-Rehabilitation Technology

dimension video is captured [58].

Combating the set-back on service qualities, Fook et al. [59] introduced a body-worn sensor as an addition to video conference. During the exercise session, accelerometers embedded in body-worn sensor were used by producing motion data via a 3D Studio Max model. As a result, both doctor and patient have a better vision spotting incorrect movement and correct them. Therefore, the direction of this study is to utilize the most suitable human motion tracking system for home rehabilitation.

2.1.5 Human Motion Tracking System

With respect to the potential of human motion tracking system to assist in tele-rehabilitation (home), the system is expected to be able to handle dynamic real-time data processing to position change of a human body with reference to mature motion sensing technology [60]. Currently, motion tracking systems can be based on mechani-

cal tracking, electromagnetic tracking, acoustic tracking, optical tracking and inertial, magnetic tracking. For usage, they are categorized into three main groups: non-visual tracking, visual tracking and robot-aided tracking [38]. Figure 2.6 illustrates the various types of human motion tracking systems and its core component.

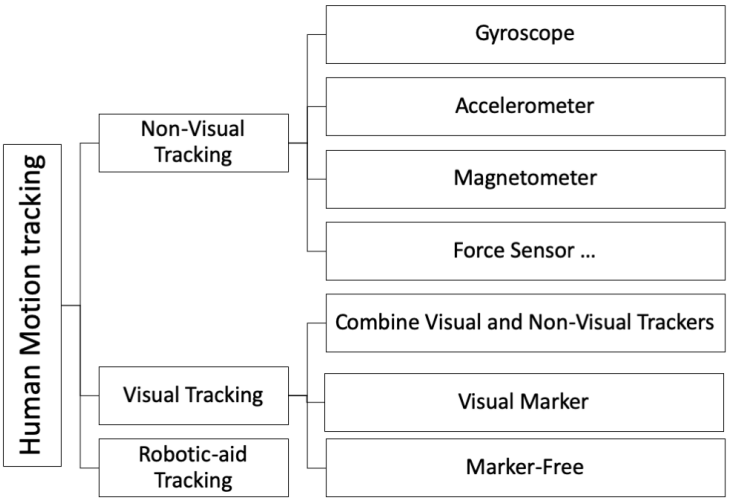

Figure 2.6: Motion Tracking Systems Overview

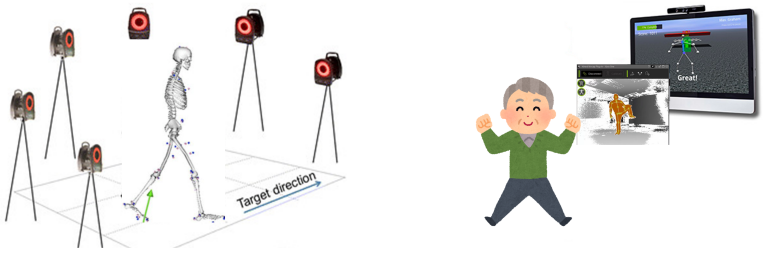

Figure 2.7: Visual Tracking Systems

Visual tracking system refers to the use of single or multiple cameras in capturing user motion. It is grouped into three types such as visual marker [61], non-visual marker [62,63] and hybrid [64]. Visual tracking system is widely used in motion research lab and clinical rehabilitation to analyse the the motion. The disadvantages of visual tracking system is either not economical using multiple-view visual tracking or the

required space is unsuitable for the home environment.

Robotic-aided tracking system provides a customized range of rehabilitation solutions by embodying sensors with the electro-mechanical or electromagnetic tracking. In addition, it brings high accuracy, good support, and feedback mechanism to users in the form of exoskeleton. The disadvantages of exoskeleton are the inconvenience in setting up and its inflexible to support multi-purpose rehabilitation for home rehabilitation [33].

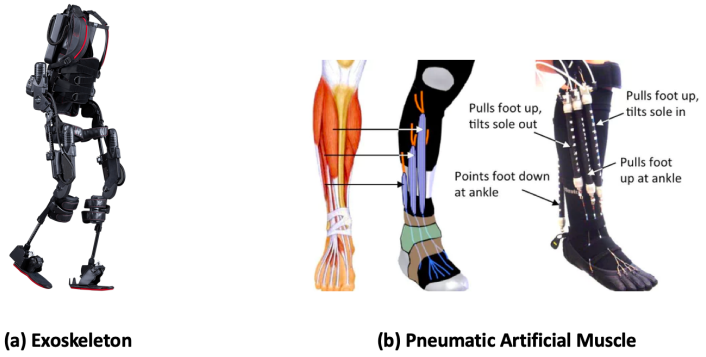

Figure 2.8: Robotic Tracking Systems [9, 10]

Non-visual tracking systems are sensor-based systems that include inertial based, magnetic based, ultrasound based and glove based tracking systems. For everyday usage, in particular taking into consideration the uncontrolled and compact space in a patient's home, non-visual tracking system is preferred. The inertial and magnetic based systems are the prominent choice for their flexibility and customizability and are affordable to be used in wearable devices. In fact, the study by Zhang et al. [2] had shown that among non-visual tracking systems, accelerometer, gyroscope and magnetometer are most discussed and ranked at the top three.

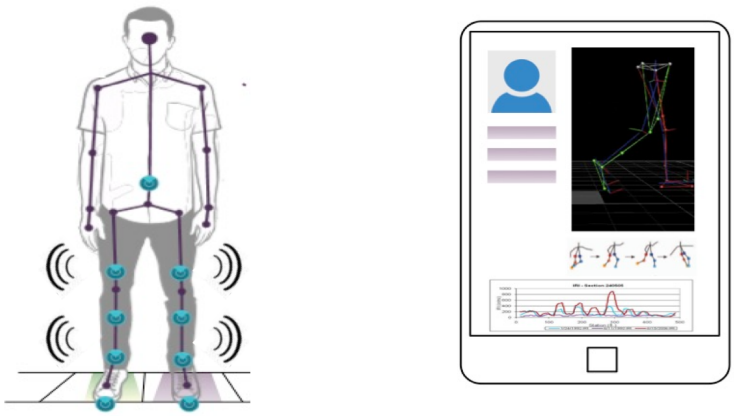

Figure 2.9: Non-Visual Tracking Systems

2.1.6 Characteristics of Wearable Sensors as Motion Tracker

The main factors that contribute to the choice of hardware component are its ability to track movements accurately enough for the physiotherapist to track a user's recovery progress as well as the placement of sensors. At the same time, it has to be compact and lightweight so that it would not interfere with the user's movement. Besides M. Ayoadeand L. Baillie [27] who have built their motion tracking system from inertial sensors units, many other researchers have used this for Gait analysis methods [3]. Therefore, Non-visual tracking system, adopting IMUs, has been chosen in both academia and commercial usage.

Inertial Measurement Unit (IMU) refers to a device that produces integrated quantities of angular rate, linear and gravitational force as well as earth magnetic field. The key components are accelerometer, gyroscope and magnetometer to track motion and report the measurements in the form of angular displacements. Integrating components in IMU could provide high accuracy but it suffers greatly from drift [65], especially in low-cost sensors. In an ideal world, the body-frame sensor orientation can be obtained by performing integration on the gyroscope data. Due to white noise from the reading, integration actually accumulates the noise effects resulting in drift from the expected

values [19].

In summary, in order to obtain high accuracy from low-cost IMU sensor, it is crucial to understand its key components as well as the signal combination techniques which use the mutual yet uncorrelated characteristics to mitigate for the noise and drift from the angular rate.

2.1.6.1 Gyroscope

Gyroscope is a sensor that measures rotation rate of an object. Due to its low cost, small size and low power consumption, gyroscopes are popular among products such as cars, robotics, games consoles and smartphones. Triple axes MEMS gyroscope can measure rotation velocities around three axes: x, y, z based on Coriolis force [19]. In other words, it uses vibrating mechanical element to sense the rotation. Coriolis force is proportional to both angular velocity of rotating object and the velocity of object moving towards or backwards with respect to the axis of rotation. The movement is then converted to electrical signals that can be read by a microcontroller [66]. Gyroscope is often used on objects that are not spinning very fast like aircrafts.

2.1.6.2 Accelerometer

Accelerometer is an electromechanical device that measures acceleration forces which is the rate of velocity change of an object. It contributes not only static forces of gravity but also dynamic forces of acceleration while there exists vibration or movement. Acceleration is generally measured when capacitance changes between internal capacitive plates [67]. Accelerometer has a certain advantage for holding static gravity force. This gravity force helps correct any gyroscope drift with reference to the ground. For a drastic movement, it is a challenge to seperate translation acceleration and gravity

in the accelerometer.

2.1.6.3 Magnetometer

Magnetometer is an instrument used to measure the strength and direction of the magnetic field in the surrounding area of the instrument. Magnetic field includes both earth's magnetic field and any magnetic field created by nearby objects, especially metal. The earth magnetic refers to a magnetic dipole with one end near the North Pole and the other near the South Pole. Its main advantage is its measurement of direction assisting the accelerometer to correct the gyroscope drift where the accelerometer cannot use gravity force to obtain the orientation estimate. The main drawback of the magnetometer is that it is easily corrupted by distortions called hard iron and/or soft iron. Hard iron distortion is created by objects that produce magnetic field while soft distortion is altered by existing magnetic field such as metals. In indoor environment, hard iron has a bigger impact on error compared to soft iron [68].

2.2 Wearable Sensor Fusion Techniques

In order to track rotation estimate accurately, inertial sensors are fused using signal processing techniques, while offset is calculated by calibration technique. Hence, new solutions for sensor fusion and advanced signal processing methods are continuously being proposed. The key components to track orientation in real-time are accelerometer, gyroscope and magnetometer. In an ideal scenario, 3D sensor orientation can be obtained by integrating gyroscope data. Gyroscope integration causes errors by accumulating white noise over time from the reading. The accumulated errors are called drift [19, 65].

Hence, in order to improve the performance of gyroscope integration, accelerometer and magnetometer are used to compensate for the drifts since they have mutual yet uncorrelated characteristics.

The main challenges of sensor fusion performance often boil down to the design of the system model and the corrector input obtained from the accelerometer and magnetometer. The design of the system model is usually adopted in a flexible manner, depending on the designer's interpretation. In other words, the system model differs depending on the variable representation used as well as the components which are combined. For example, one design uses Euler angles which fuse gyroscopic data with corrector input from the combination of gravity and earth magnetic field [69]. Others design a rotation matrix based algorithm by combining the accelerometer and gyroscope data first. Thereafter, magnetic field is applied for compensation when necessary [70].

The prominent fusion techniques are Kalman Filter, Extended Kalman Filter [3] [71] [72] [73], complementary Filter [28], Madgwick AHRS [74], etc. For orientation estimates, Kalman Filter often uses Matrix or Quaternion Representation as system model. However, Kalman Filter could be further extended to non-linear system model called the Extended Kalman Filter (EKF) [75] and Indirect Kalman Filter [76]. The non-linear characteristic allows EKF to repetitively correct the raw input. The bottleneck of EKF lies in the system complexity and computation time resulting in high latencies in a real-time environment. Kim, J., et al. [28] introduces StrokeTrack that uses complementary filter as a light-weight alternative to the complex Kalman Filter. Complementary Filter makes use of the fact that gyroscope data is accurate for short periods while accelerometer and magnetometer data are used as complement over long time periods. Therefore, complementary Filter implements a combination of low-pass filter for the accelerometer and magnetometer data and high-pass filter for the gyroscope data. Complementary Filter has evolved to a non-linear system as well by adding

a feedback loop to a high-pass filter and/or low-pass filter [40].

In practical implementation, especially for low-cost sensors, one must take note of adjustable parameters in order to obtain accurate orientation estimate. P. Zhou proposed a solution to drift by using periodic correction [19]. However, refreshing the integrated data could only take effect at the starting point of correction. In the scenario of sudden movements right before the end of the interval, the corrected data could end up with an error due to the accelerometer or the magnetometer. The candidate proposes to tackle the drift problem by adding a feedback loop to the Complementary Filter and tune the adjustable threshold theta (Section 3.2). This solution does not depend solely on the accelerometer and magnetometer fusion but the filtered orientation.

R. Mahony [40] has proposed various additional methods to the Complementary Filter by using feedback loop. However, its algorithmic complexity is unsuitable for limited computation power device such as smartphone. The candidate proposes to reduce the complexity of the feedback loop on the selected parameters. In addition, to overcome the inflexible predefined threshold (theta) of the Complementary Filter, the candidate proposes to study the stabilizing quaternion-based Kalman Filter, using Gradient Descent fusion for attitude error correction (Section 3.3).

Similarly, Magwick filter [74] introduced orientation estimates for both IMU and MARG that address the limitation faced by the Mahony filter [40] in computational expenses and its compatibility with only IMU system. Q. Mourcou [77] evaluated the performance of smartphone inertial sensor. While comparing Mahony and Magwick filters, Magwick filter has better performance. However, it takes the form of the Mahony which is an extension of the Complementary Filter. Thus, Madgwick filter is thus a good benchmark against the candidate proposed methods (Section 3.5). Madgwick filter has already been proven to be better than both the baseline Kalman Filter and the Complementary Filter.

2.3 Home Rehabilitation Feedback and Motion Assessment

In order to realise meaningful home rehabilitation, there is a need for exercise monitoring and biofeedback in the home/community setting with motion tracking technology. The automated system is required to guide the patient at home to do the exercise correctly and generate the progress summary reports for physiotherapists so that they can attend to a larger number of patients.

2.3.1 Motion Assessment Techniques

The exercise assessment and screening are designed to analyse the posture, stability and movements to see what injuries the patient is at risk of developing and what exercises will best improve his/her deficiencies to achieve the health goals. Exercise assessment can be broadly divided into two categories, namely, learning-based and rule-based. Rule-based methods use a set of rules to identify the unseen activity. Learning-based methods refer to machine learning models that train data using pre-defined labels and predict the outcome of the data.

2.3.1.1 Rule-Based Approach

Rule-based approach focuses on setting rules based on the perception of correct postures and movements. For rehabilitation exercise, the rule-based framework is commonly defined using the joint angles and orientation of the body segment to distinguish rules for gestures and repetitive count.

Rule-based framework has been introduced as a gesture recognition method using the joint angles (parameters) obtained by sensor devices (equipment) in order to cre-

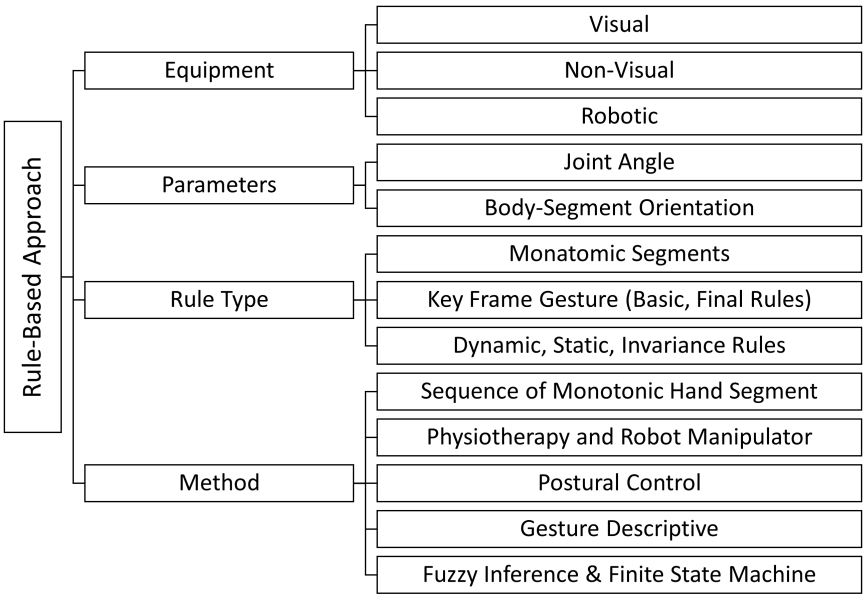

Figure 2.10: Exercise Assessment: Rule-Based Approach

ate sequences or sets of rules (rule types and methods). As the clinician uses visual assessment for the prognosis, visual equipment are frequently used for the rule-based framework. In particular, Kinect is used to extract the body segment orientation [78] and joint angles [79,80] as the inputs to form rules. However, other types of equipment such as Inertial Sensors [81] and robotics [82] are also been used to obtain sensor data to derive the joint angles and orientation.

Figure 2.10 summarises the development of rule formation. It evolves from the monatomic configuration to the clearly defined types of rules. The evolution of rule-based methods could be considered to start by defining sequences for finger joints angle [79]. Each hand configuration is called a monotonic segment. Thereafter, Gesture Description Language (GDL) is introduced to extend from the hand configuration to body gesture recognition to create a structure for the previously known monotonic segment [80]. A gesture to be recognised has to pass a set of rules, which includes basic and final rules instead of a monotonic segment. The basic rule is made of one or

more keyframes for joint positions, while the final rule consists of one or more basic rules. However, GDL focuses only on a snapshot of movements which lack the rules that involve the fluidity of movements. W. Zhao introduced 3 types of rules for the rule-based approach: dynamic, static and invariance rules [83]. The static rule covers the rules for stationary joints or body segments while dynamic rule represents the sequence of monotonic segments. Invariance rule is included to specify the requirements of moving joints or body segments. Upon obtaining the kinematic rules, the similarity between measured and ideal motions are calculated and put into the fuzzy inference system. After kinematic rules are combined and defuzzied, the patient will receive live feedback. A finite state machine is used to track the maximum and minimum values of the metric of interest in each state.

The advantages of rule-based approach are being more robust to errors as compared to exercise assessment prediction systems, and easily extensible to biofeedback after the rules are formed. Moreover, less data is required compared to the database to train the prediction model. As rule-based approach uses the knowledge base derived from the data while ignoring the external factors such as the type of exercise, it is easily extended to feedback system once it detects any deviation from the defined gesture recognition rules. However, the setback of this approach lies in the cost of obtaining the general knowledge in order to form the sets of rules. It is inflexible when the scenario or application changes from that in which the rules have been derived.

2.3.1.2 Learning-Based Approach

Learning-based approach trains the prediction model to classify activities or gestures without describing it fully. The main advantage of this approach is the less time-consuming cost of acquiring the knowledge to build the rules (unlike section 2.3.1.1). Therefore, it only requires sufficient data in order to generalise the prediction through

various types of exercises.

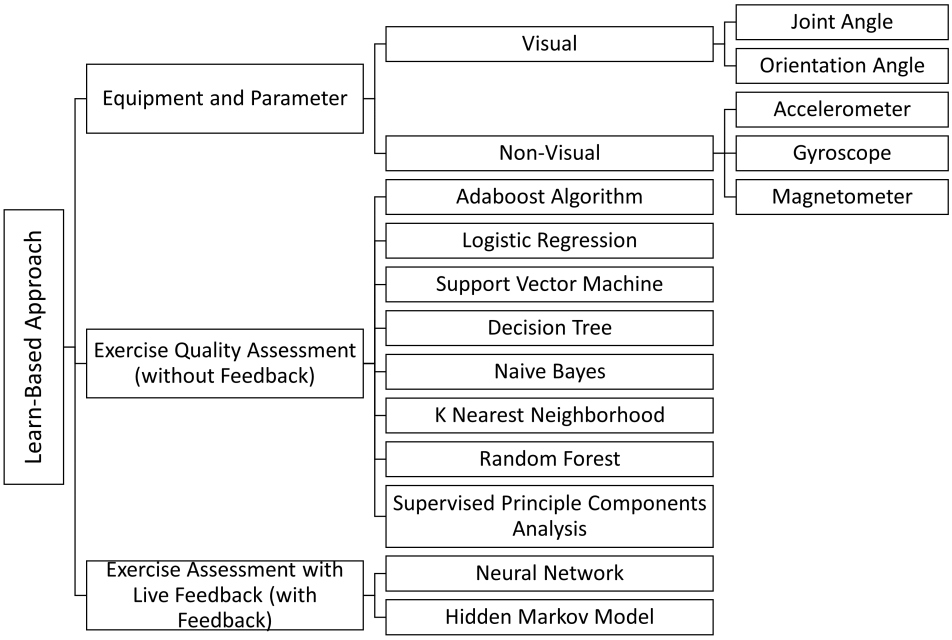

Figure 2.11: Exercise Assessment: Learn-Based Approach

Figure 2.11 groups the learning-based approach into two types: exercise quality assessment (without live feedback) and learning-based live feedback. Neural Network (NN) and Hidden Markov model (HMM) are two main methods proposed to automate exercise assessment (with feedback). Unlike finite state machine, HMM predefines the number of states and state transitions; henceforth, gesture recognition is predicted periodically at the end of each segment. Jonathan. et al. proposed the near real-time classification that incorporates periodic velocity patterns for segmentation [84]. Specifically, the pattern is divided based on zero and peak velocity while using joint angles at the setup stage in comparison. The segmentation enables the feedback to be almost real-time and is capable of identifying correct repetition despite unspecific feedback for incorrect movements. Neural Network (NN) is listed as capable of assessing the speed of exercise to be too fast, too slow or wrong static joint angle after being trained [85] in less than 2 seconds. However, it has yet to provide informative

feedback to patients. To address the problem of the lack of informative feedback in the real-time system, exercise quality assessments focus on the classes of error types. More significantly, it is used to predict the consequences of detected error. In particular, R. Kiaifar proposed a model to predict the risk of knee injuries after Dynamic Knee Valgus was detected [86]. Thus, exercise quality assessment evaluates the quality of the patient's overall implementation. The classification training is done in a way where quality labels are manually marked by observing the recorded video frame or involving the experts to rate the session. For example, P.E. Taylor adopted the adaboost algorithm [87] using frequency computation on the accelerometer as the feature extraction process. However, this method did not manage to identify multiple errors per exercise. For that reason, other machine learning methods such as Support Vector Machine [88, 89], Logistic Regression (LR) [86], Decision Tree (DT) [90], Naive Bayes (NB), K Nearest Neighborhood (KNN), Random Forests [91, 92] are adopted.

2.3.1.3 Feature Extraction for Learning-Based Approach

Feature extraction plays an important role in the application of machine learning algorithms since its intent is to draw out the informative and non-redundant features that facilitate the classification training. Feature extraction methods range from frequency computation that could be extracted from the accelerometer [87], to statistical time domain features [92]. Vision sensor is one type of general sensors used in the rehabilitation assessment system. Kinect camera directly outputs joint angles as extracted features since it captures the depth of both filed and real-time image data [93]. In a motion capture system, the joint angles and body-segment orientation (Euler angles) are calculated using the body rotation coupled with marker trajectories. [94] uses a Kinect sensor for real-time assessment using a combination of kinematic modelling with fuzzy inference in different exercises. The disadvantage of the visual sensor in

motion tracking is the need of space and the conversion from 2-dimensional perception to 3 dimensional. Therefore, wearable sensors are introduced to derive the orientation and joint angles from the motion data.

Using wearable sensors, the raw signals are commonly employed as input features more than the estimated angles. It is due to the fact that angle frames are more likely to suffer more consequences from the accumulated noise in the raw signals, namely, drift [95]. Since human-readable rules are not required to be enforced in order to train the prediction model, sensorial data could be efficiently classified. The majority uses the accelerometer because it makes use of gravitational force and it can compute the flexion/extension and abduction/adduction of the body-segment orientation. O. M. Giggains performed cross-sectional analysis and concluded the accelerometer holds the most impact over quality assessment classification compared to the gyroscope and magnetometer [92]. Although the accelerometer input is highlighted, gyroscope, magnetometer, Euler angles and joint angles are still being used as input features in some applications and techniques. For instance, when inertial sensors (accelerometer, gyroscope and magnetometer) are combined with Euler angle, Principal Component Analysis (PCA) was used for feature selection [92]. Interestingly, R. Kianifar proposed supervised PCA to the data for comparison with SVM, LR and DT. The result was better in terms of accuracy and the features are clinically interpretable.

2.4 Summary

In this chapter, the candidate presents the existing research work on home rehabilitation in both clinical and technical perspectives. Firstly, the clinical requirements, in the form of gait analysis and anatomical plane of the rotation of body segment are introduced. Secondly, the gap between gait analysis and rehabilitation exercise is

bridged by the introduction of human motion tracking system. While discussing the various types of motion tracking systems, the inertial tracking system is chosen for its flexibility, availability and cost-effectiveness. Thirdly, the characteristic of IMU sensor as well as its sensor fusion are detailed which has inspired the candidate's first and second contributions. Lastly, the intervention system for home rehabilitation is compared and contrasted between the rule-based and learning-based approaches. This has been adopted in the third contribution detailed in this thesis.

Chapter 3

Robust Sensor Fusion Algorithm for Low-Cost IMU Orientation Estimate

This chapter presents the background studies and problem statements of low-cost sensor fusion for 3-dimensional orientation estimates (Section 3.1). The candidate proposes two fusion techniques (Sections 3.2 and 3.3) [1] in comparison with the off-the-shell XSENS Awinda and the prominent Madgwick algorithm (Section 3.4). Using the use case of early-stage rehabilitation exercise, the placement of sensors and system representation are recommended to avoid the effect of gimbal lock.

[1] The contributions in this chapter has been published in
-**Seanglidet Yean**, Bu Sung Lee, Chai Kiat Yeo, and Chan Hua Vun, "Algorithm for 3D orientation estimation based on Kalman Filter and Gradient Descent ", 7th IEEE Information Technology, Electronics and Mobile Communication Conference (IEMCON), New York, USA, 2016, pp. 1-6.
-**Seanglidet Yean**, Bu Sung Lee, Chai Kiat Yeo, Chan Hua Vun, and Hong Lye Oh, "Smartphone Orientation Estimation Algorithm combining Kalman Filter with Gradient Descent ", IEEE Journal of Biomedical and Health Informatics, vo. 22(5), 2017, pp. 1421-1433.

3.1 Background Studies

The number of smartphone owners has increased from 10% in 2011 and projected to be 35% of the world population by 2020 [96]. Nowadays, smartphones are by default, equipped with integrated motion sensors, namely, accelerometer, gyroscope and magnetometer. Owing to the accessibility of smartphones, motion data collection is now easy and widely available to users. As a result, it has a huge potential to render itself useful for rehabilitation besides everyday use. Therefore, in this chapter, the IMU in smartphone is selected to be used for the experiment as the non-visual tracking system for home rehabilitation (detailed in Section 2.1.5)

The challenge is the tradeoff between the quality and accessibility of the inertial sensors in smartphone and the motion tracking accuracy. Specifically, the affordable sensors or inertial sensors integrated in smartphones are limited in range and sensitivity compared to costly commercial inertial sensors. The proposed solutions are to exploit signal processing techniques to fuse the smartphone sensor data and calibration techniques to configure the sensor settings and correct for the errors to obtain a more accurate orientation estimation from smartphone sensors.

3.1.1 Smartphone Sensor Fusion's Drift

Smartphone has become an indispensable companion in our daily life. The all-in-one nature of smartphone brings great flexibility to our needs with just a few taps of a button. In recent years, it has embedded affordable motion sensors to enable tracking of our daily activities such as walking, running. Where progress tracking for tele-rehabilitaiton is concerned, more precise and accurate measurement is required.

The robustness and accuracy of Micro-Electro-Mechanical Systems (MEMS) gyro-

Table 3.1: Processed Yaw Rotation Angle's Drift of an iPhone6

Sample	1	2	3	4	5	6	7	8	9
Angle (°)	0.20	0.40	0.59	0.78	0.96	1.14	1.32	1.49	1.66

scope in smartphones are not as accurate as commercial motion tracking sensors. For example, iPhone and Android applications are reported to accumulate errors of up to 40° in 10 minutes on angular velocity alone [19]. This means that even the processed data still experiences drift despite the smartphone being equipped with its own sensor fusion algorithm. Table 3.1 presents an instance of the drift incident in a stationary position for yaw rotational angle (z-axis). The samples are collected using iPhone 6 with a sampling rate of 100Hz using the built-in CoreMotion class [97]. The reading is supposed to stay at zero degree but the drift (i.e. the rotation angle) accumulates with each sample reading despite the phone being stationary.

With the intention to use smartphone for home rehabilitation exercises, error correction and stability of motion tracking are needed, especially for long rehabilitation regimen. Therefore, it is important to understand the phone sensors' characteristics in order to apply suitable sensor fusion techniques effectively. The performance of the proposed smartphone algorithms is then being benchmarked against commercial motion tracking device such as XSENS [98].

3.1.2 XSENS Awinda for Drift Comparison

XSENS Awinda is a digital measurement suite that measures 3D angular rate, acceleration and earth-magnetic [98]. It is a commercially available inertial sensor and has been widely used in motion tracking research as shown in Table 3.2.

Table 3.3 shows XSENS's sensors specification while Table 3.4 illustrates the MEMS gyroscope configuration of two common smartphones. Series ADIS1626x [103] is com-

Table 3.2: Examples on the Use of XSENS MTx

Researchers	**MTx Usage**	**Year**
S. O. Madgwick,A. J. Harrison, and R. Vaidyanathan [74]	Estimation of IMU and MARG orientation using a gradient descent algorithm	2011
S. Qiu, Y. Yang, J. Hou, R. Ji, H. Hu, and Z. Wang [99]	Ambulatory estimation of 3D walking trajectory and knee joint angle using MARG Sensors	2014
H.-P. Brückner, B. Krüger, and H. Blume [100]	Reliable orientation estimation for mobile motion capturing in medical rehabilitation sessions based on inertial measurement units	2014
M. Crabolu, D. Pani, L. Raffo, and A. Cereatti [101]	Estimation of the center of rotation using wearable magneto-inertial sensors	2016
S Qiu, Z Wang, H Zhao, H Hu [102]	Using Distributed Wearable Sensors to Measure and Evaluate Human Lower Limb Motions	2016

Table 3.3: XSENS Performance Specification [17]

Unit	Accelerometer	Gyroscope	Magnetometer
Dimensions	3 axes	3 axes	3 axes
Dynamic Ranges	$\pm 50 m/s^2$	$\pm 1200 deg/s$	$\pm 750 mGauss$
Bandwidth (Hz)	30	40	10
Nonlinearity (% FPS)	0.2	0.1	0.2
Bias Stability ($^\circ/\sqrt{Hr}$)	0.002	1	0.1

monly found on Android phones while L3G4200D [104,105] is the equivalent on iPhones.

Tables 3.3 and 3.4 show the differences between the performance of low-cost sensors on multipurpose smartphones versus the relatively expensive and commercial motion tracking sensor. In general, the drift from MEMS gyroscope is affected not only by the gyroscope's bias but also influenced by acceleration and environmental vibration. It means the low performance sensors such as the ones in the smartphones have a high propensity to produce errors unlike higher performance MEMS gyroscope in XSENS which are mostly affected by physical factors such as vibration impact or temperature.

Table 3.4: Android and iPhone Phones' MEMS Gyroscope Specifications [18, 19]

Unit	iPhone (L3G4200D)	Android (ADIS1626x)
Dimensions	3 axes	3 axes
Dynamic Ranges	$\pm 500 deg/s$	$\pm 320 deg/s$
Bandwidth (Hz)	50	50
Nonlinearity (% FPS)	0.2	0.2
Bias Stability ($^\circ/\sqrt{Hr}$)	25.2	1.8

For instance, Bias Stability in Tables 3.3 and 3.4 represents the noise from the built-in gyroscope. The higher the Bias Stability, the more noise is added to the angular rate and hence to the orientation estimates.

Therefore, to benchmark the performance of the proposed algorithms, the candidate uses the processed data from XSENS for comparison.

3.1.3 The Effect of Gimble Lock

Location of sensors on the lower limb has high potential to positively improve the accuracy of orientation estimate. B. Zhang [2] highlights the placement of inertial sensor. When sensor placement is not limited to a participant's feet, positioning on the shank and thigh are top on the list.

The initial orientation of sensors that are attached to the shank and thigh are important as it can potentially avoid gimbal lock. Gimbal lock happens when two axes in a 3-dimensional space move in parallel (Figure 3.1). In other words, a 3-dimensional rotation is now locked onto a 2-dimensional space. Gimbal lock is related to the order of combination angles in object rotation [106]. The standard order of rotation is to rotate in yaw (z), followed by pitch (y) and finally roll (x).

To avoid the gimbal lock that happens when pitch = 90°, The recommended solution is to adjust the axis so that pitch has a low probability to reach 90°. For lower limb

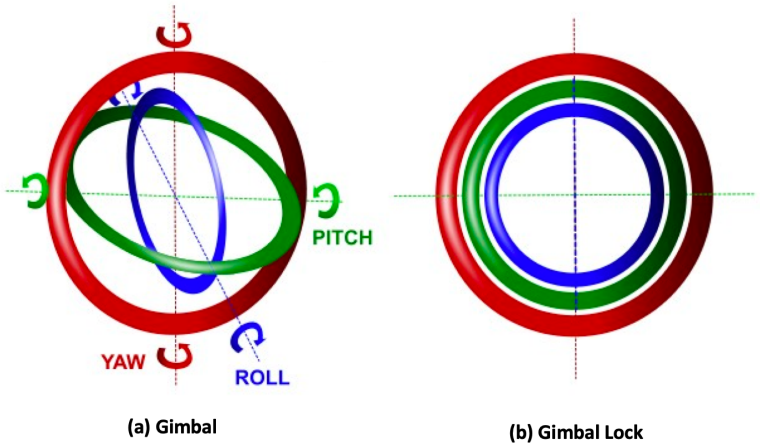

Figure 3.1: Example of Gimbal Lock [11]

kinematic, the range of rotating from side to side (abduction/adduction rotation) has less tendency to reach 90°. Thus, the tracking sensors are placed at the side of the participant's lower limb and the coordinates are adjusted as shown in Figure 3.2-C.

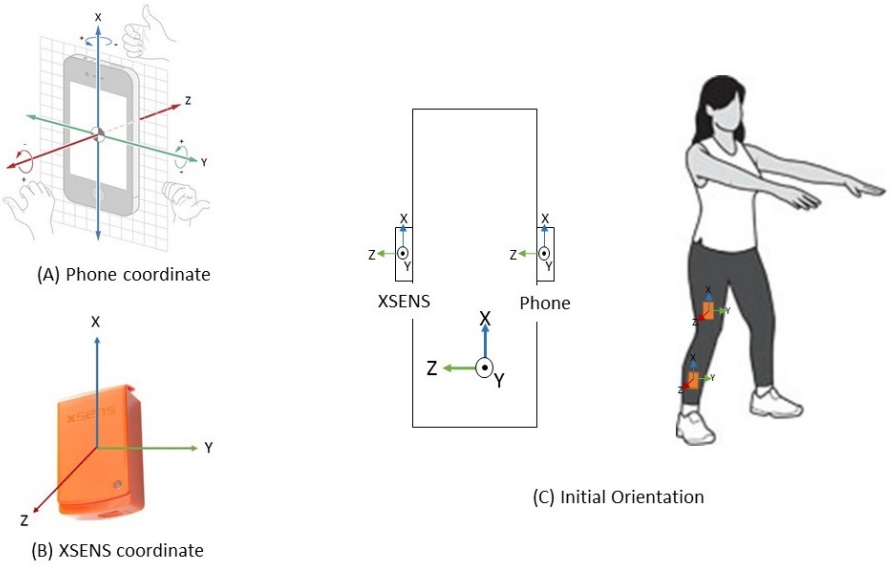

Figure 3.2: Placement and Initial Orientation of Sensors to avoid Gimbal Lock

3.2 Complementary Filter Feedback (CFF)

3.2.1 Model Overview

The evidence discussed in Section 3.1 illustrates the main issue of drift and gimbal lock effect in extracting the orientation estimates from the motion sensors, especially when using affordable sensors. Henceforth, the literatures (in Section 2.2) of innovative design of system models and correctors have been introduced to combine sensors gyroscope, accelerometer and magnetometer readings as well as complementing their uncorrelated characteristics.

Complementary Filter makes the assumption that gyroscope data is accurate for a short period while accelerometer and magnetometer data are used to complement over the long period of time. In addition, it is commonly known as the alternative to Kalman Filter [28] by fusing both the high-pass filter and the low-pass filter results as illustrated in Figure 3.3. The main goal is to reduce the drift from gyroscope by balancing with an instant attitude with constant weight. It is to be noted that Euler angles is chosen as the state representation as it is straightforward and has human-readable representation.

Low-pass filter is applied upon the accelerometer measurements that includes earth gravity and linear accelerometer. Earth gravity ($\vec{A} = \begin{bmatrix} A_x & A_y & A_z \end{bmatrix}$) is extracted via Low-pass filter trying to eliminate the short term noise presented in linear acceleration [107]. By using the acceleration force of gravity, estimated attitude ($\alpha_{attitude}$) can be obtained with respect to earth frame. However, gravity force is pulling towards the ground and thus the estimated attitude can only be obtained from tilting with respect to the ground, i.e. tilting to the side ($\alpha^z_{attitude}$) and tilting front and back ($\alpha^y_{attitude}$).

Therefore, $\vec{A}$ is combined with magnetometer ($\vec{E} = \begin{bmatrix} E_x & E_y & E_z \end{bmatrix}$). Obtain the

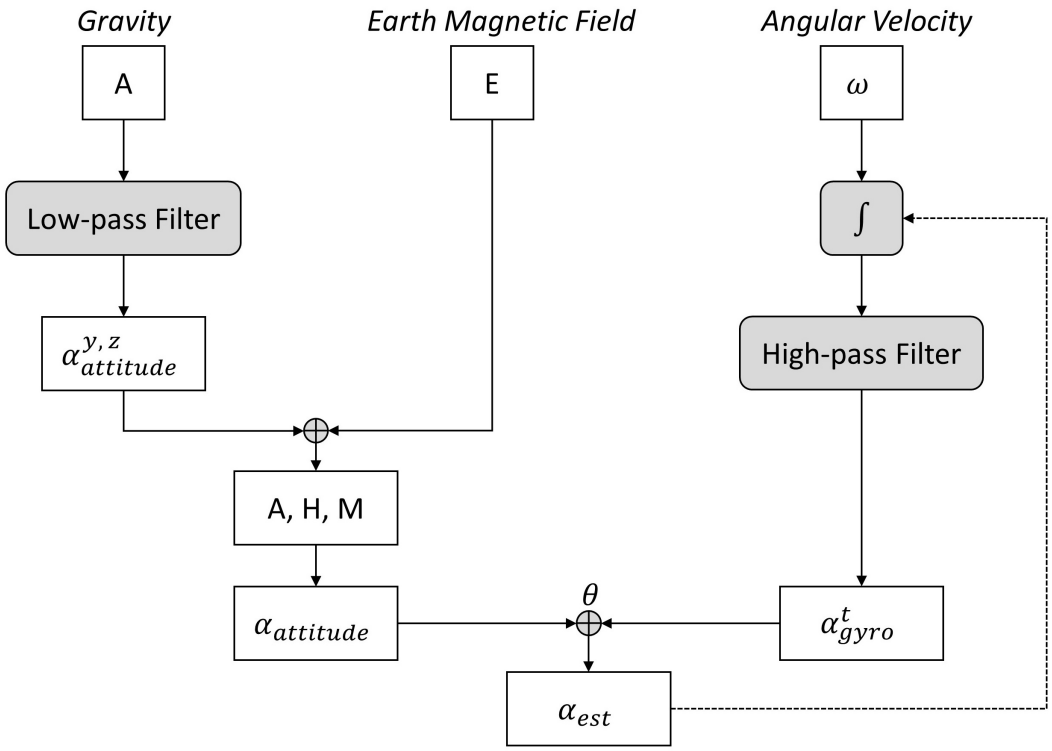

Figure 3.3: System Overview of Complementary Filter + Feedback

$\vec{H}$ and $\vec{M}$ which represent the Earth vector pointing to the East (Eq.3.1) and the North (Eq.3.2) respectively as follows:

$$\vec{H} = \vec{A} \times \vec{E} = \det \begin{bmatrix} i & j & k \\ A_x & A_y & A_z \\ E_x & E_y & E_z \end{bmatrix} \tag{3.1}$$

$$\vec{M} = \vec{H} \times \vec{A} = \det \begin{bmatrix} i & j & k \\ H_x & H_y & H_z \\ A_x & A_y & A_z \end{bmatrix} \tag{3.2}$$

According to [108] and the coordinates presented in Figure 3.2, the following is obtained:

$$\begin{cases} \alpha^{x}_{attitude} = \arctan(\frac{H_y}{M_y}) \\ \alpha^{y}_{attitude} = \arcsin(-A_y) \\ \alpha^{z}_{attitude} = \arctan(-\frac{Ax}{A_y}) \end{cases} \tag{3.3}$$

while $\alpha^{x}_{attitude}$,$\alpha^{y}_{attitude}$,$\alpha^{z}_{attitude}$ denote instant rotation about G, rotation about axis at $\alpha^{z}_{attitude}$ in the horizontal E-N plane, and angle in horizontal plane for pitch rotation respectively. Together, they are referred to as ***instant attitude***.

The angular rate of rotation from gyroscope is then integrated using Euler's method [109]. High-pass filter is implemented on the gyroscope integrated data by allowing data higher than the pre-set range to pass through. α_{gyro} is the result from the integration and high-pass filter (Eq.3.4, Eq.3.5).

$$\alpha^{t}_{gyro} = \alpha^{t-1}_{gyro} + \frac{1}{2}\, Q\left(\alpha^{t-1}_{gyro}\right)\, \omega^{t}\, \Delta t \tag{3.4}$$

$$Q\left(\alpha\right) = \begin{bmatrix} 0 & \sin\left(\alpha^{z}\right) sec\left(\alpha^{y}\right) & \cos\left(\alpha^{z}\right) sec\left(\alpha^{y}\right) \\ 0 & cos\left(\alpha^{z}\right) & -sin\left(\alpha^{z}\right) \\ 1 & \sin\left(\alpha^{z}\right) tan\left(\alpha^{y}\right) & \cos\left(\alpha^{z}\right) tan\left(\alpha^{y}\right) \end{bmatrix} \tag{3.5}$$

where Δt and ω^{t} represent the sampling rate and gyroscope measurement at current time t.

The performance of Complementary Filter depends on the weight, θ, which determines if more trust should be accorded to the gyroscope integration or to the attitude estimate (accelerometer and magnetometer fusion) as per Eq.3.6. In practice, when the time periods are shorter than time, t, the gyroscope data can be trusted and the noisy accelerometer data would be filtered out. On the other hand, for time periods longer than time, t, the averaged accelerometer data will be weighted more than the gyroscope data; the latter may have drifted at this point. Thus, the time period plays a very important role as the value of θ can be tuned accordingly. The feedback is being

illustrated in Figure 3.3 as the solid line from the orientation estimate to the integrator of the gyroscope data.

$$\alpha_{est} = \theta \times \alpha_{gyro} + (1 - \theta) \times \alpha_{attitude} \tag{3.6}$$

3.2.2 Effect and Limitation of Complementary Feedback Filter

The process of integration will cause an accumulation of error which results in gyro drift (Figure 3.4-G1) and it would affect the CF result (Figure 3.4-CF1). Therefore, a feedback from the estimated orientation angle is proposed (Figure 3.4). Using (3.7), the gyro drift from the integration will be reduced as shown in Figures 3.4-G2 and 3.4-CF2.

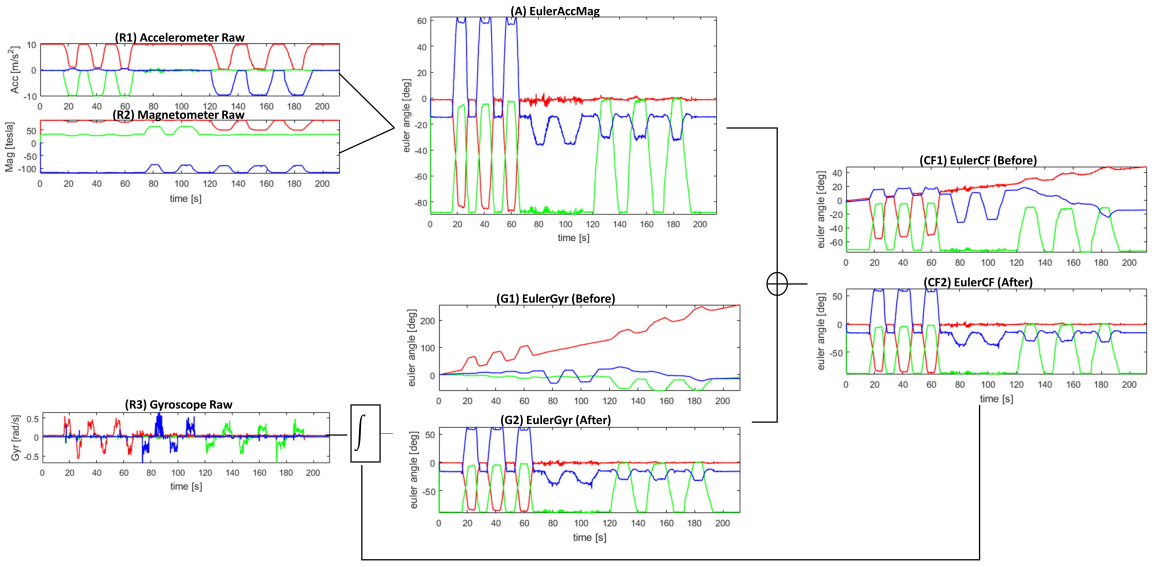

Figure 3.4: Detailed Signal in Complementary Feedback Filter

Unfortunately, the standard complementary filter does not allow θ to be adjusted. Furthermore, even if the trust can be periodically adjusted, it could only be corrected

by the instant attitude which is fused from the accelerometer and magnetometer data. Under the circumstance where the accelerometer is affected by drastic movement or the Earth's magnetic is affected by the environment, the orientation estimates are still heavily affected. Since noise is being accumulated upon integration, the candidate has proposed the feedback loop from α_{est} to the α_{gyro} from Eq.3.4 to become Eq.3.7.

$$\alpha_{gyro}^{t} = \alpha_{est}^{t-1} + \frac{1}{2}\, Q\left(\alpha_{gyro}^{t-1}\right)\, \omega^{t}\, \Delta t \tag{3.7}$$

Although the passive complementary filter proposed by R. Mahony [110] has a similar design, the proposed method is much more simplified and efficient as it is based on Euler representation. This suits our purpose towards a lightweight computation algorithm tenable on a relatively-resource constrained smartphone.

3.3 3D Orientation Estimation based on Kalman Filter and Gradient Descent (KFGD)

Section 3.2 introduces the issue of adaptively adjusting the trust weighting parameter θ. Linear Kalman Filter is chosen as the proposed KFGDs base (overview in Figure 3.6) for this purpose due to its adaptive parameters. In other words, Kalman Filter is known for its Bayesian influence characteristic in dealing with uncertain noises. It is applied in many systems from robotic to computer vision with the main purpose of producing clean output signal in the presence of White and Gaussian noises such that the output signal is to be as close as possible to the ground truth. The main purpose of Kalman Filter is to produce clean output signal regardless of the presence of White and Gaussian noises.

3.3.1 State Representation

There are various ways to represent orientation such as Euler Angle, rotation matrix, quaternion (Figure 3.5). Although Euler representation is easily understood by human, it limits the full range of movement of an object's orientation estimates because of Gimbal lock (Section 3.1.3). In addition, Euler angle's characteristics is subjected to a non-linear system model, which is contrary to the linear system model which is being formulated. Hence, Euler angle is not suitable as a system model but it is a good representation for visualization. A. Janota [111] has compared rotation matrix and quaternion with regards to their computational efficiency and accuracy. It was concluded that rotation matrix and quaternion have comparable potential.

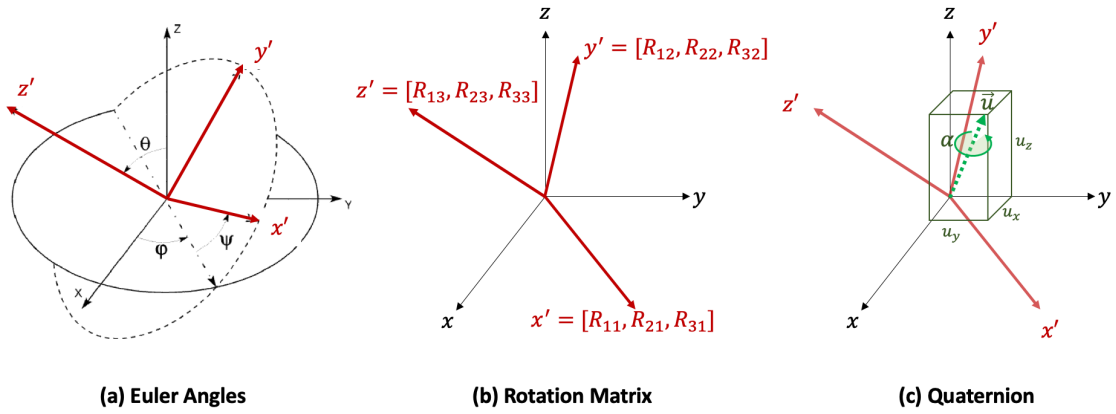

Figure 3.5: Orientation Representation

For KFGD method, quaternion notation is chosen to represent orientation estimates (q_{k+1}). q_k is formulated according to [112]. It combines angular integration ($\bar{q}_{k+1}$) and instant attitude (q_z) of the accelerometer and the magnetometer. According to Euler's rotation theorem, Eq.3.8 represents quaternion rotation of rotated angle α about a rigid body's unit vector $\vec{u}$. Eq.3.10 is selected to portray quaternion rotation instead of Eq.3.9 for simplicity.

$$q = \cos\frac{\alpha}{2} + (iu_x + ju_y + ku_z)\sin\frac{\alpha}{2} \tag{3.8}$$

$$q = q + iq_x + jq_y + kq_z \tag{3.9}$$

$$q = q + q_x + q_y + q_z \tag{3.10}$$

To establish the relationship between quaternion with angular velocity (ω), angular rotation, q_k^-, is equal to the integration of angular velocity from the gyroscope. The ideal result could be obtained if drift is not presented.

Quaternion differentiation with respect to the angular rate is derived as

$$\dot{q} = \frac{1}{2}\omega \times q \tag{3.11}$$

$$\dot{q} = \frac{1}{2}\begin{bmatrix} 0 & -\omega_z & \omega_y & \omega_x \\ \omega_z & 0 & \omega_x & \omega_y \\ -\omega_y & \omega_x & 0 & \omega_z \\ \omega_x & \omega_y & \omega_z & 0 \end{bmatrix} \tag{3.12}$$

where $\omega = (\omega_x, \omega_y, \omega_z)$ are the angular velocities of gyroscope output.

3.3.2 Quaternion-Based Kalman Filter

Kalman Filter fuses sensor signals mainly at 2 critical stages: gyroscope data propagates to the next predicted state variable, and instant attitude from the accelerometer and the magnetometer corrects the predicted state variable (Refer to the Measurement Stage of Figure 3.6). Section 3.3.2 focuses on the prediction and operation of the quaternion-based kalman filter while section 3.3.3 will elaborate on the estimation.

Quaternion-based Kalman Filter formulates its system model from the linear state

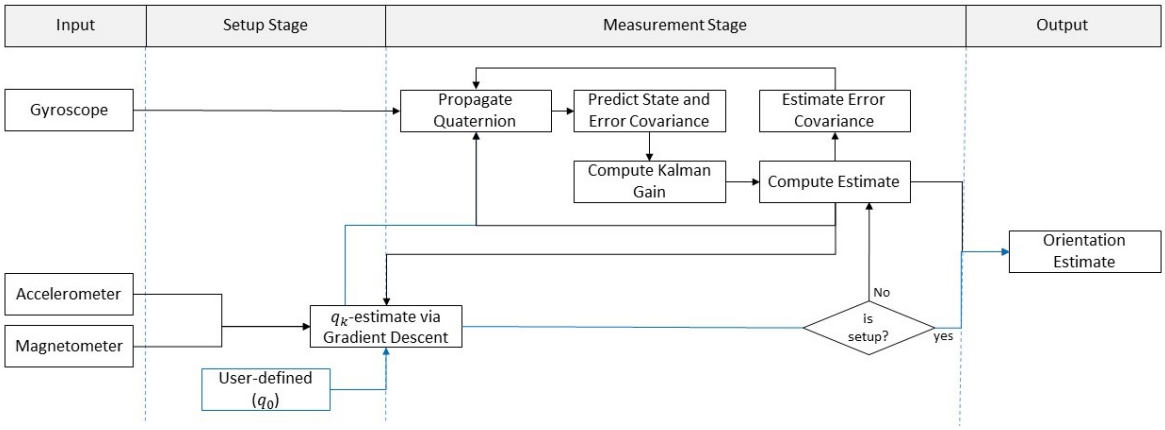

Figure 3.6: KFGD System Model Overview

variable $q = (q, q_x, q_y, q_z)$, while following the guideline procedures in [69]. From Eq. 3.11 and Eq. 3.12, the predicted state at stage 1 is integrated from the angular velocity. Hence,

$$q_{k+1} = q_k + \frac{1}{2}\dot{q}\Delta t \tag{3.13}$$

where q_k holds the previous quaternion to incorporate at the Propagate Quaternion stage at sampling rate Δt.

$$\begin{aligned} A &= I(4)\cos(\tfrac{v}{2}) + \tfrac{2}{v}\sin(\tfrac{v}{2})\dot{q} \\ v &= ||\omega||\Delta t \end{aligned} \tag{3.14}$$

According to Eq.3.13 and Eq.3.14, the predicted state estimate of KFGD is defined as

$$q_{k+1}^{-} = Aq_k \tag{3.15}$$

$$P_k^{-} = AP_kA^T + GQ_dG^T \tag{3.16}$$

$$G = \begin{bmatrix} 1-2q_y^2-2q_z^2 & 2q_xq_y-2q_wq_z & 2q_xq_z+2q_wq_y & 0 \\ 2q_xq_y+2q_wq_z & 1-2q_x^2-2q_z^2 & 2q_yq_z-2q_wq_x & 0 \\ 2q_xq_z-2q_wq_y & 2q_yq_z+2q_wq_x & 1-2q_x^2-2q_y^2 & 0 \\ 0 & 0 & 0 & 1 \end{bmatrix} \Delta t$$

$$K_k = P_k^- H^T (H P_k H^T + R)^{-1} \tag{3.17}$$

Q_d denotes the uncertain noise covariance of the gyroscope. In other words, it depicts how much error correction is expected from external impact. Eq. 3.16 and Eq. 3.17 explain the contribution of Q_d to error covariance P_k^- and Kalman gain K_k. In practice, Q_d is adjusted to be not too high or too low, so that it will not interfere with the corrector q_z in correcting the gyroscope error. Therefore, matrix G is deliberately set to the original form with only Q_d to adjust the Gyroscope's bias.

Likewise, R is the uncertainty covariance of the sensor noise from the observed sensor readings. It represents the gap between the current reading and the real expected value. Since the additional step of Gradient Descent is being used to determine the instant attitude (Section 3.3.3), R uses the value initiated in the setup stage (Section 3.3.4).

3.3.3 Gradient Descent for instant attitude estimate

Extracting gravity from the accelerometer enables correction for the predicted state because gravity does not accumulate nor suffer from the drift. In the same way, magnetometer data provides the earth's magnetic field which is possible to calculate the change of direction especially when acceleration is affected by linear acceleration or inability to detect the direction that is parallel to the earth. Therefore, extracting gravity from the accelerometer and the earth's magnetic field from the magnetometer

forms an instant attitude estimate (q_z) to correct q_{k+1}^- error. q_z is fed into "Compute Estimate" stage of the Kalman Filter to obtain the final output q_{k+1}. Eq. 3.3 in section 3.2 has suggested a fusion formula for gravity and earth magnetic. However, it does not consider the unavoidable noises arising from the drastic change of speed which creates a bias in the accelerometer (A) and the magnetometer (E) (Eq. 3.18).

$$\begin{cases} \vec{\omega} = K_g\vec{\omega}_{true} + \vec{b}_g + \vec{v}_g \\ \vec{A} = K_a(\vec{g} + \vec{a}_{true}) + \vec{b}_a + \vec{v}_a \\ \vec{E} = K_m\vec{h} + \vec{b}_m + \vec{v}_m \end{cases} \tag{3.18}$$

where $\vec{b_i}$ and $\vec{v_i}$ are the bias and the uncorrelated white Gaussian measurement noise, K_g,K_a are the scale factor matrices. Bias and noise from the different axes are assumed to be independent.

Therefore, it is crucial in practical Kalman Filter design to filter out processed noise from the accelerometer and the magnetometer before feeding the data into the quaternion-based Kalman Filter. The focus is to extract the optimal q_z-estimate as the instant orientation. The aim is to minimize the error in the following function:

$$\begin{aligned} Err(q,g,b,E) &= \begin{bmatrix} f_g(q,g) \\ f_b(q,b,E) \end{bmatrix} \\ f_g(q,g) &= q \otimes_q g \\ f_b(q,b,E) &= q \otimes_q b \otimes_q E \end{aligned} \tag{3.19}$$

where gravity g is extracted from the accelerometer. E is the magnetometer data and $b = [\ 0 \quad b_x \quad 0 \quad b_z\ ]$ is the earth magnetic field inclination. $\otimes_q$ refers to quaternion multiplication; thus, f_g and f_b can be derived [76].

The objective function determines the optimal quaternion that yields convergence

via an iterative process using Gradient Descent method according to [74]. Thus,

$$q_{z+1} = q_z - \mu \frac{\nabla Err}{||\nabla Err||} \tag{3.20}$$

$$\text{Such that } \nabla E = J_{g,b}^T Err(q, g, b, E)$$

3.3.4 System Setup Stage

The Setup Stage (refer to Figure 3.6) is the period when a participant is getting ready to start the exercise from a resting position. In this stage, it is assumed that there is no significant movement that will corrupt the accelerometer and magnetometer. Knowing that the gyroscope would accumulate the drift error (section 3.1.1), only the Gradient Descent method and the instant attitude estimate q_z are involved to set q_0.

At the start, having known the initial orientation of the body segment (Refer to Figure 3.7), the candidate sets the "user-defined" q_0 before feeding into the q_z estimate at the beginning (Figure 3.6). Subsequently, the accelerometer and magnetometer data would stabilize the processed data. This output straight away becomes the orientation estimates until the Setup Stage is completed.

In other words, in the Setup Stage (no motion), complete trust is given to the accelerometer and magnetometer to produce the orientation estimate. When the Measurement Stage starts, the stabilized orientation estimate (q_k) is fedback to Eq. 3.13. From then on, the measurement procedure involves the gyroscope data in the Kalman Filter as well as being corrected by the Gradient Descent method. It is to be noted that KFGD's internal state models are initialized as shown in Table 3.5 where $\sigma gyro, \sigma vel, \sigma att$ are the bias of the gyroscope, the accelerometer and the observed attitude respectively.

Table 3.5: KFGD Internal State Parameters

Q_d	$I(4)\|\|\sigma gyro\|\|\Delta t$
R_d	$I(4)\|\|\sigma vel\|\|^2$
P	$I(4)\|\|\sigma att\|\|^2$
H	$I(4)$

3.4 Data Collection

3.4.1 Experiment Scenario - Early Stage Rehab Exercise

The rehabilitation is grouped into stages: first, heal the damage tissue and then progressively build muscle strength and endurance and finally adapt the tissue to functional exercises. Mobility exercises focus on restoring range of motion without putting too much stress on the injury. Since the focus is on the early recovery stage, mobility and early strengthening exercises are thus chosen. They are well-suited for not only early recovery stage of sport injuries, but also activity for elders.

Human primary activities (such as walking, running, jumping, climbing, etc) usually put pressure on the knees for stable support. As a result, knee injury commonly occurs in all ages and genders [113]. In this thesis, the focus is on two knee recovery exercises: Leg Extension and Sit-Stand.

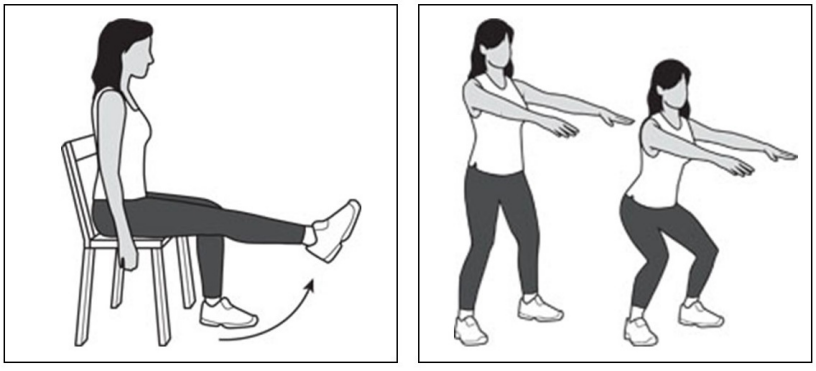

Figure 3.7: Knee Rehabilitation Exercises [12, 13]

Table 3.6: Leg Extension Exercise

Resting Position	Sit on the chair where the thigh and shank form 90 degree in the sagittal plane
Procedure	1. Raise the monitored leg as much as possible until the shank and thigh max out at the same level (normal knee extension). The leg raising takes place within a count of 5s. 2. Squeeze the thigh muscle and hold. 3. Relax the monitored leg to rest position within a count of 5s. 4. Rest. (Repeat x3)
Caution	No forceful swing momentum to lift the leg higher
Assumption	The thigh is kept as still as possible as at the rest position.

After knee injury or surgery, a patient may not be able to straighten the knee to its full range. Hence, early stage rehabilitation exercise such as Leg Extension, is used to regain the full knee extension. This exercise (Figure 3.7-A) targets the quadriceps [12]. In the panel on the right, Sit-Stand (Figure 3.7-B) set is a simple exercise that concentrates on quadriceps. It helps the patient to maintain quad strength.

Since the main focus is to produce accurate estimates for lower limb orientation in early stage rehabilitation, especially knee-related recovery, only the "Leg Extension" mobility exercise and early stage strength restoration exercise "Sit-Stand" are used.

- **Leg Extension**: Table 3.6 summarises the data collection procedure. The motion is monitored by attaching XSENS and smartphones to the sides of shank in the different experiments.

- **Sit Stand**: Table 3.7 explains the exercise procedures. The XSENS and smartphones are respectively attached to the sides of the thigh near the knee cap. It is assumed that the main motion is the thigh while the shank is kept still while performing the experiment.

Table 3.7: Sit-Stand Exercise

Resting Position	Sit on the chair where the thigh and shank form 90 degree in the sagittal plane
Procedure	1. In a slow and controlled manner and counting to 5s, the subject moves from the sitting to the standing position. 2. Stand 3. The subject, counting to 5s, sits back down at the rest position. (Repeat x3)
Caution	Ensure the knee does not fall inward (i.e. no twist or swing)
Assumption	The thigh is kept as still as possible as at the rest position.

3.4.2 Equipment Setup

During data collection, the exercise sets are performed by 5 participants. Each exercise is repeated 6 times for each device. For example, each participant repeats exercise 1 on 2 different devices: iPhone and XSENS, then Samsung and XSENS. Exercise 1 will be repeated 6 times for each pair of devices. Likewise for exercise set 2.

Smartphones (iPhone6 and Samsung Galaxy S7) and XSENS are placed at the sides of the leg. The data is collected using the custom-made application shown in Figure 3.8. The placement ensures that the smartphones and XSENS are aligned to the body segment (Figure 3.2). They are either fixed on the thigh (Sit-Stand) or the shank (Leg Extension). For the Setup Stage, the participant remains in the rest position for 15s before moving onto the Measurement Stage where they proceed with the exercise sets.

The results of the orientation estimation are compared using the off-the-shelf motion tracking system XSENS Anwida. Raw data are logged using the implemented data-collector app of the smartphones. It is then transferred to the host computer for analysis. XSENS sensor is attached to the lower limb by stretchables and placed at the opposite side from the smartphones. The placement of XSENS and the smartphones

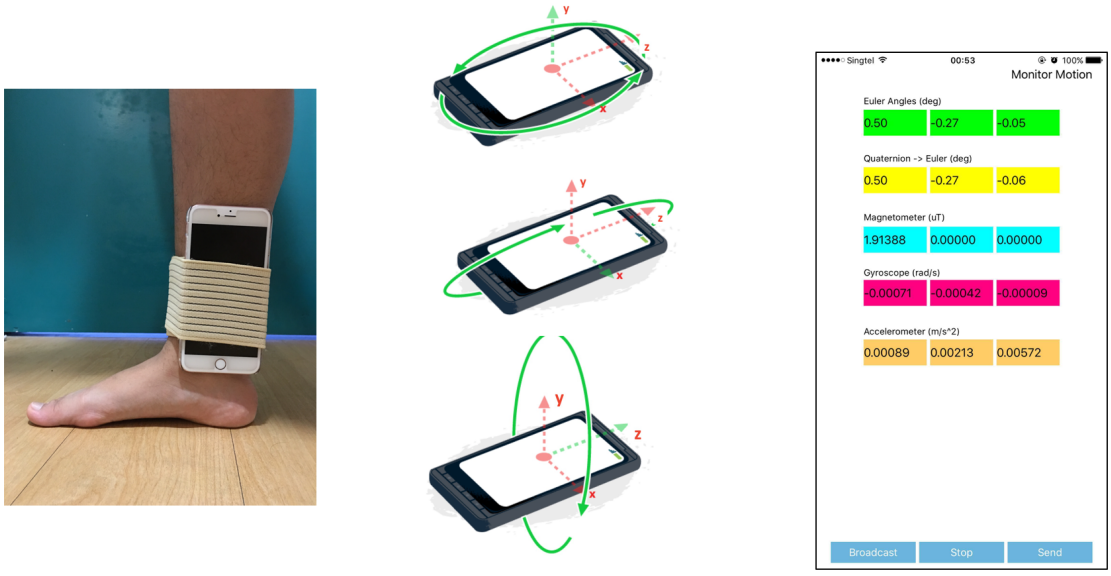

Figure 3.8: Mobile Application for Data Collection

is being alternated on the two sides of the lower limb when the exercises are repeated to stem out any placement bias.

3.4.3 Evaluation Methods

The algorithms[2] used for the performance comparison are carefully selected for their adaptive characteristic so that it would be able to monitor movements in real-time. Their abbreviations are used to discuss their performance. Table 3.8 specifies the parameters of the filters. The pre-defined values of Singapores Gravity ($g = 9.71m/s^2$) and sampling rate (Δt for 100Hz sampling rate) are set based on the geographical and the case-study settings of the data. While β is based on the Madgwick Filter specification [74], θ , $\sigma gyro$, σvel and σatt are identified are identified from observing the sensors biases via empirical approach as explained in Sections 3.2 and 3.3. Since the

[2]Among all, an additional algorithm, DCM based attitude estimation [114], has been implemented for comparison. However, it is excluded in the results of this thesis because of data incompatibility which will be unfair to DCM. DCM attitude estimate uses temperature and Kubo robotic arm data for calibration while our experiments only use XSENS and IMUs data.

Table 3.8: Filters' Setting

Symbol	Description	Value
g	Gravity (Singapore)	$9.71 m/s^2$
Δt	Sampling rate	$0.01 s$
β	Madgwick's	0.10
θ	CFF threshold	$0.80 s$
$\sigma gyro$	KFGD gyroscope processed noise	$0.01 rad/s$
σvel	KFGD accelerometer processed noise	$0.01 m/s^2$
σatt	KFGD attitude processed noise	$0.017 rad$

behavior during movement and accuracy of the movement's amplitude are important, a post processing step has been added to synchronize the beginning offset of both XSENS as well as the various filters.

- **XSENS Awinda (XSENS)**

  In comparison, the processed data is taken from XSENS Awinda (Section 3.1.2). The data is logged at 100Hz frequency. As the placement of XSENS is at the opposite side of the mobile phone, the Y and Z axis are flipped during comparison.

- **Complementary Filter + Feedback (CFF)**

  CFF's implementation is detailed in section 3.2. It does not incorporate Gradient Descent method to minimize errors nor involves the Setup Stage since it is a simplified implementation.

- **Madgwick Filter (MW)**

  [74] formulated the attitude estimation problem by combining the accelerometer and magnetometer data and solving it with gradient techniques. Unlike the proposed KFGD, MW [3] uses attitude estimate to correct the gyroscope data before it is integrated. Madgwick Filter has been tested with both high-end and

[3] It has been frequently used for comparison with newly proposed method, in particular, DCM based attitude estimation [114]. However, DCM estimate uses only gyroscope and accelerometer data for estimation.

affordable sensors. As it has been tested on smartphones which have noisy sensor data, it serves as an appropriate benchmark against which the performance of the filters proposed in this thesis. It is to be noted that the method works best in the presence of magnetometer [115]. Therefore, MW with the presence of magnetometer will be used to process experiment results.

- **Gradient Descent with Kalman Filter (KFGD)**
  KFGD is the complete implementation of Quaternion-based Kalman Filter with Quaternion-based formulation, as introduced in Section 3.3.

3.5 Experiment Results and Comparisons

3.5.1 Leg Extension

Experiment results in Figure 3.9 to Figure 3.11 illustrate the Euler angles of Leg Extension in series of moving (shaded Grey) and resting phrases. Android and iPhone processed data are denoted as subplots A and B respectively. In addition, the deviation measurements (with XSENS as the reference) are highlighted in subplots C and D.

Flexion/Extension rotation (Figure 3.9) is the main tracking angle while performing the Knee Extension exercise. Figure 3.9 shows that all filters produce results close to XSENS' for both mobile phones. Interestingly, for the Android phone, CFF tracks XESNS closely (Figure 3.9-C). This is due to the fact that beyond gyroscope data, gravity is present and the change can be sensed clearly, especially in the Sagittal plane (for Flexion/Extension rotation). CFF gives the best result because of its ability to adapt well due to the trust weight parameter (θ) which leans it toward accelerometer fusion instead of the gyroscope.

Another issue noted from the figure using iPhone data is the slight lags of MW at

the beginning of movement [19s-20.5s] (Figure 3.9-B and Fig3.9-D). On the other hand, KFGD ramps up to XSENS fairly quickly [19s-20s] while CFF is quickest at tracking XSENS.

Among the three axes (Figure 3.9 - Figure 3.11), it can be observed that the filters fall short of catching up with XSENS in the Sagittal plane (Figure 3.9). Not only are CFF and KFGD affected but also MW, in particular, for the iPhone data. These results do show a shortcoming of using mobile phones as sensors[4] where the filters could not measure up to XSENS' trend.

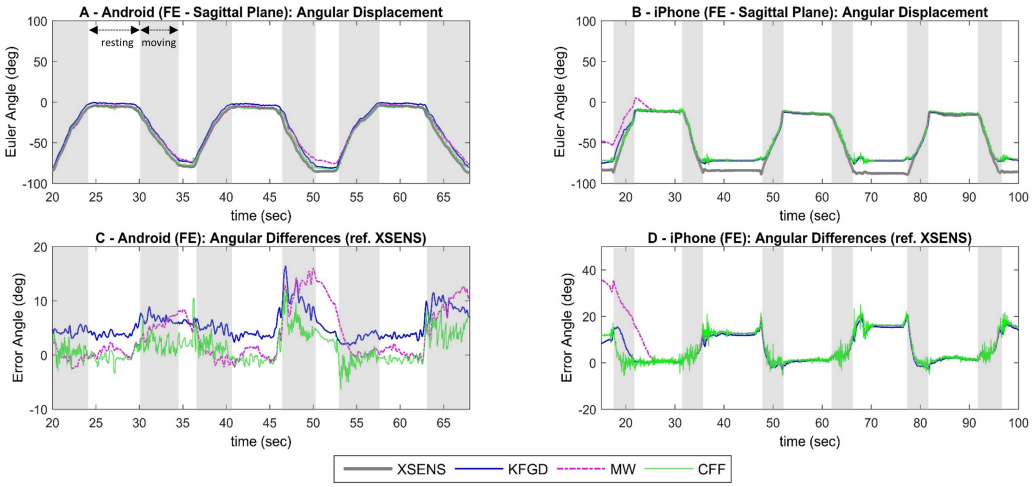

Figure 3.9: Flexion/Extension Rotation - Leg Extension

Pertaining to XSENS, it is to be noted that during the internal/external rotation in the Transverse plane (Figure 3.10-A and Figure 3.10-B), KFGD adapts best compared to MW and CFF. It is especially so during the moving state, specifically at the downward trend toward the resting state. Figure 3.10-C shows that KFGD has the least variation compared to XSENS for the Android Phone. Although, Figure 3.10-B and Figure 3.10-D show that KFGD, MW and CFF all show comparable trends, at moving states [17s-22s], [32s-37s], [47s-52s], [61s-66s], [77s-82s] and [93s-98s], KFGD

[4]The results using XSENS data are identical to what XSENS provided.

still yields the best result in terms of being closest to that of XSENS.

Another point to note is that CFF appears to ramp up before all the other filters (KFGD and MW) and XSENS (Figure 3.10-A). Although this may be reasonable given that CFF reacts fast to the movement, however it is not deemed as CFF is being more sensitive in tracking movement. In fact, it is considered worse than the others as from observation, when the movement is continuously going up or down, the rotations of other axes (IE and AA) are supposed to change at the minimum. However, CFF shoots up higher than MW and KFGD which can be attributed to the residual from the magnetometer as it would change the direction when the leg is raised. The case (Figure 3.10-D) differs when there is more prominent raise-and-hold stage rather than continuous movement as the former will hold at a certain angle for some time.

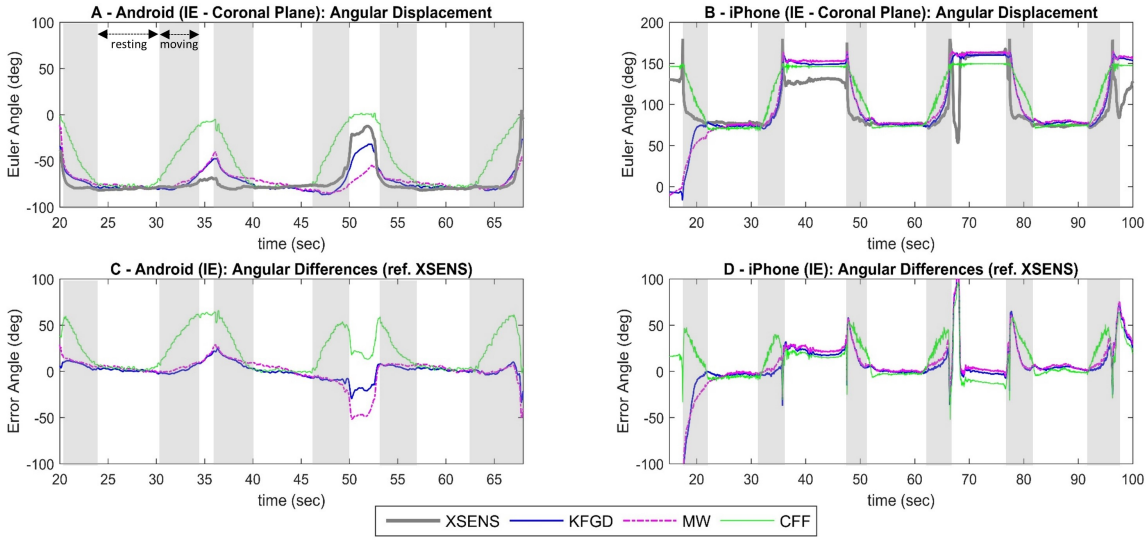

Figure 3.10: Internal/External Rotation - Leg Extension

The trend continues in the Coronal plane that tracks Abduction/Adduction rotation (Figure 3.11-A and Figure 3.11-B). The lag from MW is more prominent while it still comforms to XSENS' trend. Considering the moving phases (shaded Grey), KFGD remains at the top as it attains the desired trend using the least time to adapt.

CFF resumes the stable stage faster than the rest but tends towards the opposite direction (Figure 3.11-A). For iPhone data in Figure 3.11-B, KFGD and MW are comparable with XSENS while CFF somewhat 'amplifies' above the trends. This shows that exploiting Accelerometer and Magnetometer fusion, though inexpensive, does have shortcoming.

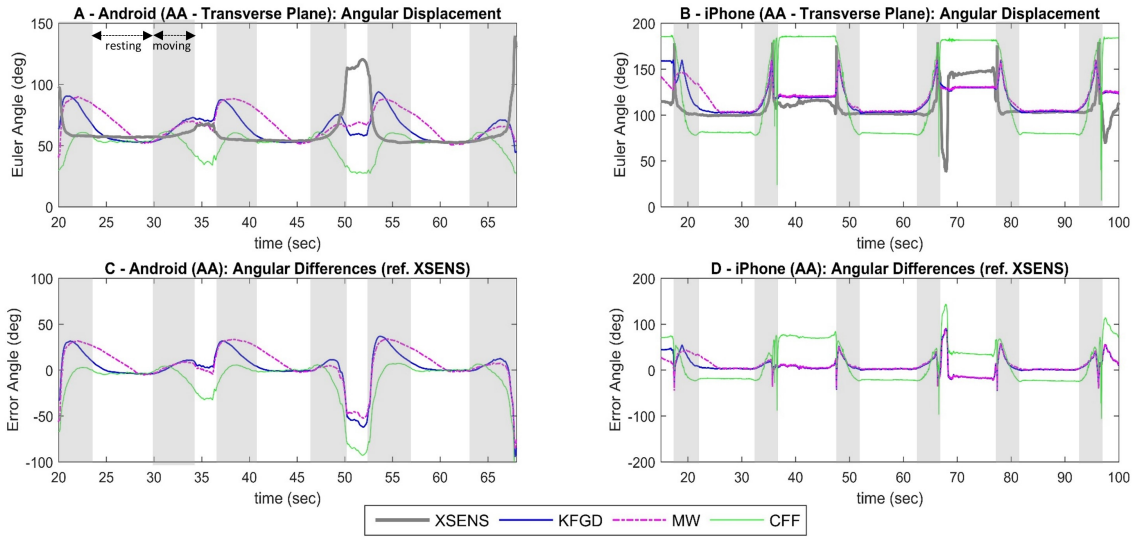

Figure 3.11: Abduction/Adduction - Leg Extension

3.5.2 Sit Stand

Figure 3.12 to Figure 3.14 represent rotation angles while performing Sit Stand exercise, engaging the quadriceps. During Flexion/Extension rotation (Figure 3.12), KFGD, MW and CFF have almost identical output compared to XSENS despite a difference of about 5 degrees (iPhone) or less (Android) at the rest-and-hold stage.

In this experiment, KFGD achieves remarkable result compared to MW and CFF. Its performance follows the characteristic of Kalman Filter by first slowly damping the fused signal and finally showing the same result as XSENS.

Notably, the trend in Android highlights the decisive performance of KFGD, using

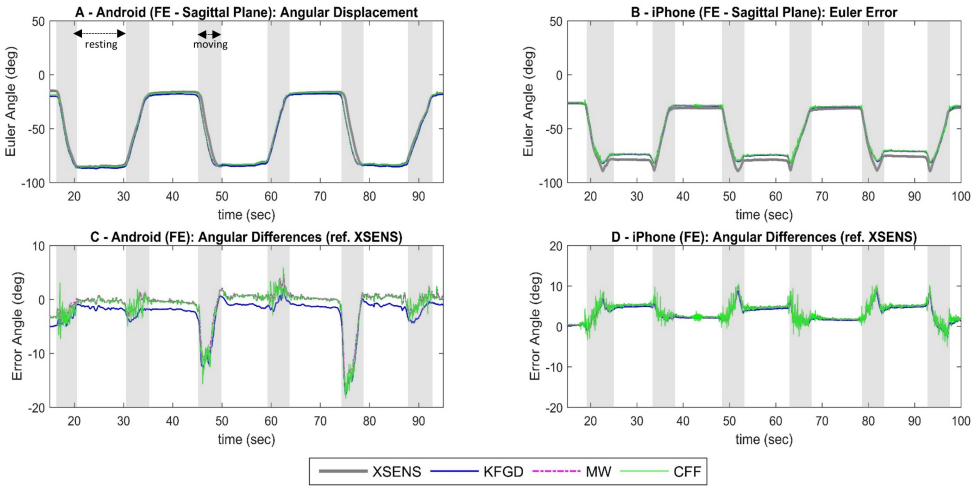

Figure 3.12: Flexion/Extension Rotation - Sit Stand

mobile phone data, where it closely tracks XSENS' (Figure 3.13 and Figure 3.14). Deviation of KFGD's data is almost zero while MW and CFF struggle with their specific offsets. CFF's inclination of its trust toward the Accelerometer and Magnetometer results instead of the gyroscope data to gain in computational efficiency and swift transformation to fit the trend results in the offsets. This shortcoming of CFF can also be seen in the trend in Android shown in Figure 3.13 and Figure 3.14. CFF rises above the expected XSENS due to th ecorrupting accelerometer and magnetometer data that results in the overcorrection of the processed data, ending in a bigger leap. KFGD adaptively fuses the gyroscope and attitude angles using Kalman Gain. Thus, KFGD gives more consistent and satisfactory result relative to MW and CFF.

It can be concluded that CFF is fast, lightweight and better when there are holding intervals in between movements. KFGD, although slighlty slower, is all-rounded in terms of its adaptation during movement and held up to the expected orientations.

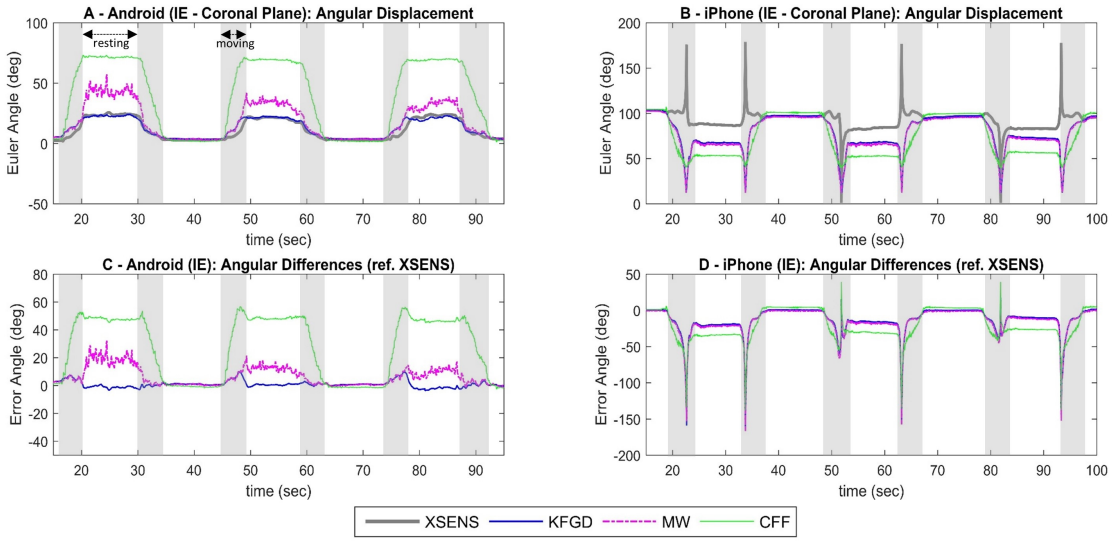

Figure 3.13: Internal/External Rotation - Sit Stand

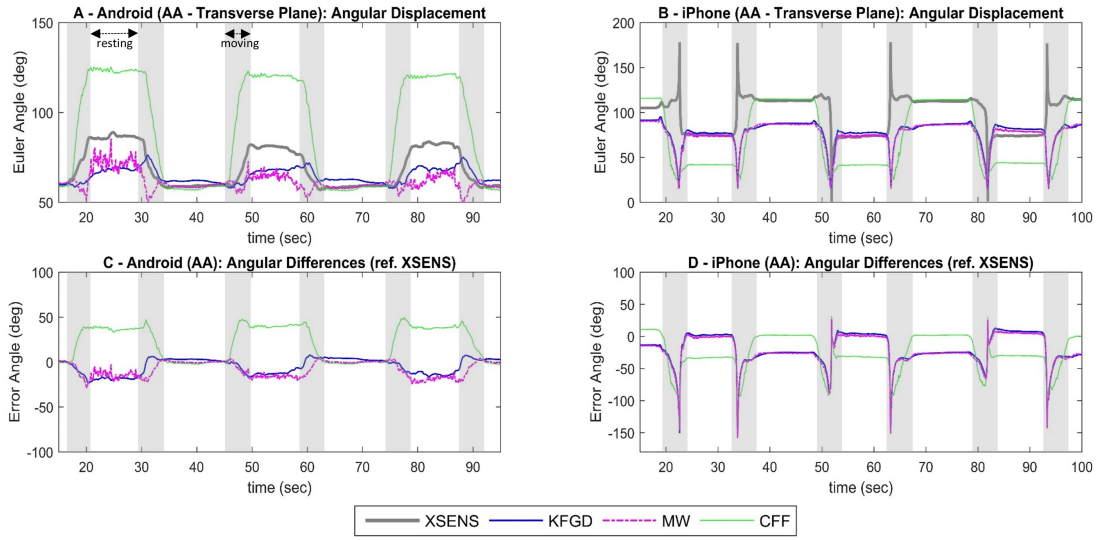

Figure 3.14: Abduction/Adduction Rotation - Sit Stand

3.6 Discussion

Overall, the output trend of Leg Extension exercise appears to oscillate more compared to Sit-Stand exercise. The reason is due to the freedom of limb movement. During Leg Extension exercise, it is tempting for the participants to flick their shank

up which results in shakiness. Although the movement is confined to 5s, twisting (Internal/External rotation) and shaking to the side (Abduction/Adduction) are bound to be present. On the contrary, Sit-Stand exercise focuses on the movement of the thigh and thus the patient has relatively more control in keeping the shank still. As a result, there is less fluctuation.

It can be concluded from the experimental results that by using our proposed CFF and KFGD, smartphones like iPhone and Android can be used for orientation estimation and on the whole, the results are close to that of the expensive, purpose-built XSENS. CFF catches up well with XSENS while its data relies more on the accelerometer and magnetometer fusion. The proposed feedback loop from the orientation estimates in CFF has been proven to be able to correct for the drift resulting from the integration of the gyroscope's data. As a result, in every iteration, CFF does not present any drift trend in the output. However, because the threshold theta is fixed, there is no way to adjust the trust weight parameter between the accelerometer/magnetometer and the gyroscope. This means exploiting Accelerometer and Magnetometer fusion does have a shortcoming despite the computational efficiency and fast response. This also means when more reliance is placed on attitude fusion (Accelerometer and Magnetometer), once it overshoots, it is hard to bring it back to the intended angles. Hence, in some cases, the gyroscope data could not bring the estimation result back to the desired inclination, leaving the accelerometer and magnetometer to incorrectly amplify the results.

For more sensitive and purpose-built sensors such as XSENS, MW performs comparably with KFGD. MW generally demonstrates good performance and is able to damp its initialization to a stable trend without calibration. However, with noisier and less sensitive sensors such as multipurpose iPhone and Android smartphones, MW takes longer to adapt to the expected trend.

The proposed KFGD aims to enable multipurpose smartphones to perform orientation estimation instead of using expensive, purpose-built sensors like XSENS. KFGD adaptively adjusts the trusting weight parameter to place emphasis either on the raw accelerometer and magnetometer data or the gyroscope data opportunistically. KFGD has outperformed MW in all experiments. In bio-feedback or motion monitoring for early stage rehabilitation, KFGD is actually a best fit as it ensures the correct orientation estimate and adapts well to the expected movement (with reference to XSENS).

The experiments have also proven that the correct placement and orientation of smartphone sensors to avoid gimbal lock has a positive impact and it prevents fluctuation in the estimate after the conversion from quaternion. Therefore, device orientation should be based on the hierarchy of Euler angles as in the middle axis of the Euler gimbal must map to the body segments such that it does not rotate to 90 degree often. In our exercise sets, the abduction/adduction rotation applies i.e. only sideway swings which is less than 90 degrees for early rehabilitation

3.7 Conclusion

This chapter has presented two fusion algorithms: complementary Filter Feedback (CFF) and Gradient Descent on Quaternion-Based Kalman Filter (KFGD). The goal is to obtain drift-free 3D orientation estimate for early stage rehabilitation. Experiments have been conducted on two exercise sets: Sit-Stand and Leg Extension with 5 participants. The two algorithms have been shown to control the drift well and produce accurate result compared to the ground truth from XSENS. A comparative evaluation shows that CFF effectively corrects the drift trend while KFGD outperforms Madgwick (MW) and adapts well to the reference from XSENS with KFGD being the best in performance. With smartphone sensor data, KFGD ensures consistent outputs while

MW reacts sensitively to direction change. CFF has shown its potential in correcting drift by setting the trust weight in favour of the accelerometer and magnetometer data instead of gyrscope data. Its overall result is quite stable and converges to XSENS data.

Chapter 4

Automated Oscillation Detection and Correction of Fused Wearable Sensor Signals using Machine Learning

In this chapter, the oscillation of post filtered signal is being addressed by defining the basis of the oscillation as well as the motivation to correct the signal (Section 4.1). An oscillation detection model as well as the framework to combine with the sensor fusion is proposed (Section 4.2). In Section 4.3, the experiment setup and labelling of data are presented. [1] . The selection and performance of detection model are evaluated in Section 4.4.

[1]This chapter's work has been published in **Seanglidet Yean**, Bu Sung Lee, Chai Kiat Yeo, and Zhaomin Chen, "Automated Oscillation Detection and Correction of Fused Wearable Sensor Signals using Machine Learning ", 16th IEEE Wireless Telecommunications Symposium (WTS), Phoenix, USA, 2018.

4.1 A Study on Post-Filter Orientation

4.1.1 Usage of Post-Filter Orientation

The post-filter orientation obtained from the wearable sensors are available for further analysis and interpretation to extract biomechanical parameters and physiological variables. They have been used in studies of motion analysis, motion tracking, Gait analysis, activity recognition that involves 3 dimensional motion data. These parameters support physiotherapists and other experts in their prognosis as well as assist patients in the recovery stage [116]. The analysis and accurate interpretation of the monitored data can thus be converted to readable reports to provide a new perspective and help in understanding the recovery process, providing biofeedback and progress monitoring.

In motion tracking, Euler angles are computed from the inertial sensor data using sensor fusion techniques [117] or are converted from the displacement of optical motion tracker coordinates [118]. The Euler angles conversion and processing techniques have since been discussed and improved. In recent years, motion tracker is able to output Euler angles ranging from commercial purpose-built wireless sensors such as XSENS Awinda [17] and Promove [119] to general purpose devices such as mobile phones and low-cost SensorTag development kits [120].

Euler angles are most commonly used in rotational coordinates due to its advantage of providing a more human readable data as it can distinctively show 3 dimensions of angle composition. It has been used in clinical report [121], visualization tool [34], kinematic analysis [122], activity recognition [123], rehabilitation [42], biofeedback [124] etc. Comparing with other conversion techniques and representation, Euler angle is irreplaceable, especially for the output's interpretation of a rigid body's orientation

over a fixed frame.

4.1.2 Observation of Oscillation

Regardless of the improvement in signal processing techniques in cleaning the processed data from the sensors, the output signal has a noticeable characteristic. While in motion, the Euler angle output would oscillate from positive to negative and vice versa. Periodically, the data stays at the opposite end and it differs from time to time. It is more pronounced in physical exercise when the rotation angle exceeds 85°. This oscillation has been noted in various studies [14–16] (Figure 4.1). However, this oscillation is often left unaddressed.

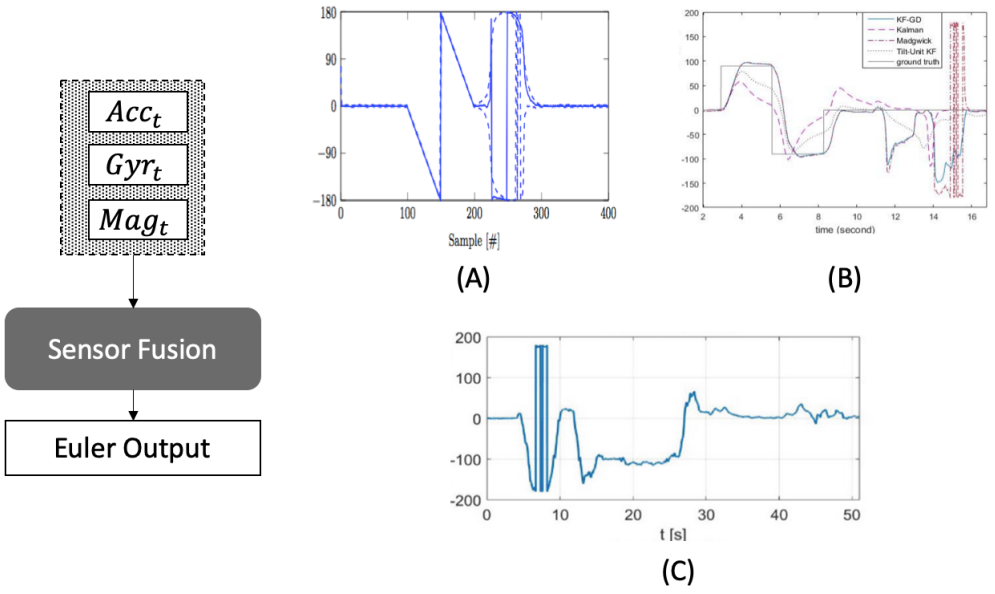

Figure 4.1: Oscillation in various studies (A- [14], B- [15], C- [16])

It is understood that the oscillation usually does not occur during a narrow range of motion such as during walking or running where the rotation angle would not exceed 50 degrees. However, during physical exercise such as leg-raise and sit-stand, the oscillations are more pronounced. The oscillation in Figure 4.1 is denoted as the

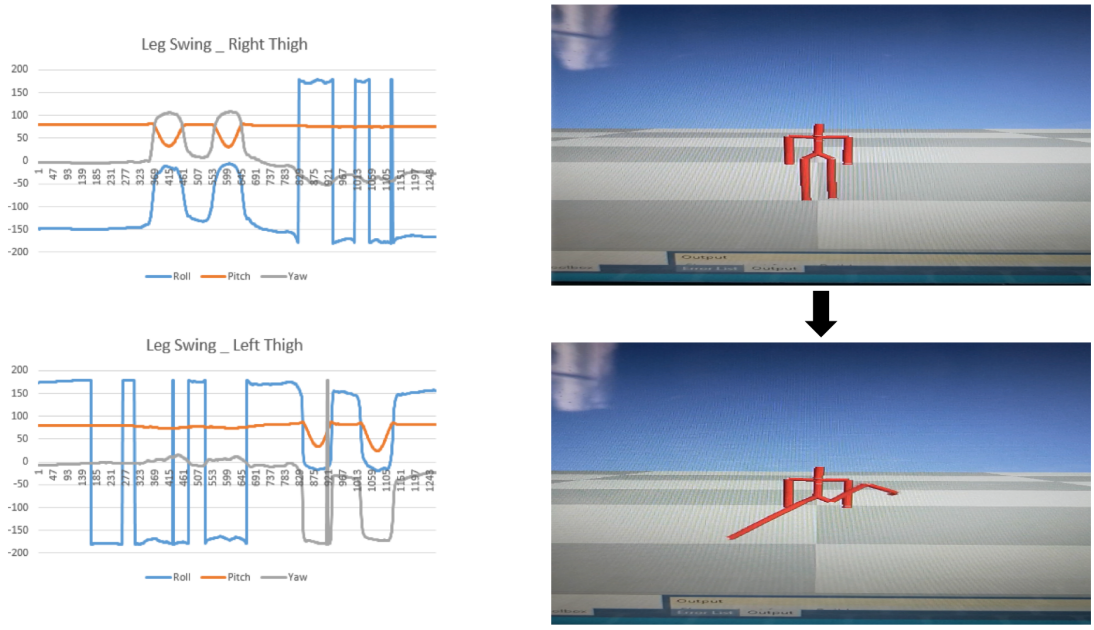

Figure 4.2: Example of Stick Figure Visualization with Oscillation

gimbal lock effect (explained in Section 3.1.3) by P.Musa et al. [125]. It is noted that the oscillation occurs inconsistently over time regardless of whether the pitch value approaches $85° - 90°$. The inconsistency could be caused by the instability from the minor vibrations in IMUs.

Figure 4.2 depicts the fact that digital representation and visualization are affected if the oscillation is left unaddressed. A fundamental solution is to convert from Euler angles to Quaternion representation. On the contrary, there is a number of analysis and applications that uses Euler angles mentioned in Section 4.1.1. Hence, the straightforward method to address such oscillations is to filter the outliers and noises offline by observing the output trend in consultation with a domain expert. Manual correction is time consuming and limits the application of such sensors since they cannot be used in real-time and home-friendly environments [126].

For this reason, this chapter explores the application of supervised-learning solution to automate the correction of post-filtered oscillation. The aim of this research is to de-

tect the oscillation from the signal data from wearable IMU sensors (i.e. accelerometer, magnetometer and gyroscope).

4.2 The Proposed Oscillation Detection Model and Correction Framework

4.2.1 System Overview

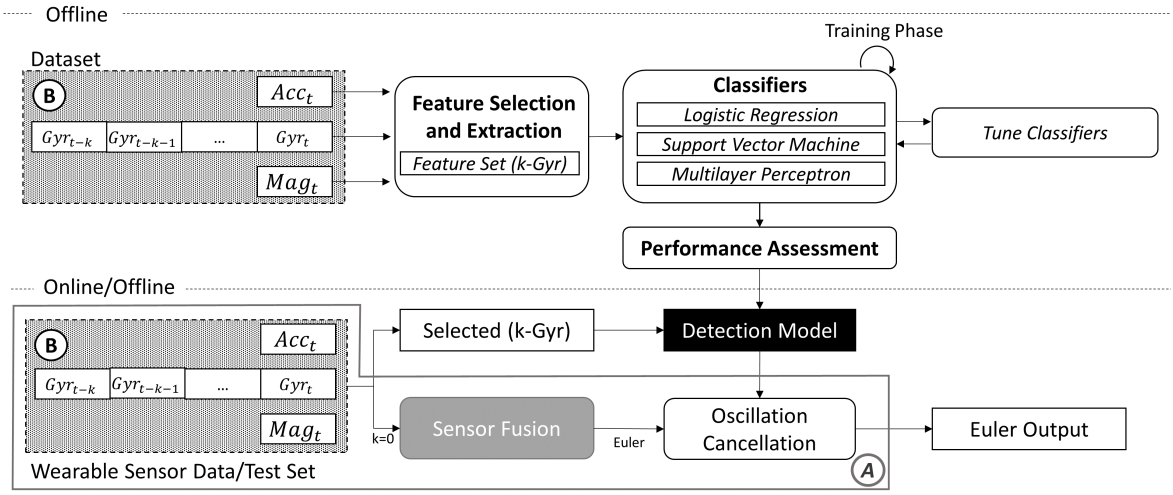

Figure 4.3: System Overview

A typical design of sensor fusion is to pre-process the signal from wearable sensors such as accelerometer, gyroscope and magnetometer. These input signals are then aggregated using sensor fusion methods [69, 74, 75, 126] in order to produce a clean and accurate orientation estimate (Figure 4.3-A). The system model of the sensor fusion methods typically exploit the sensor data characteristics and combine them via model representation such as quaternion, rotation matrix or Euler angles.

Figure 4.3 shows the framework of the proposed solution which trains a model to detect oscillation by analysing the input data. The procedure comprises two main

phases, offline training and online real-time sensor fusion.

The offline training phase aims to train the dataset to detect the oscillation automatically. The models obtained by this phase is being evaluated and chosen for the best performance in detecting the oscillation. In addition, the features are extracted from the sensor data by sampling accelerometer, magnetometer and gyroscope signals. The model's hyper parameters are being tuned during training with a set of pre-selected features. The performance assessment (Section 4.4.2) then selects the most suitable combination of features and classifier.

The online phase is the proposed framework for sensor fusion by incorporating the detection model to correct the oscillation. It is shown in Figure 4.3-A by adding the oscillation cancellation function after the sensor is fused. In other words, the trained model from the offline phase detects the likelihood of oscillation in parallel with the Euler outputs from the sensor fusion. Finally, the final output is the fusion output with the oscillation eliminated by the detection model.

4.2.2 Feature Combination

The input features for the detection model are extracted from the Accelerometer, Gyroscope and Magnetometer. The extraction of the motion signals as input signals is due to the fact that the oscillation is the product of the sensors combination and using Euler Angle as the output.

Figure 4.3-B illustrates the input features for the detection model. The accelerometer and magnetometer computed Euler angles are termed as instant attitude by P.Zhou [19]. Instant attitude is so named because its angles can be computed independently at any instance of time. Hence, an instance (at time t) of the accelerometer and/or magnetometer is sufficient to contribute to the model's features. On the con-

trary, gyroscope produces angular velocity [66]. The angular displacement (Euler angle) is computed by accumulating over time. In other words, it is the integration of gyroscope data. Intuitively, in order to incorporate gyroscope data into the feature, more than one gyroscope instance (window of $[t-k, t]$) should be used. $k = 5, 10, 15, 20, ...$ refers to the number of instances thus controlling how much history of the gyroscope data is needed.

Thus, the purpose of feature selection is to study how best to extract and combine the raw signals (i.e. 3-axis accelerometer, 3-axis magnetometer and 3-axis gyroscope) for the Euler-oscillation elimination.

4.2.3 Training Classifiers

Choosing the most suitable classifier impacts the performance of the whole system. Combining with feature selection, the decision is to choose the classification that yields higher performance at a lower computational complexity. In this thesis, the performance of several classifiers will be evaluated in order to recommend the most suitable classifier with the chosen features.

Logistic Regression, Support Vector Machine (SVM) and Multilayer Perceptron (MLP) are fundamental and are widely used in multiple areas pertaining to pattern recognition of motion data. In recent years, their popularity has risen in the areas of pose estimate, Gait analysis, activity recognition, automated assessment, etc. In particular, Kianifar, R. [86] explored the common classifiers such as SVM and LR to detect the squat quality and risk of knee injury using IMU data. Neural networks, for instance MLP, are known for Gait analysis dynamics and activity recognition [89]. A.C. Lapham et. al. [127] and SR Simon [91] discussed the potential of using neural networks in Gait analysis. Open issues include length "Gait" report and difficulty in

interpreting the captured data.

Logistic Regression, Support Vector Machine, Multilayer Perceptron are chosen to deal with the motion captured data.

4.2.3.1 Logistic Regression (LR)

Logistic Regression, or Linear Classifier, uses linear function (eq. 4.1) for prediction where thedependent variable (DV) is categorical [128]. The weight (W) and bias (b) are trained to predict logits (y). Softmax function is applied to convert logits to the probability of each class.

$$\begin{aligned} &Wx + b = y \rightarrow S(y = c) \rightarrow Y \\ &S(y = c) = \frac{e^{\beta_c \cdot \mathbf{x}}}{\sum\limits_{h} e^{\beta_h \cdot \mathbf{x}}} \end{aligned} \tag{4.1}$$

Owing to the fact that oscillation is labeled as fluctuated state (1) or stable state (0), Logistic Regression is adopted for the binary classification. For better performance, C parameter, representing the tradeoff between smooth boundary and training points, is adjusted.

4.2.3.2 Support Vector Machine (SVM)

Support Vector Machine (SVM) classifier is one of the most prominent model to optimize maximal-margin hyperplane and discover underlying non-linear pattern [88]. In each iteration, computation on the training data is done to maximize the margin which is the distance of the closest data points (support vectors) to the hyperplane. The success of tuning Support Vector Classifier relies on Kernels and C parameters. C parameter controls the tradeoff between Smooth Decision Boundary and classified training points. Kernels, in SVM implementation, defines the similarity or a distance

measure between the new data and the support vectors. The types of kernels include Linear, Polynomial, Radial and Sigmoid Functions.

Radial Basis Function kernel (eq. 4.2) is chosen for comparison as it yields the best performance after prior experimenting and tuning against other kernels.

$$K(\mathbf{x}, \mathbf{x}') = \exp(-\gamma||\mathbf{x} - \mathbf{x}'||^2) \tag{4.2}$$

where $\mathbf{x}, \mathbf{x}'$ are two input feature vectors and γ is the parameter that determines how influential each training sample is to the model.

4.2.3.3 Multilayer Perceptron (MLP)

Multilayer Perceptron (MLP) represents a group of connected units in layers that predicts the outcome by feeding forward the input data into nonlinearly-activating neurons in hidden layers and output layer [129]. In this case, Rectified linear unit (ReLU) is used as the activation function (eq. 4.3). During training, it adapts to the external data at every step through back propagation. While updating the network's weights, stochastic gradient descent optimizer called Adam, is used [130].

$$f(x) = \begin{cases} 0 & \text{for} x < 0 \\ x & \text{for} x \geq 0 \end{cases} \tag{4.3}$$

The main difference between MLP and Logistic Regression is that MLP uses non-linear activation in each neuron (connected unit except input neuron) resulting in nonlinear perceptron. This non-linear capability of MLP has the potential to benefit this model because sensor-fused Euler angle is known to have a nonlinear association with its raw data [69].

4.3 Design of Data Collection

4.3.1 Experiment Setup

The data is collected by performing two early-stage rehabilitation exercises, in particular, Sit-Stand and Leg Extension (Section 3.4.1). The data is collected using XSENS Awinda. Due to XSENS sensor having a processing unit that produces clean Euler angles as output [131], the raw data and Euler angles are transmitted to the computer via a USB dock.

The wearable sensors are strapped on the shank (for Leg Extension exercise) and thigh (for Sit-Stand exercise) of a participant. The exercises are 2 to 3 minutes in duration and are repeated 5 times for each participant. To train the classification model, the dataset is randomly divided into a training set (70%) and a test set (30%). Scikit-learn [35], Python's module, is used to facilitate the implementation.

4.3.2 Case Studies and Labelling Oscillation

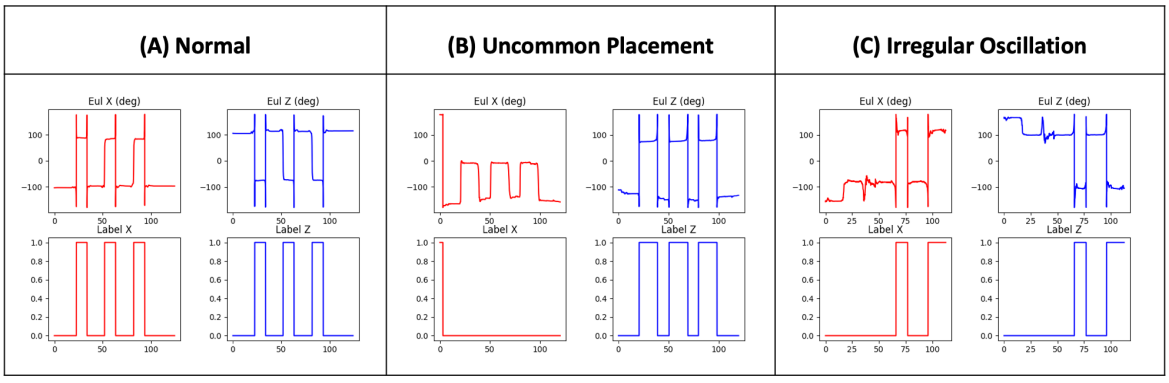

Figure 4.4: The Oscillation Case Studies

For a fair evaluation, the efficiency of the proposed detection model is compared with the manual method (Section 4.2). Figure 4.4 represents the selected test sets in

Table 4.1: Oscillation Labelling Description

Label	Description
1	when,there is oscillation occurred and while in the opposite direction.
0	when there is no effect from oscillation.

three categories:

- *Normal (Figure 4.4-A)* depicts the oscillation that takes place during the leg-raise and leg-drop movement
- *Irregular Oscillation Normal (Figure 4.4-C)* refers to unpredicted signals that occur at random.
- *Uncommon Placement (Figure 4.4-B)* refers to the test data that are collected when the tracking device is placed at the front and on the left side of the body segment. It is given that the normal placement of the tracking device is on the right side of the body segment.

For the supervised-learning training, the oscillation are labelled in binary class as described in Table 4.1.

4.4 Implementation Result and Discussion

4.4.1 MLP Architecture Performance

For Multilayer Perceptron, the crucial steps to obtain a good performance model are to find a suitable and balanced nested topology; to tune the hyper parameters and to avoid over-fitting.

The experiments are conducted to test the impact of the number of hidden layers and number of neurons on the performance. Figure 4.5 shows an apparent improve-

ment over the generic combination of H(15,3) neurons. While the y-axis depicts the prediction?s accuracy, the x-axis represents the case studies depicting the number of hidden layers as well as the number of neurons for each layer. For instance, H (15,10, 4) describes the meta-parameters of 3 hidden layers comprising 15, 10 and 4 neurons respectively. Precision-wise, the new accuracies of X and Z axes are (77.08%, 76.65%), (75.22%, 72.52%) and (71.55%, 75.33%) while using 0, 10, 15 gyroscope instances with MLP (Table 4.2) respectively. This result confirms that parameter tuning of MLP impacts the prediction.

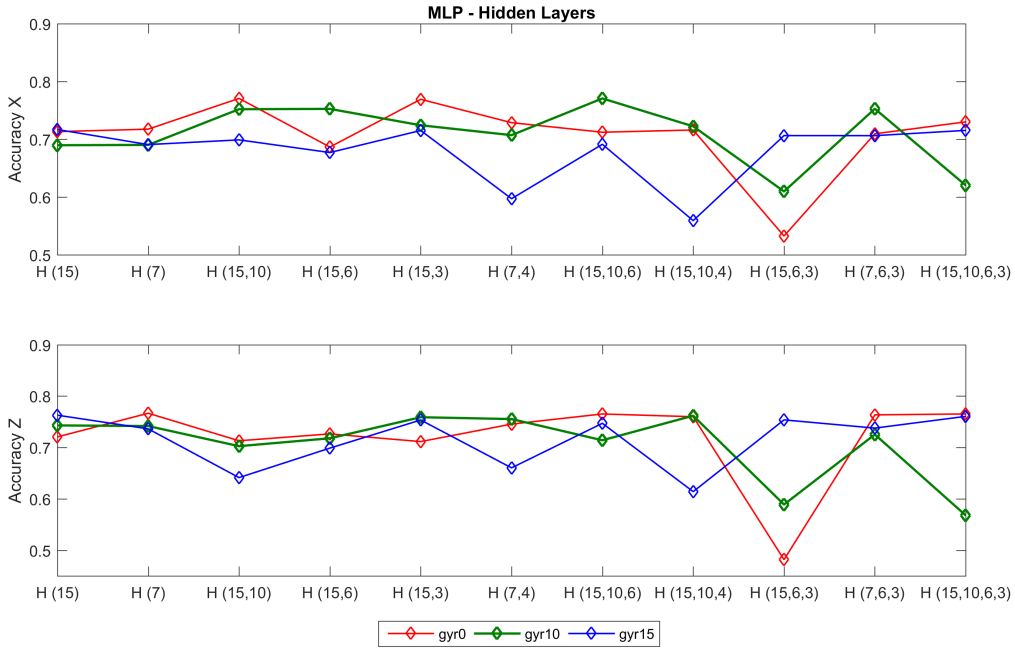

Figure 4.5: MLP - Hidden Layers

4.4.2 Input Features Performance

Figure 4.6 illustrates the general accuracy of the model with respect to the presence of the input signals (from the accelerometer, magnetometer and gyroscope). Furthermore, it is used to determine a sufficient window size for the gyroscope data. Since

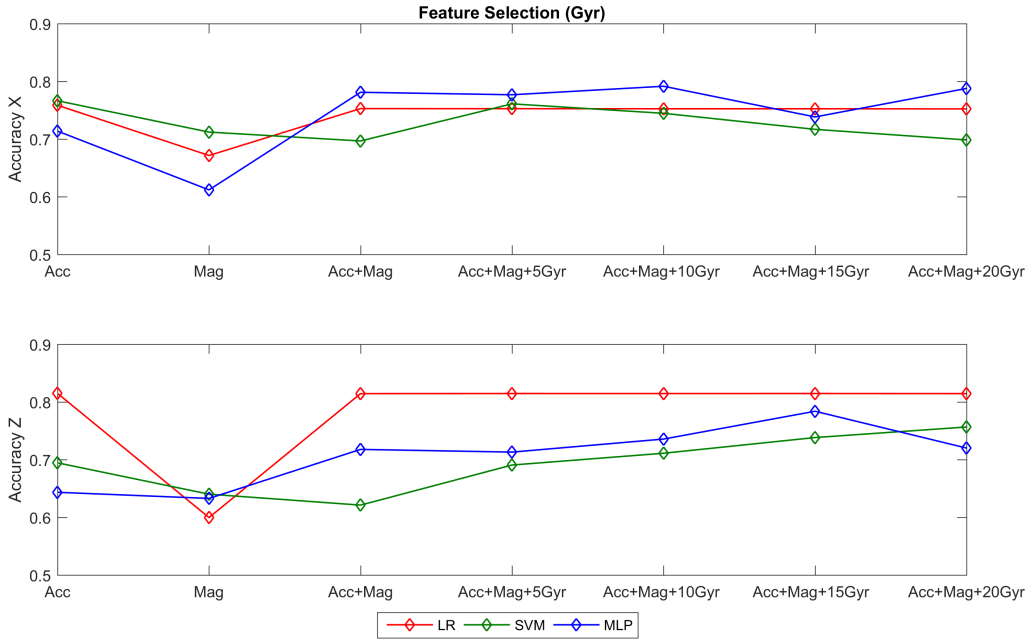

Figure 4.6: Feature Selection (Gyroscope)

the oscillation appears only in the X and Z axes, the accuracy of both axes are presented. LR and SVM have been tuned for this experiment while MLP uses a generic combination of 2 hidden layers with 15 and 3 hidden neurons each.

Pertaining to input features, LR creates a straight line regardless of the gyroscope instances being added. It could be deduced that gyroscope data does not contribute to LR's performance or oscillation detection much like accelerometer and magnetometer.

In contrast, SVM and MLP improve their accuracy upon the addition of rotational velocity (gyroscope data). Although SVM seems to be better with a bigger window size, it does not outperform LR and MLP. Therefore, SVM is shelved from further investigation. Since MLP peaks at 0 and 10 (Accuracy X) and 15 (Accuracy Z), these MLP combinations and LR will be added for the following investigation in Section 4.4.3.

Table 4.2: Selected Classifier Models

Model	Description
LR	Logistic Regression model uses Accelerometer and Magnetometer
MLP (Gyr 0)	MLP uses Accelerometer and Magnetometer. The chosen hidden layers are H(15,10) and H(7) respectively for X and Z axes
MLP (Gyr 10)	MLP uses 10 Gyroscope instances in addition to Accelerometer and Magnetometer. The chosen hidden layers are H(15,10) and H(7,6,3) respectively for X and Z axes
MLP (Gyr 15)	MLP uses 15 Gyroscope instances in addition to Accelerometer and Magnetometer. The chosen hidden layers are H(15,10,6,3) and H(15,3) respectively for X and Z axes

4.4.3 Selected Classification Performance

To analyze the results in details, the best performance models of MLP and LR are investigated. Table 4.2 describes the chosen classifiers and their features.

LR is usually preferred because its model parameters are interpretable and easy to use [128]. In Figure 4.7, LR is doing fairly well in general. The noticeable drop is in Test 4 and Test 6 which represent the untrained placement. That means LR is lightweight but its weakness shows while facing unfamiliar trend of the wearable sensor data.

In Section 4.4.2, it is observed that MLP (Gyr 0) and MLP (Gyr 15) have slightly higher accuracy than MLP (Gyr 10). Figure 4.7 shows that MLP (Gyr 0) and MLP (Gyr 15) are of comparable performance and their accuracies decrease in Test 6-8. Interestingly, MLP (Gyr 10) displays a more stable trend.

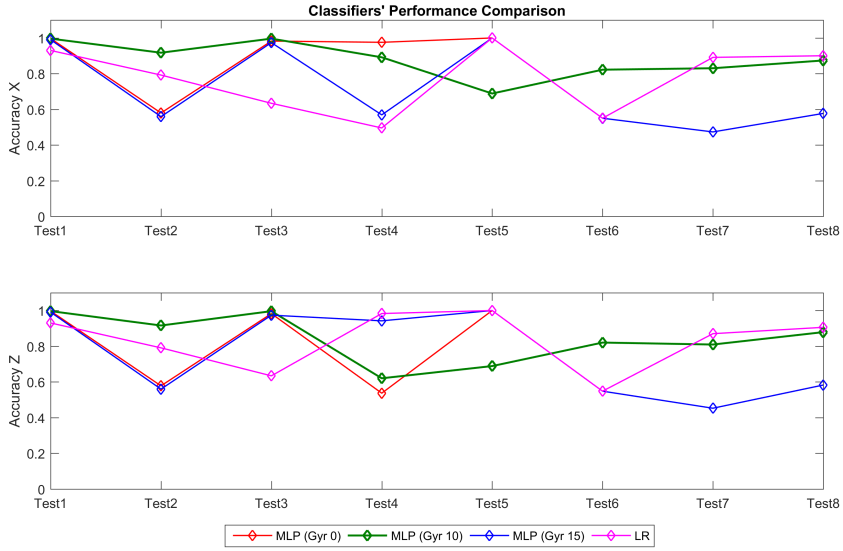

Figure 4.7: Classifiers' Performance on Test Sets

4.4.4 Discussion: Manual vs Detection Model

It is known that when oscillation occurs, it cannot be fully filtered unless it is plotted offline after the data is recorded. From observation, in order to avoid omitting useful information in real-time, the detection is set during the known movements. Thus, *manual* detection is indexed. The aims of this section are to assess the capability of classifiers MLP and LR and whether their predictions are able to identify the occurence of oscillations against the manually indexed oscillations denoted as *Manual* method.

The oscillations are often found as a result of continuous movement reaching above 85° because accelerometer and magnetometer are sensitive to direction. Figure 4.8-A shows that all methods are doing well. It proves that MLP and LR can measured up to *Manual*.

A more robust result shall determine whether MLP and LR are stable during placement and movement. Instead of placing the sensor at the right side of the lower limb, it is placed in front. Hence, the plotted signal in features would differ. All the methods

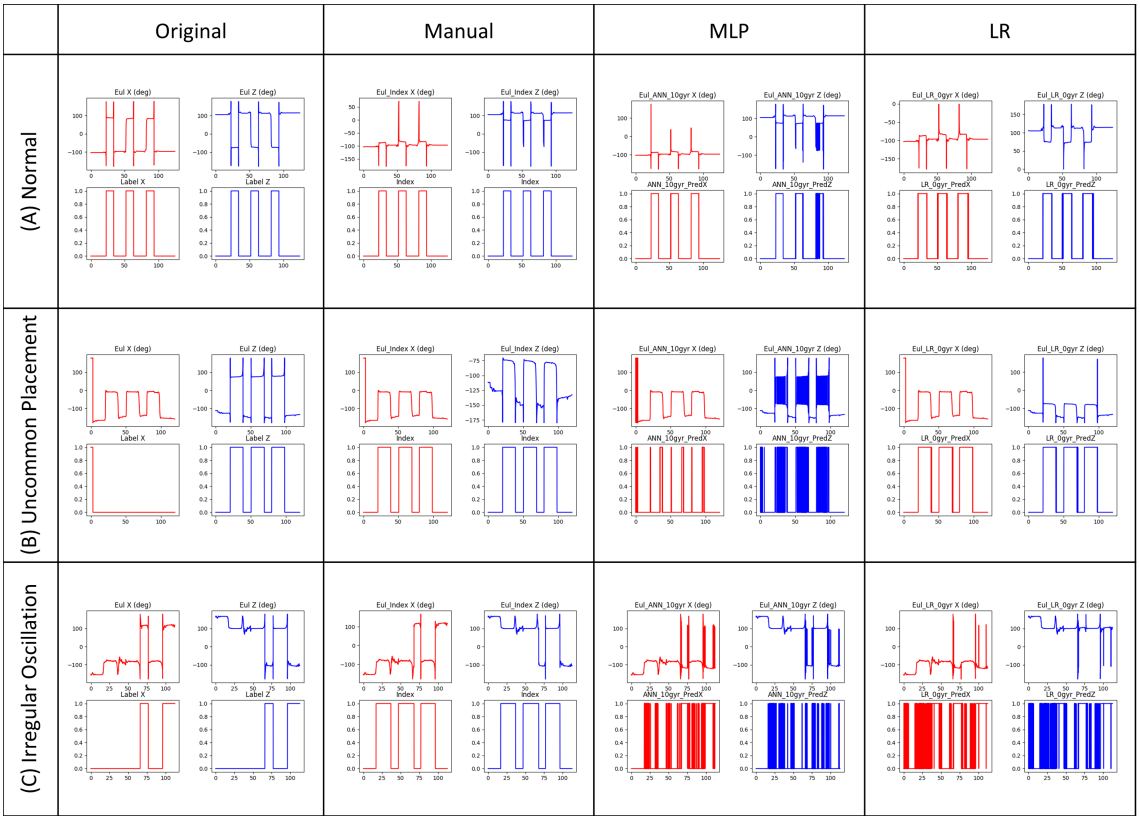

Figure 4.8: Comparison - Manual vs Classified Output

are able to clear the oscillation in the Z axis of Figure 4.8-B. Although MLP detection fluctuates, the output could be smoothened to match the result of LR. Originally, there should not be any detection as there is no oscillation in the X axis. For Logistic Regression (LR), X axis prediction resembles that of Z axis, resulting in misjudging the oscillation. MLP performs better in this case.

There are rare cases where oscillation does not occur during movement (Figure 4.8-C). It is understandable that *Manual* is not indexed to handle this occurrence and is unable to eliminate the oscillation. MLP and LR predict the fluctuation where LR has a better correction at Z axis. If prediction results are considered, MLP has a much cleaner detection. In other words, MLP detection is more precise as it does not fluctuate across the time-line.

All in all, the proposed model has been evaluated and proven that it has the capability and potential to post-filter the oscillations after sensor fusion. From this study, accelerometer, magnetometer and 10 instances of gyroscope are used as features for the MLP classifier to produce a generic and stable oscillation detection model for Knee Extension and Sit-Stand exercises. For devices with limited memory and processing power, Logistic Regression using only accelerometer and magnetometer is a more suitable model and straight forward while producing satisfying results.

4.5 Conclusions

This chapter discusses the issues of oscillation that occurs after sensor fusion of IMU sensors. The proposed supervised-learning detection model contributes in finding the automated solution to correct the fluctuated Euler angles. In other words, the main goal is to efficiently detect the oscillation and correct them without the presence of domain experts. A detailed study has been performed to draw conclusions on the impact of sensor data and the suitable classifier for the model. The feature selection ranges from incorporating accelerometer data to deciding the combination of gyroscope instance's window size. Classifiers such as Support Vector Machine (SVM), Logistic Regression (LR) and Multilayer Perceptron (MLP) have been used.

From the experimental results, the best combination of features are selected to train the model. It is found that only accelerometer and magnetometer play an important role in LR while adding instances of gyroscopes improves the accuracy of SVM and MLP. In fact, 10 instances of gyroscope (equivalent to 0.1 second window) contribute to the best performance of MLP. All in all, LR with accelerometer and magnetometer is capable of predicting and correcting the oscillation while MLP with accelerometer, magnetomer and 10 instances of gyroscope appears to be more stable but less accurate

overall.

In conclusion, this method has the potential to be used in real time to detect regular and irregular oscillations and remove them.

Chapter 5

Pattern Recognition for Rehabilitation Exercise Segmentation

This chapter provides realisation of home rehabilitation by proposing software tools for patients and physiotherapy. In Section 5.1, RehabPartner is a pilot mobile application developed to bring the IMU motion tracking algorithm (explained in Chapter 3) [1] to the patients and patient management for the physiotherapist. Aiming to obtain continuous qualitative feedback software, an intermediate exercise segmentation is proposed 5.4.4 [2] in Section 5.2 and following by the evaluation and discovery (Section 5.3) of features'

[1] This section's contribution has been published in Shao Loong Lim, **Seanglidet Yean**, Bu Sung Lee, and Chai Kiat Yeo, "RehabPartner: Motion Tracking Assistant Using a Novel Complementary Feedback Filter ", in IEEE Consumer Communications & Networking Conference (CCNC), Las Vegas, USA, 2018.

[2] This section's contribution have been published in **Seanglidet Yean**, Bu Sung Lee, and Chai Kiat Yeo, "Lower-limb Rehabilitation at Home: A Survey on Exercise Assessment and Initial Study on Exercise State Identification toward Biofeedback ", in International Journal of Interdisciplinary Telecommunications and Networking (IJITN), 2019.
The extended work been submitted to **Seanglidet Yean**, Bu Sung Lee, and Chai Kiat Yeo, "Feature Engineering and Pattern Recognition for Rehab Exercise Segmentation ", submitted to Sensors, 2019.

insight (Section 5.4).

5.1 RehabPartner: Motion Tracking Assistant for Home Rehab Exercise

5.1.1 Rehabilitation and Feedback Mobile Application

There is a rapid growth in mobile phone usage in both developing and developed countries. Therefore, to reach out to provide the healthcare services and health monitoring for larger group of the population, the healthcare-related program has shifted from face-to-face to the mobile application, called *mHealth*, under the tele-health umbrella. The trend of mHealth apps for lowerlimb rehabilitation has been booming to augment healthcare services globally. In fact, [132] reported that among mHealth apps in the field of rehabilitation, out of 104 applications developed, there are 14 and 11 apps created targeting stroke and musculoskeletal rehabilitation respectively.

Although many applications are developed with the objective to monitoring and feedback, they neither provide the tracking performance of the rehabilitation exercise nor intervention feedback. The existing application usually only shows users how to perform the exercises via video and keeps track of the repetition count or range of motion. For instance, *KneeDecide* [133] and *Pain Theraphy* [134] provide videos for rehabilitation exercises. *PT Pal Pro* [135] and *PT Timer* [136] offer exercise management and reminder. However, these applications do not consider the actual record of how user moves. *CMV* [137] makes use of image processing and produces on-the-spot instructions but it only applies for limited types of sports and it is not suitable for a more confined space like the home. The app that could track user progress is Ginometer [138], which measures a user's range of motion, detecting only flexion/extension

rotation angle.

5.1.2 RehabPartner 1.0

RehabPartner is an application that is designed to assist the elderly in rehabilitation exercises. It features functionalities that provide feedback as intervention to correcting movement during rehabilitation and tracking the progress of patients doing exercise at home.

5.1.2.1 System Overview

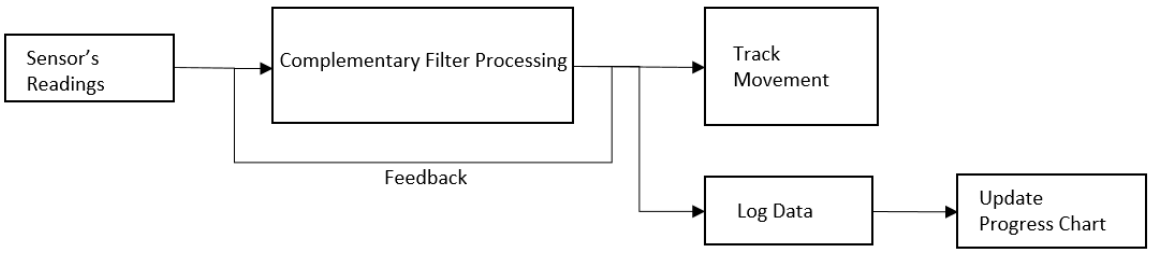

Figure 5.1: RehabPartner Application Overview

Figure 5.1 shows the overview of RehabPartner Application. The building blocks of this application can be broken down into four main modules: sensor readings, complementary filter feedback (CFF), logging of data and tracking of movement. Sensor readings refer to the three motion sensors found in smartphones, namely the accelerometer, magnetometer and gyroscope. The three sensors will provide readings and pass the readings to the complementary filter processing. RehabPartner uses the motion tracking algorithm, Complementary Filter Feedback (CFF) proposed in Chapter 3 to obtain the 3-dimension orientation of the phone. It then tracks the movement of the users during rehabilitation with the obtained orientation angle from the proposed CFF.

5.1.2.2 Application User Interface Design

Figure 5.2-A depicts a primitive menu of the app where users can track their progress and see how much improvements they have made in their rehabilitation exercises.

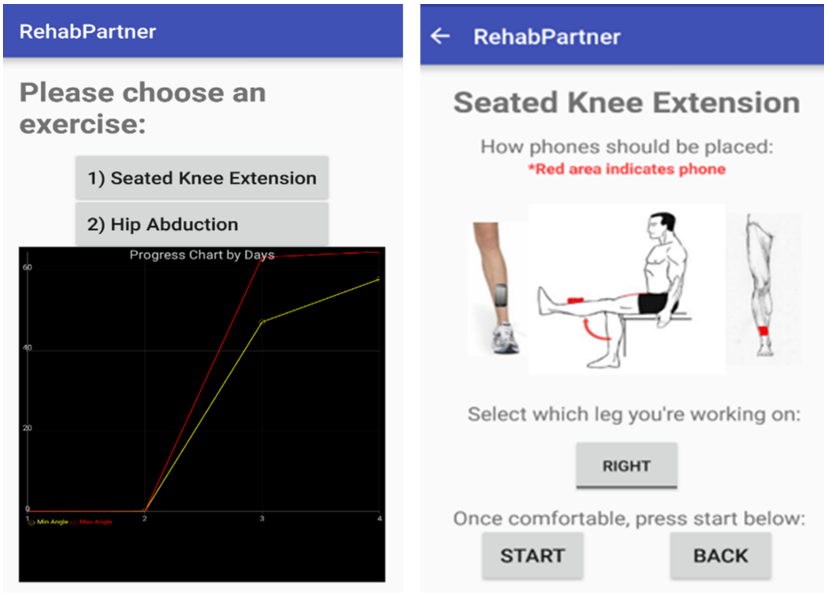

(A) Main Menu *(B) Selection Menu*

Figure 5.2: Application Menu

Figure 5.2-B shows a menu where users will be able to select which leg they are going to work on. It also illustrates how the exercises should be done and where the smartphone should be placed. After the user has clicked the start button, the appropriate steps and sequence for the exercise will be displayed as shown in Figure 5.3-A. In this page the number 2 shown in Figure 5.3-A refers to the command which goes to a timer showing the time spent in each action [start, up, down, hold]. The smartphone screen is duplicated on the TV so that the patient can follow the commands (Figure 5.3-B).

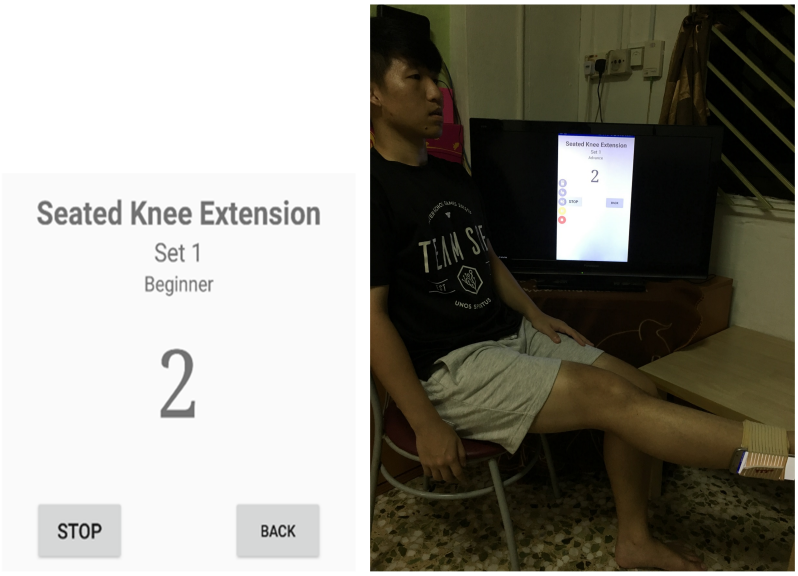

Figure 5.3: Application Exercise Interface

5.1.2.3 Implementation

The Rehab Menu background tasks consist of the four building blocks as described above, namely, collecting sensor readings, complementary filter processing, logging of data and tracking of movement.

Figure 5.4 shows the background tasks of RehabPage. A timer task will be initialized to run the complementary filter continuously. After the initial five seconds, it will set the initialisation readings which signals the synchronization of the user's body parts to the phone's readings at the starting point. In addition, the timer task ensures that certain tasks are being carried out; for example, tasks such as every five seconds, it will display a command such as Up, Down or Hold. This is to notify the user of what to do during the exercise. Up means raising of the leg as shown in Figure 5.3-A, Down refers to the lowering of the leg back to the initial position and Hold is to hold that position. During the Up process, it will detect the range of movements and any deviation from the intended movement made by the users. From past experience, the

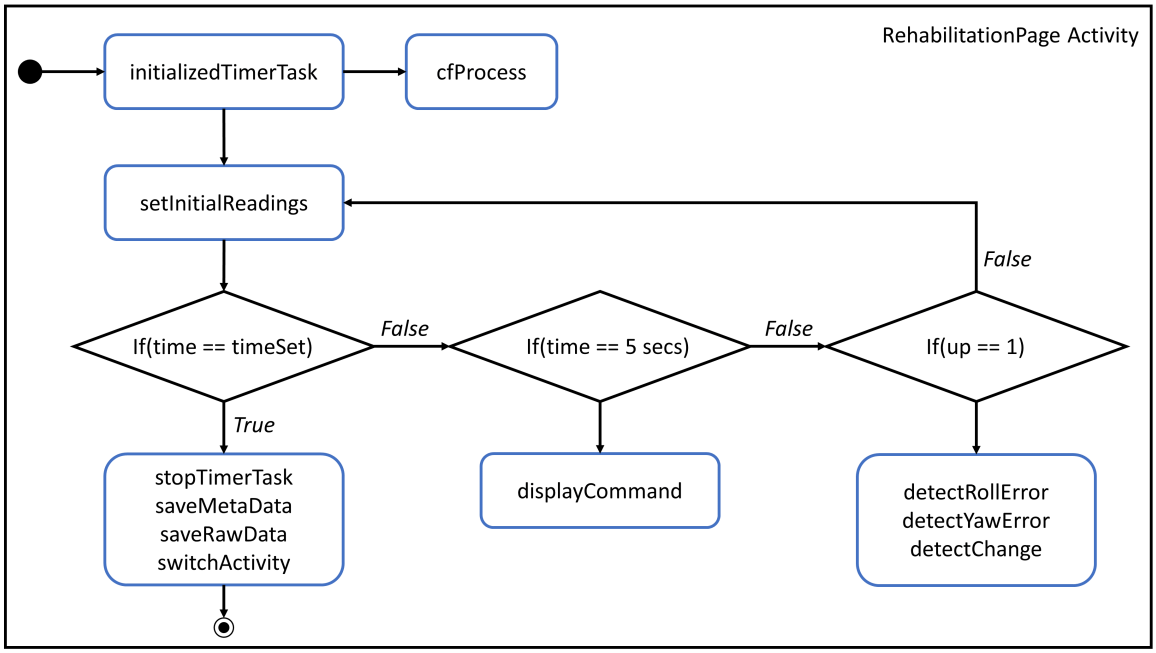

Figure 5.4: RehabPartner Flow Diagram

deviation threshold is predefined as $\pm 8^o$. In other words, if the movement is out of range by 8^o, it will be considered as an error and a beeping sound will be heard. All complementary filtered readings, raw sensor readings, range of movement and errors will be logged into two separate files. These files are used to analyse the patients' progress as well as the motion they are having difficulties with which are very useful for the therapist and the users.

5.1.2.4 Summary of RehabPartner

All in all, RehabPartner has been prototyped to demonstrate the practical use of motion tracking with home intervention. By obtaining the angle estimate, this application acts as a non-visual three-dimension motion tracking system. While exercising, commands are displayed and with the availability of smart TVs, this application could be projected on the TV screen which enhances visibility for the users. This makes the application

very applicable for community use. The prototype further highlights its ability to detect if there are any errors in the motion during the rehabilitation. The application produces sound beeps when errors are detected thereby informing the user in real-time of an incorrect movement.

It is to be noted that the pilot application was developed in collaboration with Shao Loong Lim [139]. RehabPartner 2.0 is the improved version by including a web-base application for the patient management, such as providing performance results and getting feedbacks from the physiotherapist. It is a collaboration with National Yunlin University of Science and Technology.

5.1.3 The Challenges of Continuous Augmenting Feedback to Lower Limb Motion Tracking

RehabPartner shows the potential of home exercise intervention while tracking the thigh or shank movement. It specifically tracks the information of limb's internal/external angle in order to raise the alert on whether the patient is over twisting their body segments. Beyond the threshold-setting, it may be feasible for an automated system that guides the patients at home continuously.

Figure 5.5 conceptualises the bridge between the advancement of hardware with the existing solutions where intermediate steps are needed to realise assistive home rehabilitation. In Section 2.3, exercise assessment is discussed extensively for the solution of continuous feedback in two categories: learning-based and rule-based.

Briefly, Rule-based approach uses a set of rules that is based on the perception of correct movement and posture. Hence, it is used to identify the correctness for the non-visual activity. Rule-based approach is commonly introduced for biofeedback [78, 81] as it is more robust to errors as compared to a prediction model and is easily extensible

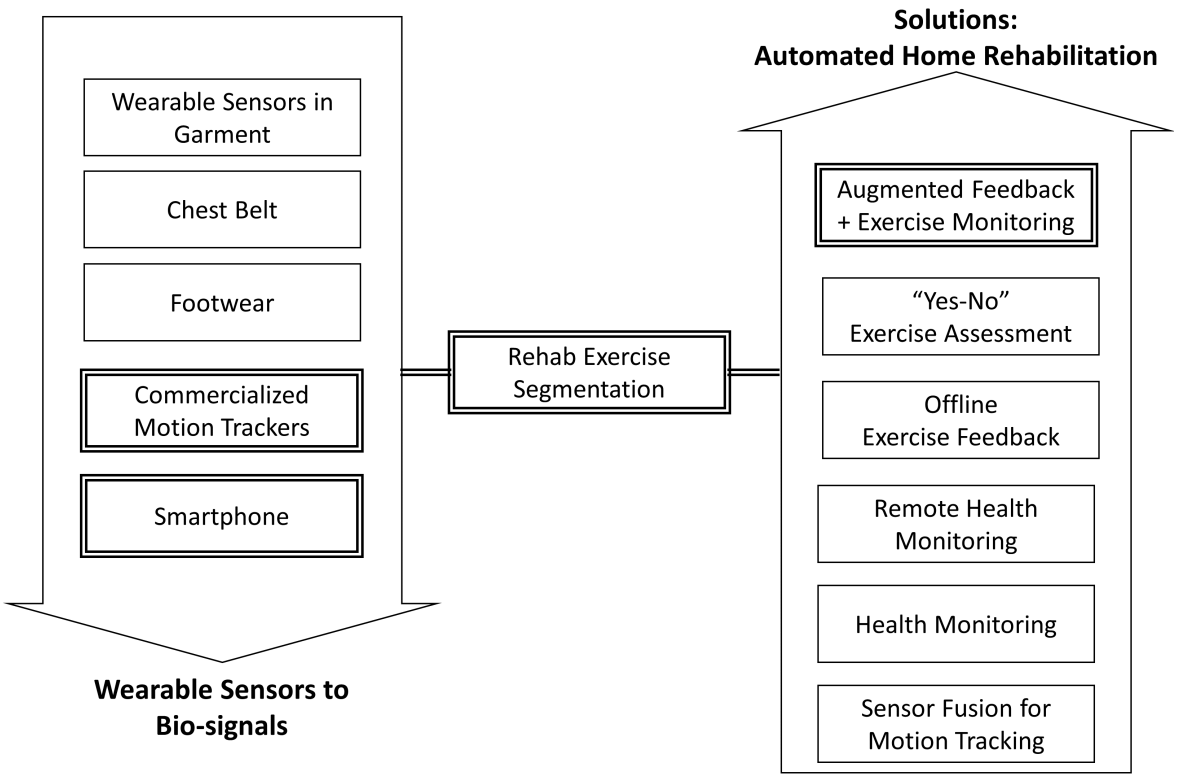

Figure 5.5: Bridge between Motion Tracking to Automated Home Rehabilitation System

to biofeedback from a set of rules. It relies on clearly defined rules derived from the data; for example, focusing on the snapshot of movement using gesture recognition rules [80] or more complex rules [83]. However, the setback of this approach is the cost of obtaining the knowledge which is generic enough to construct the rules. The rules could turn out to be inflexible if the data lacks the different application scenarios.

On the other hand, learning-based method constructs the prediction model using machine learning algorithm involving feature engineering and training. It requires less resources compared to rule-based approach which requires lots of data of different scenarios in order to derive the rules. The challenge of using the learning-based method is the trade-off between how informative and how frequent the feedback should be. Hidden Markov Model (HMM) [84] and Neural Network (NN) [85] show the potential

for real-time feedback system by making prediction periodically. However, the feedback is limited to a "yes" or "no". For example, the model predicts whether the movement is too slow, too fast, wrong static joint angle, or correct repetition. R. Kianifar et. al. aimed to provide more explanatory feedback by using predictive model to infer the consequences from the movement [86]. However, the prediction could only be done at the end of the exercise.

The more informative feedback and quality assessment could be obtained by selectively segmenting an exercise into states and identifying the abnormal sequences against the correct pattern. P-C Huang et al. proposed a State Identification method [42] to divide the exercise motion into four states. The experiment was conducted using angle frame (joint and body-segment orientations of lower-limb) with Support Vector Machine (SVM) algorithm. However, the justification of SVM as well as feature extraction and insights were not elaborated.

5.2 Pattern Recognition for Exercise State Segmentation

The human motion segmentation system is proposed using wearable sensor signals with machine learning techniques to recognise the motion segments. A comparative performance evaluation will be conducted between using the readable clinical data (i.e. Angular Displacement called Angle Frame(AF)) and the proposed wearable sensors' data (i.e. Signal Frame (SF)).

Figure 5.6 shows the overall training flow of the proposed learning based exercise state identification and illustrates the features extracted from MEMS signals (i.e. accelerometer, gyroscope and magnetometer) and the derived angular displacement (i.e.

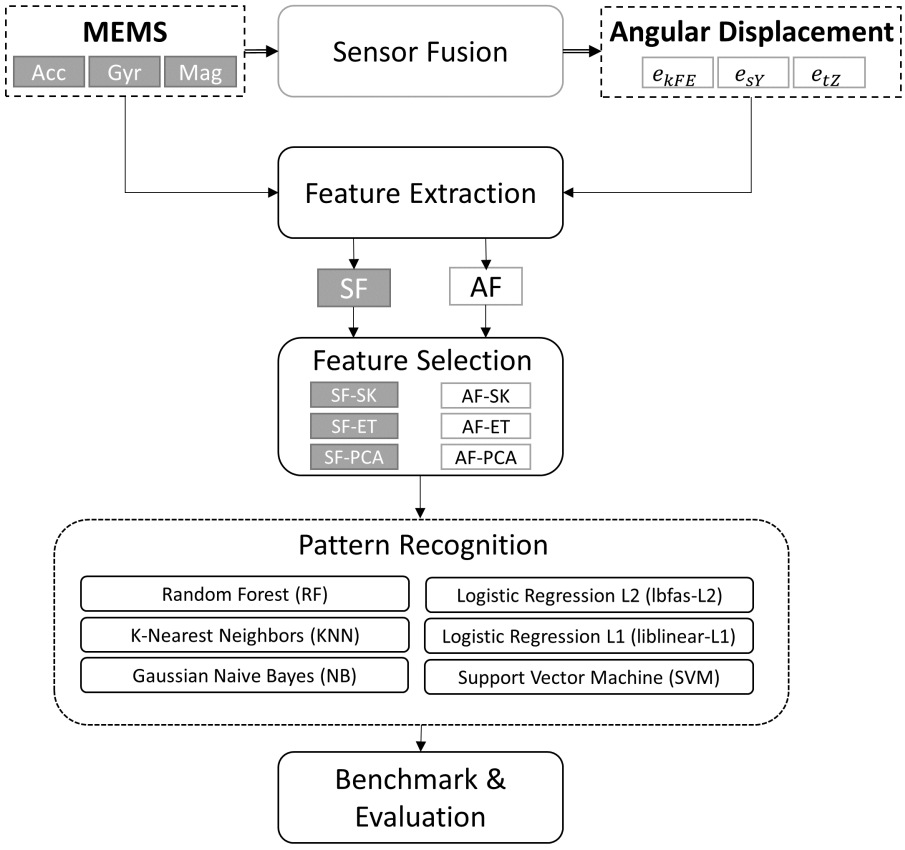

Figure 5.6: Training of Learning-based Exercise State Segmentation

euler angle), which is the post-processing result from MEMS data. The data is used for comparison purpose. The aim is to study the impact of signal data and select the significant features for the exercise segmentation pattern recognition and generic human motion classification.

If the SF is proven to be better, it has the potential to speed up the training and to be preprocessed for motion classification. This is because AF requires more computational resources and is prone to error from sensor fusion. The features, namely, the properties of both frames (SF and AF) are extracted using statistical feature extraction and chosen feature selection techniques. Lastly, the SF and AF are fed into the machine learning algorithms for evaluation. Thus, the recommended framework (see

Section 5.4.4) will be a subset of Figure 5.6.

5.2.1 Feature engineering

Feature engineering is a preprocessing stage in machine learning. It transforms the raw inputs into application-based features and possibly at a lower dimension for the training. It includes feature extraction and selection process. Section 2.3.1.3 presented the features created for learning-based method. Hence, for this case, Statistical time-domain feature extraction is frequently applied to motion data [86, 140]. Eight properties (mean, standard deviation, skewness, kurtosis, 25-percentile, 75-percentile, energy and range) are extracted from the wearable sensor signals and anglar displacements to create the SF and AF respectively. In total, there are 24 (AF-all) and 144 (SF-all) extracted features for AF and SF respectively.

Feature Selection reduces the dimensional presentation by selecting the subset of features which are most relevant to the predictive model and target output. Thus, three feature selection techniques, namely, SelectKBest (SelectK), ExtraTree (ExtraTree) and Principle Component Analysis (PCA) are used. They are chosen for their different characteristics in feature selection.

- **SelectKBest** [141] is a filtering method that uses one variation of statistical measure to assign the feature score. The features are then sorted and a predefined number of the top features are selected. Half of the top features are chosen as the candidates for SelectK method.

- **Extra-Tree method**, or extremely randomised trees, adopts the decision tree module. It builds the tree based on the numerical input features and chooses a random cut-point. This method usually improves the accuracy due to the variance reduction effect. It entails less computation cost from choosing a random

instead of an optimal cut-point. The uniqueness of ExtraTree is the calculation of the feature's importance by reducing the node impurity weight so that it is less likely to reach the node [142].

- **Principle Component Analysis (PCA)** normalises data by decorrelating the axis and picking the k dimension that has the highest amount of variance. PCA is an unsupervised method that reduces the original features to fewer lower dimension features [143].

It is used mainly to identify the hidden pattern of the data as well as removing the redundancy of correlated features. Figure 5.7 further explains the extraction of features.

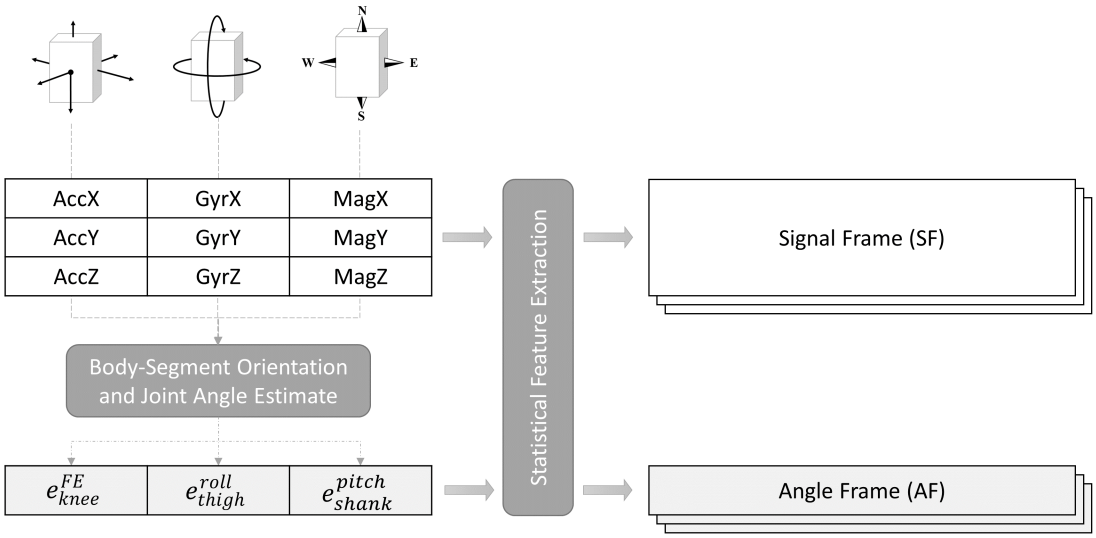

Figure 5.7: Feature Frames

5.2.1.1 Fundamental Features: Angle Frame (AF)

Angle Frame (AF) refers to the Euler angles that are human-readable movement representation. AF is incorporated in some rule-based approaches such as [80] and learning-

based approaches such as [94]. In recent years, state identification has applied AF to train a prediction model [42]. However, the exercise cases tested in the study included Knee Extension, Leg Raise and Leg Swing from side to side, which are similar in movements. Furthermore, the paper has not provided any performance comparison results nor details of the feature engineering process. It specified the orientation of the lower limb (translated to e_T_z and e_S_y based on [144]), hip abduction-adduction (side swing) and knee joint flexion-extension (e_K_FE) although the choice of angles was not fully elaborated. For comparison, AF is used to benchmark the performance against SF and to provide insight into its use in feature engineering. Hip adduction-adduction would not be included since only thigh and shank sensors are used.

5.2.1.2 Technical Feature: Signal Frame (SF)

Signal Frame (SF) is the data collected from the accelerometer, gyroscope, and magnetometer embedded in the wearable sensors such as MEMS. AF has been commonly used in both rule-based and learning-based approaches because AF is often the angle translated from the Kinect device. That could be one of the reasons that SF is not widely explored since SF is not so human readable. The idea of using SF is because it poses less bias and requires less computation. Figure 5.8 shows examples of the raw data of the motion signal and euler angles (angular displacements) of the body segment at different states in an exercise cycle. Although the angular data are readable to end users, it is not clear cut as to whether it is needed to segment the states of the human motion since obtaining angular displacement entails an additional sensor fusion procedure over a MEMS sensor. Moreover, MEMS sensors are widely used in classifying human activity recognition [145, 146]. Thus, the aim of this specification is to determine whether SF performs better than AF while reducing the preprocessing time and computation load.

5.2.2 Machine Learning Algorithms

5.2.2.1 Support Vector Machine (SVM)

For human motion pattern recognition, Support Vector Machine (SVM) is the first choice because it could produce good performance with less need for customisation. It is considered a very competitive choice for its ability to recognise particular features and its ease of implementation [42]. From the experiment, the linear kernel delivers the most desired results since it is less prone to overfitting.

5.2.2.2 Random Forest (RF)

Random Forest (RF) is a form of supervised learning which is the ensemble method of the decision tree. RF creates random subsets of features building smaller decision trees and uses the bagging method to improve the overall result. It was being used in [147].

5.2.2.3 K-Nearest-Neighbor (KNN)

K-Nearest-Neighbor (KNN) classifies the pattern by storing the training vectors. KNN provides test vectors by relying on majority voting on the classes of k nearest training vector, which is closest to the feature space. KNN has been introduced in multi-sensor and on-line recognition of body positions and activities [148].

5.2.2.4 Logistic Regression (LR)

Logistic Regression (LR) is a statistical model that analyses the dataset that finds the most fitting relationship between the outcome-correlated variables and a set of predictor variables. LR generates the coefficients to predict the logit (outcome) transformation from the probability of interest (correlated variables). It is an effective algorithm, even

for complex problems.

5.2.2.5 Naive Bayes (NB)

Naive Bayes is a probabilistic classifier that is based on the Bayes' theorem. Naive Bayes has been successfully deployed for the lower limb patient monitoring system, abnormal Gait detection and activity recognition in [42]. In this experiment, the Gaussian distribution is adopted (GNB) for continuous motion data.

5.2.3 Data Overview

The input data for this experiment is collected using XSENS Awinda [17], wireless wearable sensors that include a 3-axis accelerometer, a 3-axis gyroscope and a 3-axis magnetometer. The sensors are strapped on the shank and thigh of the participants at a sampling rate of 100Hz. In order to avoid the bias of sensor placements, the sensor are placed in 3 positions: facing front, right hand side, and left hand side of the lowerlimb.

10 participants were invited to take part in this study by performing SitStand and LegExtension exercise. Each participant is instructed to perform 15 repetitions, which last about 5 minutes, for each exercise type and placement. It means a participant needs to do 6 exercises and for each exercise, they need to repeat 15 cycles of *Rest*, *Raise*, *Hold*, and *Drop*. Figure 5.8 shows the segmentation of exercise's state. Lastly, the collected data are divided into 70% training and 30% testing datasets.

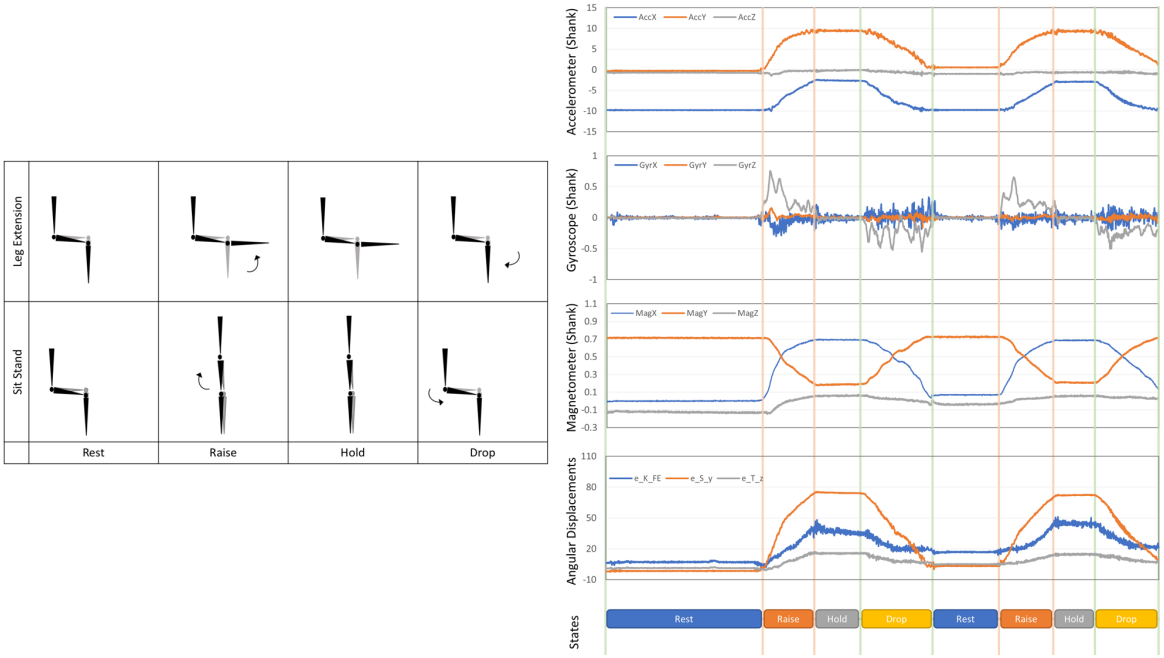

Figure 5.8: Example of Exercise State Segmentation

5.3 Results and Comparisons

The experiment evaluated two processes: the performance of the pattern recognition and the selection of motion features (in Section 5.2.1). The pattern recognition performance is benchmarked using the accuracy of the classification methods (mentioned in Section 5.2.2). Due to the 4 states within an exercise, the pattern is classified using two approaches: binary and multi-label classifications. Figure 5.9 lays out the different ways of approaching the classification problem by transforming the training model into 4 single-class classifiers (Binary Class) or using the algorithm to directly address the 4 classes at once (Multi-Label) taking into account that each label is related. It is to test whether a feature should be isolated and which features should be the focus for each exercise state.

Different feature selection methods are adopted to study the average accuracy and identify the signficant features. As mentioned in Section 5.2.2, after the statistical

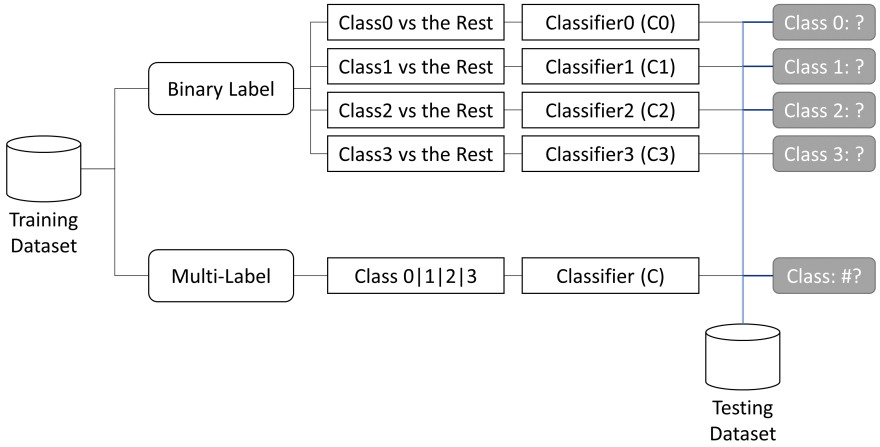

Figure 5.9: Binary vs Multi-Label Classification Overview

	AF-all	AF-SelectK	AF-ExtraTree	AF-PCA	SF-all	SF-SelectK	SF-ExtraTree	SF-PCA
Random Forest (RF)	87.45	88.24	88.78	80.33	91.14	91.90	**94.90**	79.76
K-Nearest Neighbors (KNN)	90.39	90.66	92.28	88.17	93.84	93.57	**94.82**	79.76
Gaussian Naive Bayes (GNB)	79.61	80.79	80.94	69.78	77.79	76.89	83.29	**84.04**
Logistic Regression - L2 Regulation (LR-l2)	86.91	87.28	87.15	81.08	91.69	**95.89**	***95.78***	82.41
Logistic Regression - L1 Regulation (LR-l1)	87.34	87.16	87.18	81.08	82.70	**94.97**	***94.48***	83.99
Support Vector Machine (SVM)	86.76	85.83	87.00	81.16	86.87	***95.83***	**95.89**	80.46

Table 5.1: Average Accuracy - Binary Classification (%)

feature extraction, 144 features have been derived for SF(SF-all) and 24 for AF (AF-all). To reduce the dimension of the extracted features, feature selection methods, namely, SelectKBest (-SelectK), Extra Tree (-ExtraTree), and PCA (-PCA) have been employed.

Feature selection methods are tested for its significance while studying the average accuracy. As mentioned in Section 5.5.2, after the statistical feature extraction, 144 features have been derived for SF (SF-all) and 24 for AF (AF-all). To reduce the dimension of the extracted features, feature selection methods, namely, SelectKBest (-SelectK), Extra Tree (-ExtraTree), and PCA (-PCA) have been employed.

Table 5.1 and Table 5.2 show the accuracy derived from the different input features. It can be seen that SF results in better performance than AF, especially after feature selection. The best results are from SF-SelectK and SF-ExtraTree for both the binary

	AF-all	AF-SelectK	AF-ExtraTree	AF-PCA	SF-all	SF-SelectK	SF-ExtraTree	SF-PCA
Random Forest (RF)	74.70	74.79	74.65	61.67	78.68	**85.08**	82.65	48.57
K-Nearest Neighbors (KNN)	80.72	82.76	84.45	76.24	87.67	88.83	**90.32**	55.26
Gaussian Naive Bayes (GNB)	52.20	56.89	56.89	41.08	84.09	83.93	**85.78**	68.74
Logistic Regression - L2 Regulation (LR-l2)	73.19	71.24	71.24	57.64	84.81	92.14	**92.74**	67.62
Logistic Regression - L1 Regulation (LR-l1)	74.98	71.70	71.70	57.63	71.10	91.07	**93.22**	70.36
Support Vector Machine (SVM)	73.04	69.48	69.48	56.7	84.60	**94.04**	***93.95***	31.69

Table 5.2: Average Accuracy - Multi-label Classification (%)

	Rest	**Raise**	**Hold**	**Drop**	**MultiClass**
AF	***24***	***24***	***24***	***24***	***24***
AF-SelectK	12	12	12	12	12
AF-ExtraTree	12	15	12	7	14
AF-PCA (0.95)	7	7	7	7	7
SF	***144***	***144***	***144***	***144***	***144***
SF-SelectK	72	72	72	72	72
SF-ExtraTree	47	37	43	45	63
SF-PCA (0.95)	4	4	4	4	4

Table 5.3: Number of Features Selected

and multi-label approaches. While binary classification acts as the baseline, it (best at 95.89%) performs slightly better than the multi-label pattern recognition (best at 94.04%). Interestingly for multi-label (Table 5.2), AF achieves a worse outcome on 4 out of 6 classification methods after feature selection. This may be due to the already small feature set of 24 in AF and hence further reduction of the feature set may lead to loss of useful information.

The results from binary and multi-label show that reducing the number of features contributes positively to the overall performance. The increase in accuracy is especially true for SF features. For AF, given its already small feature set of 24, the performance does not benefit from further reduction in the features. For SF features, the reduction is about 50-65% as can be seen from Table 5.3. The ExtraTree method for feature selection greatly impacts the final performance of the classification as it yields better performance for the majority of the classification methods for both binary and multi-label classification. SelectK and ExtraTree are more or less on par with the latter performing slightly better. SelectK exploits the univariate correlation between

features while ExtraTree weighs the importance of features by measuring the errors of the prediction models derived from the various permuted features. The meticulous computation of feature importance in ExtraTree has therefore a greater impact on the overall performance.

Merging features to reduce dimension, PCA produces significantly lower number of selected features as can be seen in Table 5.3. PCA selects 4 features for SF and 7 for AF. Intuitively, the drastic reduction could be explained since AF and SF are respectively derived from the original 3 Euler angles and 9 motion signals. Therefore, it is not a coincidence that a much smaller feature set has been derived by PCA upon removing the redundancy. However, the next question to answer is whether the cutback on the features compromises the pattern recognition accuracy of the exercise segments. For time-series application, the linear relationship of PCA is a shortcoming which can affect the results of the prediction models [149].

In this experiment, the top performer for pattern recognition is SVM. In general, SVM returns the most robust result against other classification methods, especially if there is imperfection of data [150]. It is unsurprising that SVM performs best in this classification problem and it shows that SVM has great potential not only in activity recognition but human motion pattern recognition in general.

Logistic regression (LR) produces the second best performance after SVM. It exhibits inconclusive performance improvement when changing the regulation from L1-norm to L2-norm. Avoiding over-fitting, L2-norm minimizes the sum of squared differences while L1-norm focuses on the sum of the absolute differences. L2-norm encourages the prediction model to compute the closed form of solution, especially the binary classification. The performance as reflected in Table 5.1 shows that L2-norm and SelecK are on par with SVM for binary classification. LR-l2 is known for working well with feature selection since LR-l1 may have redundancy with its built-in feature

selection. In Table 5.2, LR-l2 presents consistently good performance regardless of the feature selection method although LR-l1 produces slightly better result when combined with ExtraTree feature selection. We could argue that feature selection methods selected more generic features for the labels. LR-l1 coincidently provides better result because it further selects the largest set of correlated features to the results.

In summary, SF not only saves on the computational resources, it also avoids the cumulative errors when processing the raw sensors data into the angular displacement. SF also performs better in the exercise segment recognition for both multi-label and binary pattern recognition. Multi-label incorporates the chain of label information on top of the independent labels of binary class. It is concluded that SVM with ExtraTree feature selection is best for the exercise segment predictive model.

5.4 Features Insight and Analysis

In this section, the impact of features is discussed based on the selected features chosen by SelectK and ExtraTree. Figures 5.10 to 5.13 illustrate the features' scores whereby the higher the value, the more important and more correlated the feature is in the exercise states. The relevance and properties extracted from both Angle Frame (AF) and Signal Frame (SF) are discussed as well as how the various selection methods prioritise the features. It is to be noted that PCA is not included because the PCA features are a combination of the original AF and SF. Therefore, which are the important features in AF and SF cannot be separately differentiated.

5.4.1 Binary Classification - Angle Frame Features

Universally, kurtosis and skewness have the lowest feature score for both selection and training methods. It means they do not have any correlation to the exercise states. Hence, the shape of the sample distribution is concluded to be insignificant.

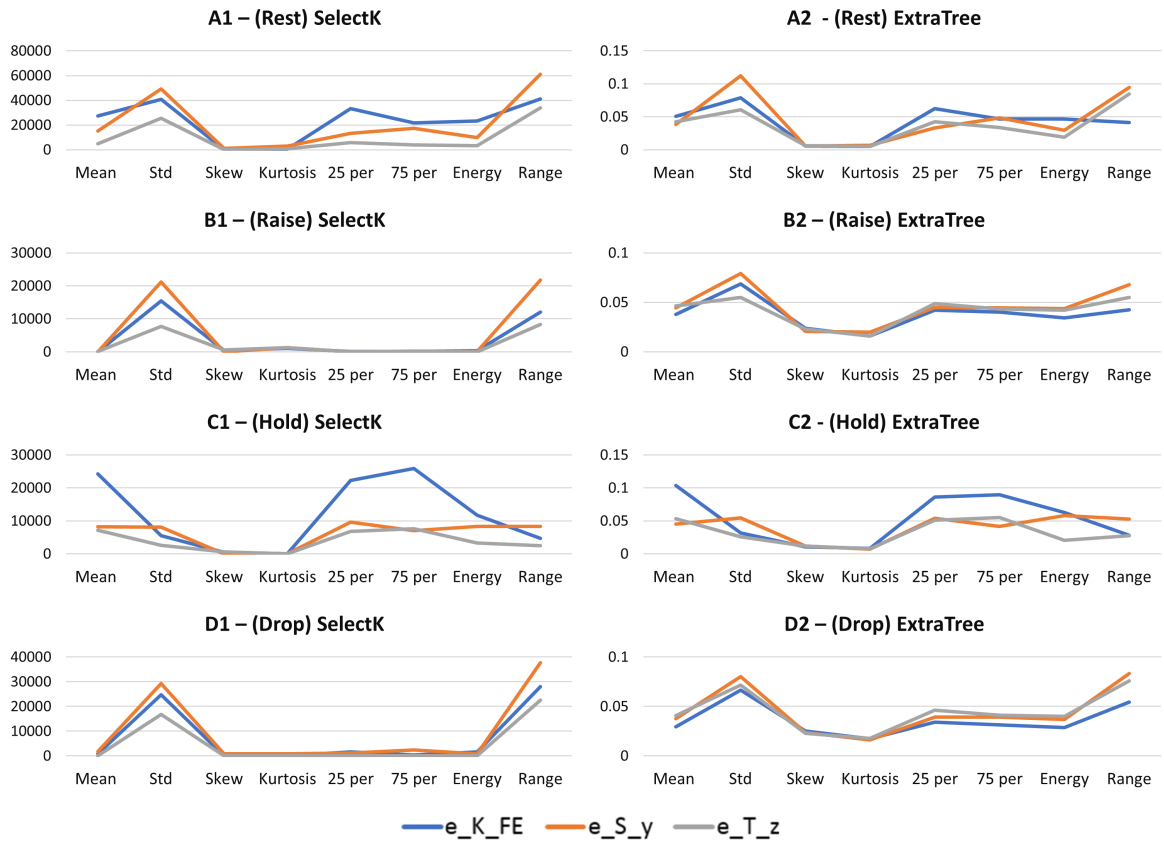

Figure 5.10: Angle Frame (AF) - SelectK and ExtraTree Feature Selection for Binary Class

Angle Frame (AF) was proposed by [42] making use of the euler angles derived from the signals of the sensors being placed on the lowerlimb. AF is used here as a benchmark for first-hand comparison of the accuracy of using the proposed SF to classify motion at each state. Figure 5.10 presents the feature scores (Y axis) of SelectK and ExtraTree while the X axis shows the statistical properties of the Euler Angles (e_K_FE,e_S_y and e_T_z).

SelectK and ExtraTree have similar trends for both moving (B, D) and non-moving (A,D) states. For the non-moving state of *Rest* and *Hold*, the difference is that *Rest* depicts the preparation state before starting of the cycle while *Hold* signifies the middle of state of the exercise. Hence, *Hold* could be used to output the patients' progress in terms of maximum range of motion and strength of the muscle (shakiness while holding the position). Knee-joint angle dominates the other two angles. In *Rest* state (Figure 5.10-A1 and A2), it can be inferred that Standard Deviation, range and 25 percentile play an important role on the Flexion/Extension angles. *Hold* differs by relying on Mean instad of standard deviation.

Distinctively, during moving state (Figures 5.10-B and D), ExtraTree seems to compromise in its performance with the 25, 75 percentiles and Energy while SelectK does not consider them at all. Nonetheless, Standard Deviation and Range are the main properties for the moving states. It aligns with the fact that one usually looks at the range of motion when the limb is in motion. It is to be noted that there is no stark differences between Raise and Drop. Therefore, the accuracy of these two states are similarly lower than the non-moving state (Appendix A). It may be due to the fact that the features' statistical properties are figuratively similar; hence the prediction model could not differentiate the two states and resulting in lower accuracy.

5.4.2 Binary Classification - Signal Frame

The proposed Signal Frame (SF) generated 144 features which are extracted from the motion signal instead of angular displacement. Feature selection methods, SelectK (Figure 5.11) and ExtraTree (Figure 5.12), have results for moving phases but contradicting results for non-moving phases.

During *Rest* state of Figure 5.11, Standard Deviation and Range have the highest

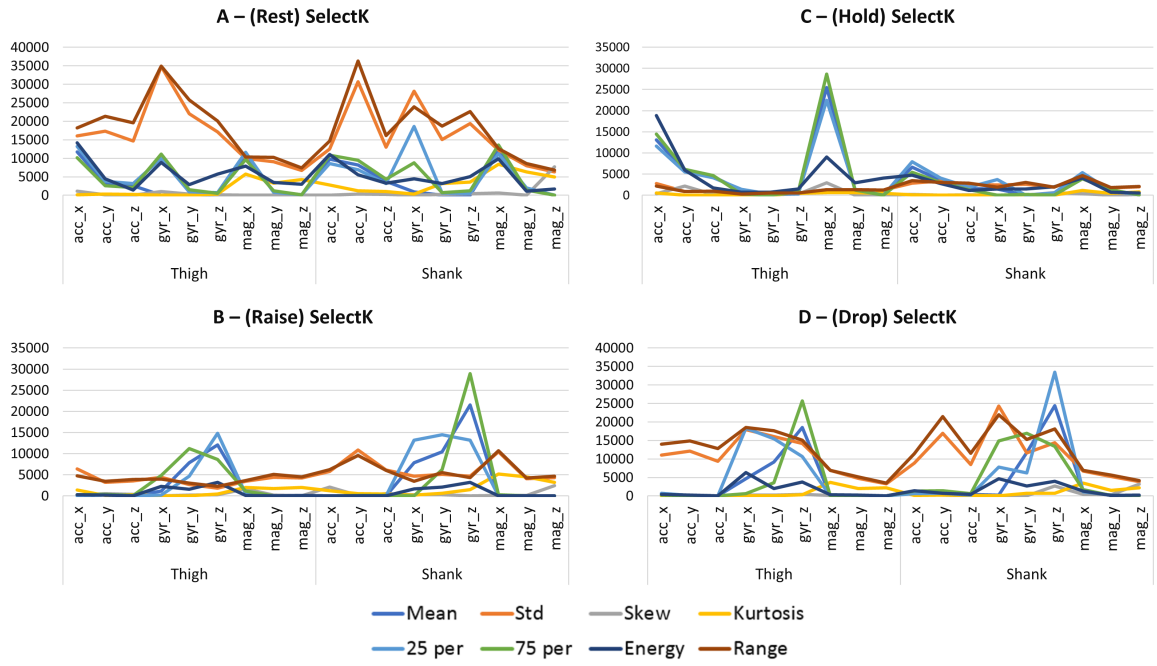

Figure 5.11: Signal Frame (SF) - SelectK Feature Selection for Binary Class

correlation to the output while Hold (Figure 5.11-B) relies on 75 percentile, 25 percentile and Energy. Considering the input signals, accelerometer and magnetometer on the x-axis always show the high peak for both thigh and shank placement. The differences are that *Rest* would consider gyroscope data on the x-axis and the acceleormeter reading of the shank data. On the other hand, *Raise* and *Drop* spike at the gyroscope data for the statistical properties which characterised the study on the range of motion (Energy, 25 percentile and 75 percentile). The distinction between these two moving states can be seen in the location of the peak feature score for the Thigh and Shank data. For example, during *Raise*, SelectK pays attention to the 25 percentile on the Thigh's gyroscope data and 75 percentile on the Shank's gyroscope data. For *Drop*, it is the reverse. In addition to raise moving, *Drop* state takes into account of Standard Deviation and Range.

ExtraTree (Figure 5.12) has similar conclusion as SelectK method, except that its

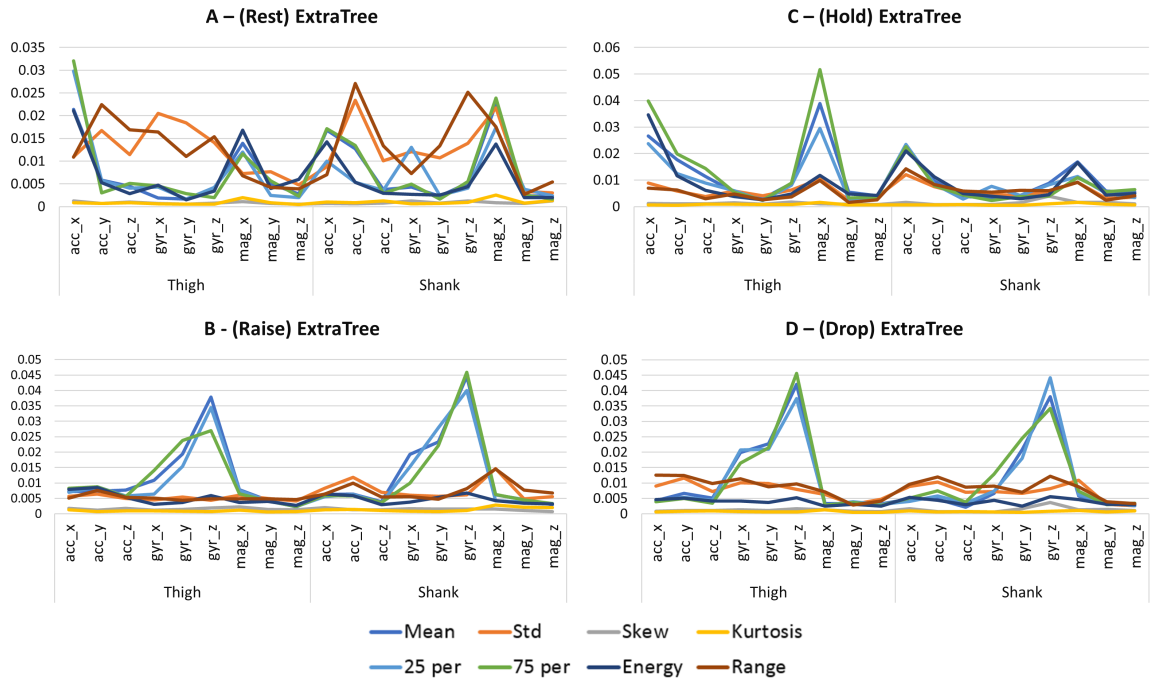

Figure 5.12: Signal Frame (SF) - ExtraTree Feature Selection for Binary Class

trend is more precise. In particular, ExtraTree illustrates the influence of Standard Deviation and Range on *Rest* state and 25 percentile, 75 percentile and Mean on *Hold* state. However, it does not favor the gyroscope data like SelectK does at *Rest* state. To break the tie between ExtraTree and SelectK, refer to Appendix A which shows that ExtraTree produces better performance on average during *Rest* state compared to SelectK. This is in line with the fact that gyroscope data does not contribute to non-moving state compared to accelerometer and magnetometer data. For moving states, only 25, 75 percentile and Energy shows significance. The ExtraTree analysis is similar to that of SelectK.

5.4.3 Multi-Label Classification

Although Multi-Label produces slightly lower accuracy than the Binary label, studying the feature scores would yield the overall knowledge of important features as well as

properties applied on the motion signal. Left Hand Side (Figure 5.13-A1 and B1) and Right Hand Side (Figure 5.13-A2 and B2) show the feature score for Signal Frame and Angle Frame respectively.

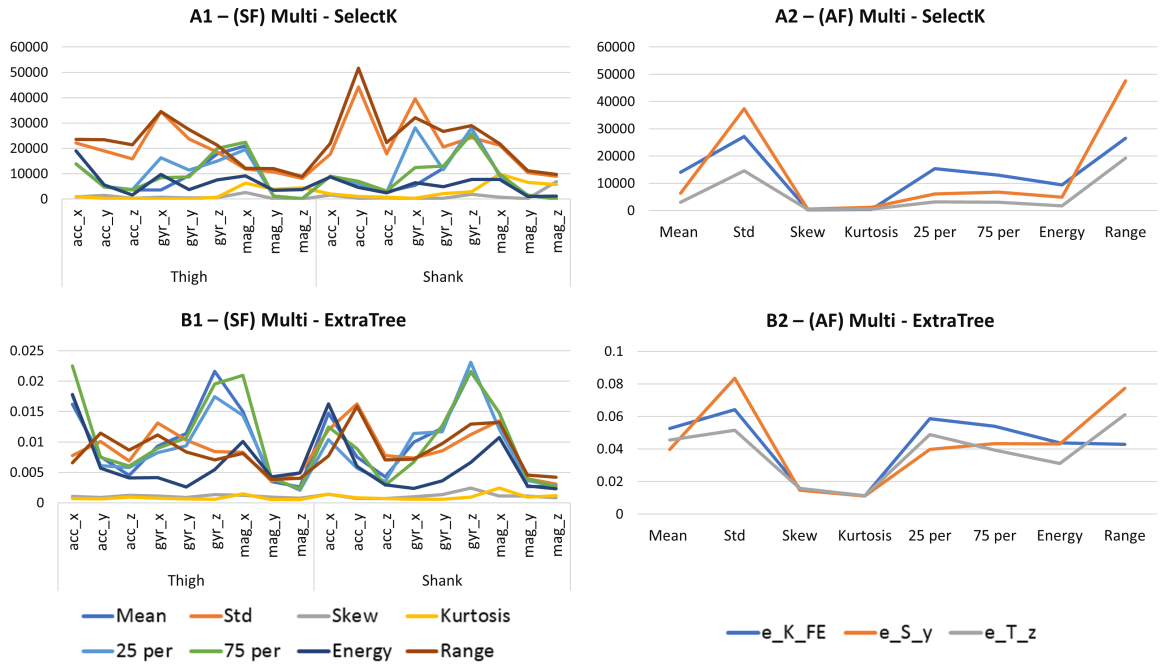

Figure 5.13: Multi-label - Angle Frame vs. Signal Frame

For Angle Frame (AF), Standhard Deviation and Range are the main properties with the highest correlation to the label by applying on the e_S_y angle. With similar trend, the same performances are reflected in AF-SelectK and AF-ExtraTree in Table 5.2.

For Signal Frame (SF), SelectK and ExtraTree focus on different properties. SelectK looks at Standard Deviation and Range while ExtraTree focus on Mean, 25 percentile and 75 percentile. According to Table 5.2, ExtraTree performs SF training with KNN, GNB, LR, and SVM. The ExtraTree selection will be discussed in more details under future research direction. The top score features are accelerometer (X axis), gyroscope (Y, Z axis) and magnetometer (X Axis) applying 25, 75 percentile and Mean. Addi-

tionally, on the shank, Accelerometer Y is taken into account by applying Standard Deviation and Range.

5.4.4 The Recommended Framework for Identification of Rehabilitation Exercise State

Figure 5.14 summarises the recommended architecture for intelligent identification of correct lowerlimb exercise state. Throughout the training phase, statistical properties are extracted from the training set. Feature engineering process results in the selection of the most significant features from the training dataset and the feature selection classifier used is the (*clf_SF_ExtraTree*). The selected features are then fed into the Support Vector Machine for classification training. The prediction model is trained using the Binary label from the training dataset which creates 4 classifiers for each of the states. Most significant features will be extracted from the testing dataset or real-time signals via *clf_SF_ExtraTree* classifer. It is then fed to the final classifier for the final prediction.

5.5 Conclusions

In this chapter, a mobile app prototype, RehabPartner, for home exercise intervention to prevent limb over-twisting has been developed. The application is an example of realising the home rehabilitation for community usage and patient management for the physiotherapist. It progresses from the existing methods to a self-automated continuous user feedback system. The proposed machine-learning exercise segmentation is an intermediate step to close the gap of motion tracking and feedback model for home physical rehabilitation. A framework to automate the recognition of 4 exercise states

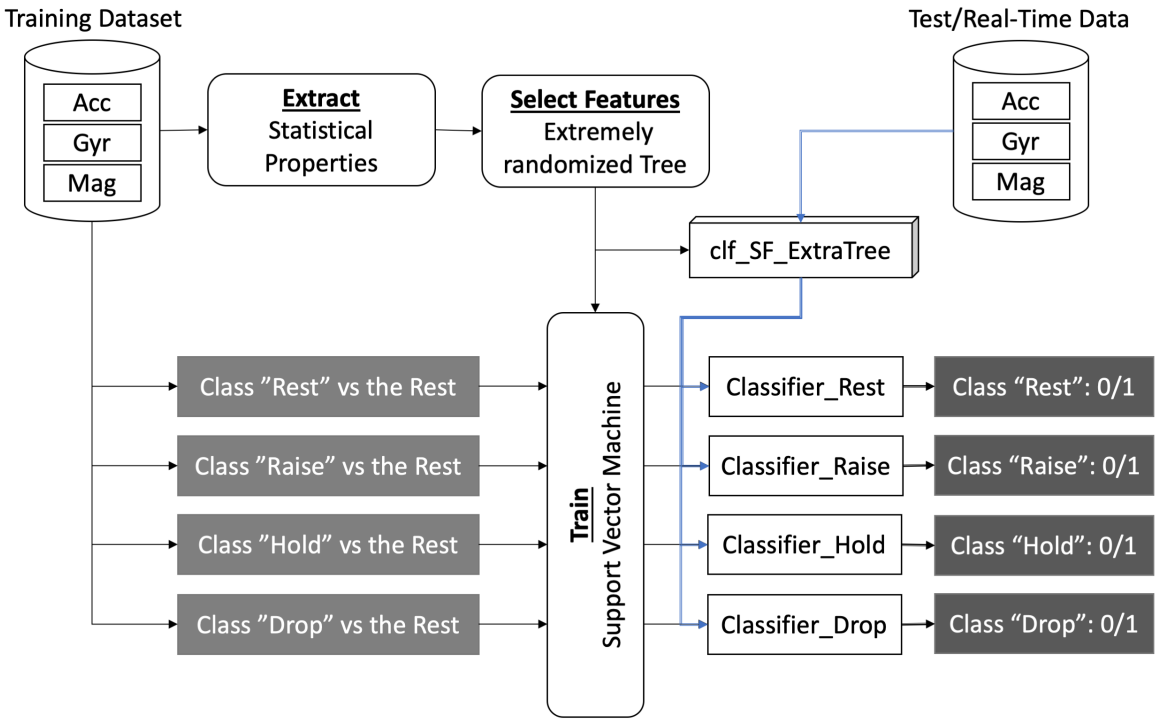

Figure 5.14: The Proposed Framework

of the lower limb: *Rest*, *Raise*, *Hold* and *Drop* are introduced. Different machine learning algorithms are explored and exploited to design the prediction models that are most suited for the recognition of the 4 states.

The evaluation compares the performance of the proposed feature Signal Frame (SF) against Angle Frame (AF). Binary classifier is used as a baseline to compare against the proposed multi-label classifier of the exercise states. The results show the impact of feature engineering, especially using SF, on the accuracy of the predictive model yielding up to 94.04% (SVM) for multi-label pattern recognition. The results show the efficiency and potential of using signal data as features in motion-based exercise pattern recognition. Specifically, the accelerometer and x-axis of the magnetometer are useful for non-moving states while gyroscope data is primarily used as features to

identify moving states.

Based on this study, a framework using motion signal is recommended with feature selection method (Extremely Randomized Tree) and training algorithm (Support Vector Machine) respectively. With binary label classification, the features are selected to be most suited for each exercise state. Accelerometer and magnetometer (x-axis) data are important features for the non-moving phase and gyroscope data for the moving phase. In particular, Rest would consider the Standard Deviation and Range, while Hold, Raise and Drop use 25 percentile, 75 percentile and Mean.

Chapter 6

Conclusion and Future Work

This thesis contributes to the development of a more accurate motion tracking system from low-cost sensors for community usage. In addition, software solutions are proposed to bring continuous intervention feedback to users realizing home rehabilitation and scaleable patient management to physiotherapist. In this chapter, the contributions of this thesis are summarized and future direction for home rehabilitation are recommended.

6.1 Conclusion

6.1.1 Robust Sensor Fusion for Low-Cost IMU Orientation Estimate

Recent development in hardware and accessibility of smartphones have created a huge potential of bringing assistive healthcare to the community, in particular tele-rehabilitaiton. For rehabilitation exercise to be monitored at home, motion sensors and its sensor fusion algorithm plays an important role. However, the main challenge

in getting the accurate readings from low-cost sensors is drift. It is the effect of shifted trend in the fusion reading caused by accumulated noise from the sensor signals. The evaluation is done on two use cases using early stage rehabilitation exercise, such as Sit-to-Stand and Leg Extension exercise.

A lightweight sensor fusion, Complementary Filter Feedback (CFF) is proposed by initiating the feedback loop from orientation estimate to gyroscope data integration. It reduces the error due to gyroscope data integration drift. Euler representation is used directly as it reduces the computation complexity compared to other representations. Furthermore, recommendation on the placement of sensors on the body segments is discussed to address the problem of Gimbal lock. There are many studies which report the placement of sensors according to the default Euler hierarchy. This recommendation has been shown to be well suited for all the lower limb rehabilitation exercises as well as for the hip joint range of motion. To overcome the limitation of CFF, a new and better orientation estimate algorithm is proposed by changing the state representation from Euler to Quaternion and combining the quaternion-based kalman filter with corrector estimates using gradient descent (KFGD).

CFF and KFGD performances are evaluated and compared with commercialized XSENS Awinda and the prominent Madgwick algorithm. The results show that CFF is capable of fast motion tracking and confirm that the feedback loop can correct the error caused by the integration of gyroscope data. The KFGD orientation estimation is comparable to XSENS Awinda and has shown itself to be more stable than and outperforms CFF. KFGD also outperforms the prominent Madgwick (MW) algorithm using mobile data. Thus, KFGD is suitable for low-cost motion sensors or mobile inertial sensors, especially during early recovery stage of sport injuries and exercise for the elderly.

6.1.2 Automated Oscillation Detection and Correction of Fused Wearable Sensor Signals using Machine Learning

Oscillation occurs in post filtered signals from both motion capture and inertial measurement sensors. This characteristic is often observed when the range of motion reaches or exceeds approximately 85 degrees. Elimination of oscillation in the filtered output signal is of significance as it means the filtered signal can be applied directly by applications such as visualization, motion tracking, clinical report, etc.

In this thesis, a detection model is proposed using feature selection and machine learning algorithm to automatically detect and correct for the artefact in the output signal. Feature extraction aims to study the impact of wearable sensor data gathered from the accelerometer, magnetometer and gyroscope, using well-known classifiers such as Logistic Regression, Support Vector Machine and Multilayer Perceptron.

As a result, the features and classification method that are most suited for the detection model are selected. Experimental results show that on average to 76% accuracy can be obtained and it can also filter out the fluctuation; the latter is more efficient than manually post-processing the data. The trained detection model has thus proved its effectiveness in eliminating the noisy fluctuations and its potential to be used in real-time.

6.1.3 Pattern Recognition for Rehabilitation Exercise Segmentation

This contribution addresses the intervention while the patient is executing the rehabilitation exercise at home. This study aims to simulate the observation of physiotherapists to track a patient's performance as well as to act as the attentive caregiver who guide

patients in the movement and correct when necessary. The system could provide the progress feedback in more details to the physiotherapist where listing of the summary, incorrect moments and accessing the limb movement are logged.

RehabPartner application is introduced to provide a platform to connect the therapist with the patients, allowing both the end users and caregivers to track the progress of rehabilitation and the movement during rehabilitation in 3 dimensions. The application monitors the motions which patients may have difficulties with. With the help of smart TVs, end users will be able to project the application onto the TVs and view the instructions for each exercise.

Nonetheless, there are challenges in providing informative feedback while adaptively monitoring and determining if the movement pattern is correct. Hence, an intermediate steps to bridge the gap between receiving the motion data to providing informative feedback is proposed. This approach uses intelligent pattern recognition to identify the 4 exercise states of lower limb movement: raise, hold, drop and raise. The the motion signals (collected via accelerometer, gyroscope and magnetometer) of the lower limb are exploited instead of the commonly used and readable Euler angles as the input features for machine learning. The different sets of features are studied and benchmarked using machine learning algorithms: Support Vector Machine, Random Forest, Logistic Regression and Naive Bayes.

The results show that the use of the proposed Signal Frame achieves the best result of 95.89% (Binary Classification) in comparison with 92.28% from the use of Angle Frame. The results show huge potential of intelligent pattern recognition from wearable sensor data in identifying the different segments of rehabilitation exercises and providing immediate feedbacks.

6.2 Future Work

6.2.1 Mobile-based Centralised System for Health Tracking using Motion and Biosignal Sensors

Since smartphone's all-in-one nature brings great flexibility and customizability, the mobile device will be used as the master device. In addition, IoT technology has enabled communication between sensors to be faster and hassle-free. A future direction is to study and design multi-sensor network [151] communicating with smart phone as well as automatic analyser.

This system has the potential to be deployed in two main areas: Network of Multiple sensors and Information Analysis from IMUs and Biosignal Sensors. Precisely, the main challenges of using multiple sensors with a limited computing power as central device are the data synchronization and management for the wireless sensor network.

With regards to a holistic motion tracking system, at least 3 low-cost IMUs could be used to obtain the major 3-dimensional joint angles: hip and knee joint. The combination of IMUs' orientation could imply the muscle activation or the affected area upon movement. From the literature of Gait analysis, Gait kinematic and Electromyogram (EMG) are linked. Therefore, there is a huge potential in using the IMU for muscle and visual cue.

Similarly, the combination of sensor could be expanded to bio-signal sensors. There are two ways to use this centralised system. It is either comparison of the devices or using multi-signals to conclude the information. For example, using EMG could confirm if IMUs have inferred the muscle activation correctly. At the same time, ECG and EEG could analyse the users' responses to the current movement.

6.2.2 Personalized Exercise Intervention and Feedback

The informative feedback from the wearable sensors could be augmented to provide end-users with more detailed real-time feedback. Instead of using one threshold while moving [139], more behaviours could be observed such as readiness at *Rest* state, twisting and unexpected swing during the *moving* states and shakiness during the *Hold* state. Therefore, the future work is to provide the system with multiple and informative feedbacks including both audio and visual feedbacks during the segmented periods of exercise. To provide the patients with real-time feedback, the main processing could be done at the server where feedback information could be retrieved by the mobile device.

6.2.3 Automatic Controller for Limb Supporters

The information from wearable sensors has more capability beyond monitoring the progress and for health analysis. This information could be used to control the limb supporters for patients. It is because the wearable sensors for motion tracking and analysis may aid the experts by enabling them to attend to more patients. However, the patients, who are severely affected from illness or injuries (e.g. hemiplegia), still requires the caregiver when doing the exercise and caryying out daily activities. In countries with ageing population, the problem is the shortage of caregivers.

Limb supporters such as Pneumatic Muscle Controller and exoskeleton become a solution to support the limb movement in patients. However, these devices movement are still set manually for personal usage. Therefore, the future work for wearable sensor information is to dynamically adjust and configure the parameters for the Limb Supporter so that it is customized for the individual patient and the patience's progress.

The candidate developed a pilot algorithm to automatically control the Pneumatic Artificial Muscle (PAM) by analyzing the PAM impact during Gait during her intern-

ship at the National Institute of Advanced Industrial Science and Technology (AIST) in Tokyo, Japan. The algorithm takes the information from a force sensor embedded at the heel of the sole of the non-PAM leg and an IMU strapped on the PAM leg to control the PAM driver.

Wireless PAM driver was developed by Digital Human Research Team at AIST [152, 153]. The driver receives the heel-strike information from force sensor in the shoes and signal PAM to contract based on the pre-defined parameters, the delay of contraction time from the event of heel strike (t_0) and the contraction duration (ΔT). The manual settings of testing all ($t_0, \Delta T$) combinations were carried out and select the best setting by evaluating the increase of hip flexion angle, decrease of variability of hip, and increase of knees peak angle. The challenge of the manual setting is finding the best combination by the exhausting search of the combination. Furthermore, as the Gait differ from individual and circumstance, the best combination varies at any event. Thus, there is a need to establish an automatic controller to adaptively set the contraction time, namely defining ($t_0, \Delta T$) from the given Gait parameters.

Figure 6.1: PAM Manual Setting Experiment

Figure. 6.1 illustrates the performance of all ($t_0, \Delta t$) combinations from 3 healthy participants based on the highest value of hip flexion angle and range of hip flexion/extension. The left y-axis represents the flexion/extension angle while the right y-axis shows the position of t_0 and Δt with respect to swing time (t_{swing}). Studying the relationship between the best PAM activation parameter with Gait swing time shows

the relationship where the PAM activation duration is about 2/3 of the t_{swing} and the delay is the fill-in to shift the contraction to end before the leg swing stops. From observation, we get (Eq.6.1) and (Eq.6.2).

$$\Delta t = \left[\frac{2}{3} t_{swing}\right] \tag{6.1}$$

$$t_0 = \lfloor t_{swing} - \Delta t \rfloor \tag{6.2}$$

where rounding is in multiple of hundred

Figure. 6.2 depicts Automatic Controller feature implemented in GaitSupporter mobile application. Hence, an additional experiment with 3 healthy participants is carried out to verify the effectiveness of the Automatic Controller by benchmarking with the best result of manual setting.

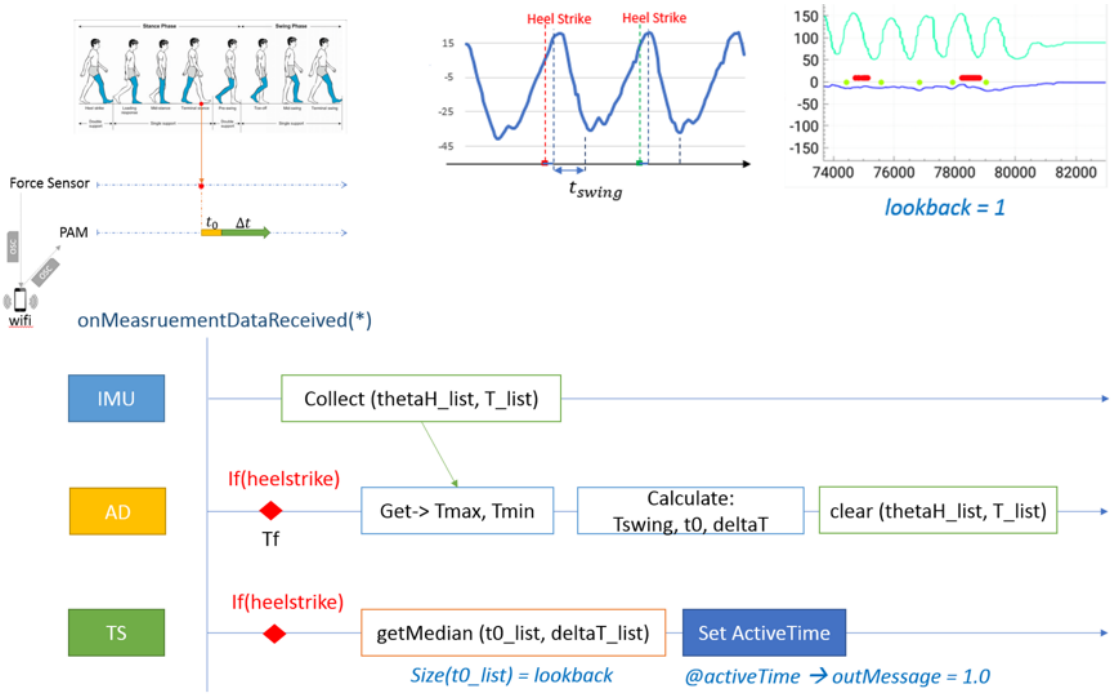

Figure 6.2: Automatic Controller Implementation

As a result, Figure. 6.3 shows that in addition to its adaptive setting, Automatic Controller is able to produce the same or better results than the best combination of manual setting. It was found that the Automatic Controller performs best with the window of 3 instances.

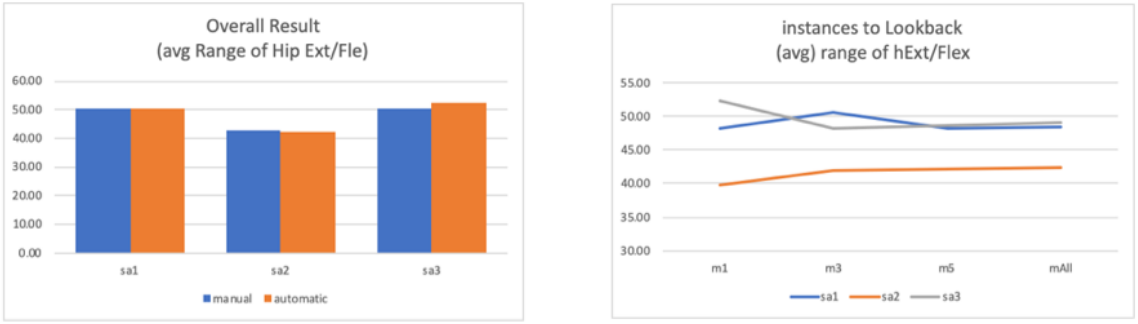

Figure 6.3: Automatic Controller vs. Manual Setting

In conclusion, this pilot study highlighted the improvement of hip flexion/extension range of motion. The collaboration on Automatic Controller is in progress where the elderly participants as well as including the emotion analysis during Gait are being discussed in future work.

Appendix A

Accuracy of Binary Classification for Exercise Segmentation

	AF			SF		
	All	**SelectK**	**ExtraTree**	**All**	**SelectK**	**ExtraTree**
Random Forest (RF)						
0 - Rest	95.41	95.38	95.77	92.32	93.73	94.55
1 - Raise	80.74	80.44	80.76	87.97	90.71	93.48
2 - Hold	95.17	95.47	95.54	95.73	87.63	96.18
3 - Drop	78.47	81.66	83.05	88.53	95.53	95.36
Average	***87.45***	***88.24***	***88.78***	***91.14***	***91.90***	***94.90***
K-Nearest Neighbors (KNN)						
0 - Rest	93.92	94.52	95.75	96.04	95.53	96.44
1 - Raise	86.22	84.76	89.01	91.58	89.48	90.74
2 - Hold	94.41	95.49	95.88	96.74	96.23	94.60
3 - Drop	87.02	87.89	88.49	90.98	93.06	97.49
Average	***90.39***	***90.66***	***92.28***	***93.84***	***93.57***	***94.82***
Gaussian Naive Bayes (GNB)						
0 - Rest	79.30	79.84	80.53	96.20	95.72	95.12
1 - Raise	67.85	68.03	68.34	75.52	74.58	82.84
2 - Hold	93.59	96.07	95.65	59.96	58.03	74.78
3 - Drop	77.67	79.24	79.24	79.48	79.22	80.40
Average	***79.61***	***80.79***	***80.94***	***77.79***	***76.89***	***83.29***
Logistic Regression - L2 Regulation (LR-l2)						
0 - Rest	96.11	95.84	96.03	96.57	95.53	95.77
1 - Raise	81.34	83.05	80.92	84.94	93.79	92.89
2 - Hold	95.04	95.06	95.02	96.55	96.40	96.59
3 - Drop	75.15	75.17	76.65	88.68	97.84	97.86
Average	***86.91***	***87.28***	***87.15***	***91.69***	***95.89***	***95.78***
Logistic Regression - L1 Regulation (LR-l1)						
0 - Rest	96.30	95.86	95.99	81.62	94.98	96.02
1 - Raise	81.72	82.59	81.14	76.57	93.34	93.55
2 - Hold	95.42	94.99	94.94	97.52	94.84	90.78
3 - Drop	75.93	75.20	76.65	75.09	96.72	97.59
Average	***87.34***	***87.16***	***87.18***	***82.70***	***94.97***	***94.48***
Support Vector Machine (SVM)						
0 - Rest	95.44	95.18	94.94	82.57	95.92	96.33
1 - Raise	80.93	78.97	78.97	89.04	93.30	94.14
2 - Hold	93.49	93.65	92.89	98.86	96.29	95.23
3 - Drop	77.17	75.51	75.67	77.02	97.82	97.87
Average	***86.76***	***85.83***	***87.00***	***86.87***	***95.83***	***95.89***

Table A.1: Accuracy of Binary Classification for Exercise Segmentation(%)

Bibliography

[1] W. F. of Occupational Therapists WFOT. Human resource project 2012. www.wfot.org/ResourceCentre/tabid/132/did/388/Default.aspx.

[2] B. Zhang, S. Jiang, D. Wei, M. Marschollek, and W. Zhang, "State of the art in gait analysis using wearable sensors for healthcare applications," in Computer and Information Science (ICIS), 2012 IEEE/ACIS 11th International Conference on. IEEE, 2012, pp. 213–218.

[3] W. Tao, T. Liu, R. Zheng, and H. Feng, "Gait analysis using wearable sensors," Sensors, vol. 12, no. 2, pp. 2255–2283, 2012.

[4] M. 107. (December 2014) Anatomical planes. https://medicine107.wordpress.com/2014/12/24/anatomical-planes/.

[5] G. Mcclure. (January 2017) Range of motion after joint replacement surgery. https://www.peerwell.co/blog/2017/01/13/range-of-motion-after-joint-replacement-surgery/.

[6] RelayHealth. Kneecap (prepatellar) bursitis rehabilitation exercises. https://www.summitmedicalgroup.com/library/adult_health/sma_knee_bursitis_exercises/.

[7] P. Tammy White, MS and D. O. Phyllis Clapis, PT. Piriformis syndrome. http://www.tzengs.com/health/Piriformis%20Syndrome/index.htm.

[8] RelayHealth. Kneecap fracture exercises. https://www.summitmedicalgroup.com/library/pediatric_health/sma_patellar_fracture_exercises/.

[9] Exoskeleton report. https://exoskeletonreport.com/product/ekso-gt/.

[10] B. Coxworth. Soft pneumatic exoskeleton could be perfect for use in rehab. https://newatlas.com/soft-exoskeleton-ankle-rehabilitation/30542/.

[11] Quaternions for quest3d. http://3dvrm.com/quat/.

[12] OrthoInfo. Knee conditioning program. http://orthoinfo.org/PDFs/Rehab-Knee-6.pdf.

[13] V. S. injury Clinic Ltd. Knee, thigh & hamstring exercises. http://www.sportsinjuryclinic.net/rehabilitation-exercises/knee-hamstring-thigh-exercises.

[14] M. Kok, J. D. Hol, and T. B. Schön, "Using inertial sensors for position and orientation estimation," arXiv preprint arXiv:1704.06053, 2017.

[15] S. Yean, B. S. Lee, C. K. Yeo, and C. H. Vun, "Algorithm for 3d orientation estimation based on kalman filter and gradient descent," in Information Technology, Electronics and Mobile Communication Conference (IEMCON), 2016 IEEE 7th Annual. IEEE, 2016, pp. 1–6.

[16] F. Caputo, E. DAmato, A. Greco, I. Notaro, and S. Spada, "Human posture tracking system for industrial process design and assessment," in International Conference on Intelligent Human Systems Integration. Springer, 2018, pp. 450–455.

[17] Xsens. Mtw development kit. https://www.xsens.com/products/mtw-development-kit/.

[18] STMicroelectronics. (December 2010) L3g4200d mems motion sensor. https://cdn.sparkfun.com/datasheets/Sensors/Gyros/3-Axis/CD00265057.pdf.

[19] P. Zhou, M. Li, and G. Shen, "Use it free: instantly knowing your phone attitude," in Proceedings of the 20th annual international conference on Mobile computing and networking. ACM, 2014, pp. 605–616.

[20] M. Electronics. Wearable devices and the internet of things. http://www.mouser.sg/applications/article-iot-wearable-devices/.

[21] D. Contruction. (July 2012) The future of healthcare. http://www.dpr.com/assets/docs/the-future-of-healthcare.pdf?/futureofhc.

[22] N. U. of Singapore. (08 April 2014) Tele-rehabilitation solution for stroke patients to boost physical recovery. http://news.nus.edu.sg/highlights/7560-tele-rehabilitation-solution-for-stroke-patients-to-boost-%20physical-recovery.

[23] W. H. Organization. (2015) Disability and health. http://www.who.int/mediacentre/factsheets/fs352/en/.

[24] H. Health. (2015) Who needs physiotherapy? http://www.hullhealth.co.uk/?p=486.

[25] D. Murphy, D. Connolly, and B. Beynnon, "Risk factors for lower extremity injury: a review of the literature," British journal of sports medicine, vol. 37, no. 1, pp. 13–29, 2003.

[26] W. H. O. WHO. Global atlas of the health workforce. http://www.who.int/workforcealliance/knowledge/resources/hrhglobalatlas/en/.

[27] M. Ayoade and L. Baillie, "A novel knee rehabilitation system for the home," in Proceedings of the 32nd annual ACM conference on Human factors in computing systems. ACM, 2014, pp. 2521–2530.

[28] J. Kim, S. Yang, and M. Gerla, "Stroketrack: wireless inertial motion tracking of human arms for stroke telerehabilitation," in Proceedings of the First ACM Workshop on Mobile Systems, Applications, and Services for Healthcare. ACM, 2011, p. 4.

[29] C. Lee, Y. Terada, Y. Liu, and B.-S. Lee, "A motion accuracy evaluator based on body parts movement by mapreduce video processing," in IEEE-EMBS International Conference on Biomedical and Health Informatics (BHI). IEEE, 2014, Conference Proceedings, pp. 644–647.

[30] D. M. Rouleau, A. Place, M. Bérubé, Y. G. Laflamme, and D. Feldman, "Rehabilitation after lower limb injury: development of a predictive score (ralli score)," Canadian Journal of Surgery, vol. 58, no. 4, p. 278, 2015.

[31] V. Tangcharoensathien, W. Witthayapipopsakul, S. Viriyathorn, W. Patcharanarumol et al., "Improving access to assistive technologies: challenges and solutions in low-and middle-income countries," WHO South-East Asia journal of public health, vol. 7, no. 2, p. 84, 2018.

[32] OptiTrack. Optitrack for movement sciences. https://optitrack.com/motion-capture-movement-sciences/.

[33] A. S. Gorgey, "Robotic exoskeletons: The current pros and cons," World journal of orthopedics, vol. 9, no. 9, p. 112, 2018.

[34] D. Roetenberg, H. Luinge, and P. Slycke, "Xsens mvn: full 6dof human motion tracking using miniature inertial sensors," Xsens Motion Technologies BV, Tech. Rep, vol. 1, 2009.

[35] I. Technology. Promove mini. http://inertia-technology.com/promove-mini.

[36] V. Draper and L. Ballard, "Electrical stimulation versus electromyographic biofeedback in the recovery of quadriceps femoris muscle function following anterior cruciate ligament surgery," Physical Therapy, vol. 71, no. 6, pp. 455–461, 1991.

[37] D. A. Padua, D. R. Bell, and M. A. Clark, "Neuromuscular characteristics of individuals displaying excessive medial knee displacement," Journal of athletic training, vol. 47, no. 5, pp. 525–536, 2012.

[38] H. Zhou and H. Hu, "Human motion tracking for rehabilitationa survey," Biomedical Signal Processing and Control, vol. 3, no. 1, pp. 1–18, 2008.

[39] J. R. Flanagan and A. K. Rao, "Trajectory adaptation to a nonlinear visuomotor transformation: evidence of motion planning in visually perceived space," Journal of neurophysiology, vol. 74, no. 5, pp. 2174–2178, 1995.

[40] R. Mahony, T. Hamel, and J.-M. Pflimlin, "Complementary filter design on the special orthogonal group so (3)," in Proceedings of the 44th IEEE Conference on Decision and Control. IEEE, 2005, pp. 1477–1484.

[41] N. B. Reese and W. D. Bandy, Joint range of motion and muscle length testing. Elsevier Health Sciences, 2016.

[42] P.-C. Huang, K.-C. Liu, C.-Y. Hsieh, and C.-T. Chan, "Human motion identification for rehabilitation exercise assessment of knee osteoarthritis," in Applied System Innovation (ICASI), 2017 International Conference on. IEEE, 2017, pp. 246–249.

[43] N. U. of Singapore. Tele-rehabilitation solution for stroke patients to boost physical recovery. http://news.nus.edu.sg/highlights/7560-tele-rehabilitation-solution-for-stroke-patients-to-boost-%20physical-recovery.

[44] J. J. Baskett, J. B. Broad, G. Reekie, C. Hocking, and G. Green, "Shared responsibility for ongoing rehabilitation: a new approach to home-based therapy after stroke," Clinical Rehabilitation, vol. 13, no. 1, pp. 23–33, 1999.

[45] F. Cavallo, M. Aquilano, L. Odetti, M. Arvati, and M. C. Carrozza, "A first step toward a pervasive and smart zigbee sensor system for assistance and rehabilitation," in 2009 IEEE International Conference on Rehabilitation Robotics. IEEE, 2009, pp. 632–637.

[46] T. Seel, J. Raisch, and T. Schauer, "Imu-based joint angle measurement for gait analysis," Sensors, vol. 14, no. 4, pp. 6891–6909, 2014.

[47] J. Michalak, K. Rohde, and N. F. Troje, "How we walk affects what we remember: Gait modifications through biofeedback change negative affective memory bias," Journal of behavior therapy and experimental psychiatry, vol. 46, pp. 121–125, 2015.

[48] D. Levine, J. Richards, and M. W. Whittle, Whittle's gait analysis. Elsevier Health Sciences, 2012.

[49] Q. Fang, Z. Zhang, and Y. Tu, "Application of gait analysis for hemiplegic patients using six-axis wearable inertia sensors," in IECON 2014-40th Annual Conference of the IEEE Industrial Electronics Society. IEEE, 2014, pp. 3993–3996.

[50] L. S. Lippert, Clinical kinesiology and anatomy. FA Davis, 2011.

[51] J. Rueterbories, E. G. Spaich, B. Larsen, and O. K. Andersen, "Methods for gait event detection and analysis in ambulatory systems," Medical engineering & physics, vol. 32, no. 6, pp. 545–552, 2010.

[52] P.-F. Yang, A. Kriechbaumer, K. Albracht, M. Sanno, B. Ganse, T. Koy, P. Shang, G.-P. Brüggemann, L. P. Müller, and J. Rittweger, "On the relationship between tibia torsional deformation and regional muscle contractions in habitual human exercises in vivo," Journal of biomechanics, vol. 48, no. 3, pp. 456–464, 2015.

[53] H. Dejnabadi, B. M. Jolles, E. Casanova, P. Fua, and K. Aminian, "Estimation and visualization of sagittal kinematics of lower limbs orientation using body-fixed sensors," IEEE Transactions on Biomedical Engineering, vol. 53, no. 7, pp. 1385–1393, 2006.

[54] N. Wyndow, A. De Jong, K. Rial, K. Tucker, N. Collins, B. Vicenzino, T. Russell, and K. Crossley, "The relationship of foot and ankle mobility to the frontal plane projection angle in asymptomatic adults," Journal of foot and ankle research, vol. 9, no. 1, p. 1, 2016.

[55] M. Tousignant, P. Boissy, H. Corriveau, and H. Moffet, "In home telerehabilitation for older adults after discharge from an acute hospital or rehabilitation unit: A proof-of-concept study and costs estimation," Disability and Rehabilitation: Assistive Technology, vol. 1, no. 4, pp. 209–216, 2006.

[56] S. J. J. K. F. H. M. S. T.-S. M. e. a. Grembowski, D., "Model of the role of complexity in the care of patients with multiple chronic conditions," Medical Care, no. 52, pp. S7–S14, 2014.

[57] G. C. Koh, S. C. Yen, A. Tay, A. Cheong, Y. S. Ng, D. A. De Silva, C. Png, K. Caves, K. Koh, Y. Kumar et al., "Singapore tele-technology aided rehabilitation in stroke (stars) trial: protocol of a randomized clinical trial on tele-rehabilitation for stroke patients," BMC neurology, vol. 15, no. 1, p. 161, 2015.

[58] P. Boissy, M. Tousignant, H. Moffet, S. Nadeau, S. Brière, C. Mérette, H. Corriveau, F. Marquis, F. Cabana, P. Ranger et al., "Conditions of use, reliability, and quality of audio/video-mediated communications during in-home rehabilitation teletreatment for postknee arthroplasty," Telemedicine and e-Health, 2016.

[59] V. F. S. Fook, S. Z. Hao, A. A. P. Wai, M. Jayachandran, J. Biswas, L. S. Yee, and P. Yap, "Innovative platform for tele-physiotherapy," in e-health Networking, Applications and Services, 2008. HealthCom 2008. 10th International Conference on. IEEE, 2008, pp. 59–65.

[60] T. Beth, I. Boesnach, M. Haimerl, J. Moldenhauer, K. Bös, and V. Wank, "Characteristics in human motion–from acquisition to analysis," in IEEE International Conference on Humanoid Robots. Citeseer, 2003, pp. 56–75.

[61] Motion capture system, vicon. https://www.vicon.com/.

[62] S.-F. Wong and K. Wong, "Reliable and fast human body tracking under information deficiency," in Proceedings of the IEEE Intelligent Automation Conference. IEEE., 2003.

[63] X. X. R. W. M. Li and S. C. Jia-hua, "Accuracy of the microsoft kinecttm for measuring gait," European Journal of Medicine, vol. 7, pp. 176–182, 2012.

[64] Y. Tao and H. Hu, "Building a visual tracking system for home-based rehabilitation," in Proc. of the 9th Chinese Automation and Computing Society Conf. In the UK, 2003, pp. 343–448.

[65] X. Ji, S. Wang, Y. Xu, Q. Shi, and D. Xia, "Application of the digital signal procession in the mems gyroscope de-drift," in 2006 1st IEEE International Conference on Nano/Micro Engineered and Molecular Systems. IEEE, 2006, pp. 218–221.

[66] S. Education. (2013) Gyroscope. https://learn.sparkfun.com/tutorials/gyroscope.

[67] ——. (2013) Accelerometer basics. https://learn.sparkfun.com/tutorials/accelerometer-basics.

[68] V. Technologies. (2013) Magnetometer. http://www.vectornav.com/support/library/magnetometer.

[69] P. Kim and L. Huh, Kalman filter for beginners: with MATLAB examples. CreateSpace, 2011, vol. 4.

[70] D. Giansanti, G. Maccioni, and V. Macellari, "The development and test of a device for the reconstruction of 3-d position and orientation by means of a kinematic sensor assembly with rate gyroscopes and accelerometers," IEEE transactions on biomedical engineering, vol. 52, no. 7, pp. 1271–1277, 2005.

[71] H. Zhou and H. Hu, "Inertial motion tracking of human arm movements in stroke rehabilitation," in IEEE International Conference Mechatronics and Automation, 2005, vol. 3. IEEE, 2005, pp. 1306–1311.

[72] H. J. Luinge, Inertial sensing of hun movement. Twente University Press, 2002.

[73] J. Lobo and J. Dias, "Vision and inertial sensor cooperation using gravity as a vertical reference," IEEE Transactions on Pattern Analysis and Machine Intelligence, vol. 25, no. 12, pp. 1597–1608, 2003.

[74] S. O. Madgwick, A. J. Harrison, and R. Vaidyanathan, "Estimation of imu and marg orientation using a gradient descent algorithm," in 2011 IEEE International Conference on Rehabilitation Robotics. IEEE, 2011, pp. 1–7.

[75] J. L. Marins, X. Yun, E. R. Bachmann, R. B. McGhee, and M. J. Zyda, "An extended kalman filter for quaternion-based orientation estimation using marg sensors," in Intelligent Robots and Systems, 2001. Proceedings. 2001 IEEE/RSJ International Conference on, vol. 4. IEEE, 2001, pp. 2003–2011.

[76] N. Trawny and S. I. Roumeliotis, "Indirect kalman filter for 3d attitude estimation," University of Minnesota, Dept. of Comp. Sci. & Eng., Tech. Rep, vol. 2, p. 2005, 2005.

[77] Q. Mourcou, A. Fleury, C. Franco, F. Klopcic, and N. Vuillerme, "Performance evaluation of smartphone inertial sensors measurement for range of motion," Sensors, vol. 15, no. 9, pp. 23 168–23 187, 2015.

[78] R. A. Clark, Y.-H. Pua, A. L. Bryant, and M. A. Hunt, "Validity of the microsoft kinect for providing lateral trunk lean feedback during gait retraining," Gait & posture, vol. 38, no. 4, pp. 1064–1066, 2013.

[79] B. C. Bedregal, A. C. Costa, and G. P. Dimuro, "Fuzzy rule-based hand gesture recognition," in IFIP International Conference on Artificial Intelligence in Theory and Practice. Springer, 2006, pp. 285–294.

[80] T. Hachaj and M. R. Ogiela, "Rule-based approach to recognizing human body poses and gestures in real time," Multimedia Systems, vol. 20, no. 1, pp. 81–99, 2014.

[81] A. Bo, M. Hayashibe, and P. Poignet, "Joint angle estimation in rehabilitation with inertial sensors and its integration with kinect," in EMBC: Engineering in Medicine and Biology Conference, 2011, pp. 3479–3483.

[82] E. Akdoğan, E. Taçgın, and M. A. Adli, "Knee rehabilitation using an intelligent robotic system," Journal of Intelligent Manufacturing, vol. 20, no. 2, p. 195, 2009.

[83] W. Zhao, M. A. Reinthal, D. D. Espy, and X. Luo, "Rule-based human motion tracking for rehabilitation exercises: Realtime assessment, feedback, and guidance," IEEE Access, vol. 5, pp. 21 382–21 394, 2017.

[84] J. F.-S. Lin and D. Kulic, "Online segmentation of human motion for automated rehabilitation exercise analysis," IEEE Transactions on Neural Systems and Rehabilitation Engineering, vol. 22, no. 1, pp. 168–180, 2014.

[85] S. Nomm and K. Buhhalko, "Monitoring of the human motor functions rehabilitation by neural networks based system with kinect sensor," IFAC Proceedings Volumes, vol. 46, no. 15, pp. 249–253, 2013.

[86] R. Kianifar, A. Lee, S. Raina, and D. Kulić, "Automated assessment of dynamic knee valgus and risk of knee injury during the single leg squat," IEEE journal of translational engineering in health and medicine, vol. 5, pp. 1–13, 2017.

[87] P. E. Taylor, G. J. Almeida, T. Kanade, and J. K. Hodgins, "Classifying human motion quality for knee osteoarthritis using accelerometers," in Proc of the Intl Conf of the Eng in Med and Biol Soc, 2010, pp. 339–343.

[88] P. Mirowski. (2010) Support vector machines: Maximum margin classifiers. https://cs.nyu.edu/~yann/2010f-G22-2565-001/diglib/lecture03a-svm-2010.pdf.

[89] T. Zebin, P. J. Scully, and K. B. Ozanyan, "Inertial sensor based modelling of human activity classes: Feature extraction and multi-sensor data fusion using machine learning algorithms," in eHealth 360. Springer, 2017, pp. 306–314.

[90] R. Kianifar, A. Lee, S. Raina, and D. Kulić, "Classification of squat quality with inertial measurement units in the single leg squat mobility test," in Engineering in Medicine and Biology Society (EMBC), 2016 IEEE 38th Annual International Conference of the. IEEE, 2016, pp. 6273–6276.

[91] S. R. Simon, "Quantification of human motion: gait analysisbenefits and limitations to its application to clinical problems," Journal of biomechanics, vol. 37, no. 12, pp. 1869–1880, 2004.

[92] O. M. Giggins, K. T. Sweeney, and B. Caulfield, "Rehabilitation exercise assessment using inertial sensors: a cross-sectional analytical study," Journal of neuroengineering and rehabilitation, vol. 11, no. 1, p. 158, 2014.

[93] A. Schmitz, M. Ye, R. Shapiro, R. Yang, and B. Noehren, "Accuracy and repeatability of joint angles measured using a single camera markerless motion capture system," Journal of biomechanics, vol. 47, no. 2, pp. 587–591, 2014.

[94] W. Zhao, R. Lun, D. D. Espy, and M. A. Reinthal, "Realtime motion assessment for rehabilitation exercises: Integration of kinematic modeling with fuzzy inference," Journal of Artificial Intelligence and Soft Computing Research, vol. 4, no. 4, pp. 267–285, 2014.

[95] S. Yean, B. S. Lee, C. K. Yeo, C. H. Vun, and H. L. Oh, "Smartphone orientation estimation algorithm combining kalman filter with gradient descent," IEEE journal of biomedical and health informatics, vol. 22, no. 5, pp. 1421–1433, 2018.

[96] Statista. Number of smartphone users worldwide from 2014 to 2020 (in billions). https://www.statista.com/statistics/330695/number-of-smartphone-users-worldwide/.

[97] A. Developer. (September 2010) Cmattitude. https://developer.apple.com/documentation/coremotion/cmattitude.

[98] XSENS. Mtw development kit. https://www.xsens.com/products/mtw-development-kit/.

[99] S. Qiu, Y. Yang, J. Hou, R. Ji, H. Hu, and Z. Wang, "Ambulatory estimation of 3d walking trajectory and knee joint angle using marg sensors," in Innovative Computing Technology (INTECH), 2014 Fourth International Conference on. IEEE, 2014, pp. 191–196.

[100] H.-P. Brückner, B. Krüger, and H. Blume, "Reliable orientation estimation for mobile motion capturing in medical rehabilitation sessions based on inertial measurement units," Microelectronics Journal, vol. 45, no. 12, pp. 1603–1611, 2014.

[101] M. Crabolu, D. Pani, L. Raffo, and A. Cereatti, "Estimation of the center of rotation using wearable magneto-inertial sensors," Journal of Biomechanics, 2016.

[102] S. Qiu, Z. Wang, H. Zhao, and H. Hu, "Using distributed wearable sensors to measure and evaluate human lower limb motions," IEEE Transactions on Instrumentation and Measurement, vol. 65, no. 4, pp. 939–950, 2016.

[103] A. Devices. Gyroscope specification adis16260. http://www.analog.com/en/products/mems/gyroscopes/adis16260.html#product-overview.

[104] C. Andrew Bookholt, iFixit. iphone 4 gyroscope teardown. https://www.ifixit.com/Teardown/iPhone+4+Gyroscope+Teardown/3156.

[105] Parallax. Gyroscope module 3-axis l3g4200d. https://www.parallax.com/sites/default/files/downloads/27911-Gyroscope-3-Axis-L3G4200D-Guide-v1.1.pdf.

[106] M. J. Baker. Maths - euler angles. http://www.euclideanspace.com/maths/geometry/rotations/euler/.

[107] S. Colton, "The balance filter: a simple solution for integrating accelerometer and gyroscope measurements for a balancing platform," white paper, Massachusetts Institute of Technology, Cambridge, MA, 2007.

[108] T. Ozyagcilar, "Implementing a tilt-compensated ecompass using accelerometer and magnetometer sensors," Freescale semiconductor, AN, vol. 4248, 2012.

[109] J. F. Vasconcelos, B. Cardeira, C. Silvestre, P. Oliveira, and P. Batista, "Discrete-time complementary filters for attitude and position estimation: Design, analysis and experimental validation," IEEE Transactions on Control Systems Technology, vol. 19, no. 1, pp. 181–198, 2011.

[110] R. Mahony, T. Hamel, and J.-M. Pflimlin, "Nonlinear complementary filters on the special orthogonal group," IEEE Transactions on Automatic Control, vol. 53, no. 5, pp. 1203–1218, 2008.

[111] A. Janota, V. Šimák, D. Nemec, and J. Hrbček, "Improving the precision and speed of euler angles computation from low-cost rotation sensor data," Sensors, vol. 15, no. 3, pp. 7016–7039, 2015.

[112] J. B. Kuipers et al., Quaternions and rotation sequences. Princeton university press Princeton, 1999, vol. 66.

[113] U. D. of Health and H. S. P. H. Service. (2014) What are knee problems? https://www.niams.nih.gov/health-info/knee-problems/knee-problems-ff.asp.

[114] H. Hyyti and A. Visala, "A dcm based attitude estimation algorithm for low-cost mems imus," International Journal of Navigation and Observation, vol. 2015, 2015.

[115] O. Bastelseiten. (2013) Imu data fusing: Complementary, kalman, and mahony filter. http://www.olliw.eu/2013/imu-data-fusing/.

[116] A. Mannini and A. M. Sabatini, "Machine learning methods for classifying human physical activity from on-body accelerometers," Sensors, vol. 10, no. 2, pp. 1154–1175, 2010.

[117] CHRobotics.

[118] D. Kim, S. W. Richards, and T. P. Caudell, "An optical tracker for augmented reality and wearable computers," in Virtual Reality Annual International Symposium, 1997., IEEE 1997. IEEE, 1997, pp. 146–150.

[119] I. Technology. Promove mini. http://inertia-technology.com/product/motion-capture-promove-mini/.

[120] Texas instruments. http://www.ti.com/ww/en/wireless-connectivity/sensortag/index.html.

[121] G. Wu, F. C. Van der Helm, H. D. Veeger, M. Makhsous, P. Van Roy, C. Anglin, J. Nagels, A. R. Karduna, K. McQuade, X. Wang et al., "Isb recommendation on definitions of joint coordinate systems of various joints for the reporting of human joint motionpart ii: shoulder, elbow, wrist and hand," Journal of biomechanics, vol. 38, no. 5, pp. 981–992, 2005.

[122] B. M. Gaffney, C. L. Christiansen, A. M. Murray, A. K. Silverman, and B. S. Davidson, "Separation of rotational and translational segmental momentum to assess movement coordination during walking," Human movement science, vol. 51, pp. 99–111, 2017.

[123] J. P. Vital, D. R. Faria, G. Dias, M. S. Couceiro, F. Coutinho, and N. M. Ferreira, "Combining discriminative spatiotemporal features for daily life activity recognition using wearable motion sensing suit," Pattern Analysis and Applications, vol. 20, no. 4, pp. 1179–1194, 2017.

[124] J. J. Jeka and P. I. Agada, "Feedback device to improve arm swing," Jan. 31 2017, uS Patent 9,558,399.

[125] P. Musa, D. A. Christie, and E. P. Wibowo, "An implementation of direction cosine matrix in rocket payload dynamics attitude monitoring," in 2016 International Conference on Informatics and Computing (ICIC). IEEE, 2016, pp. 271–276.

[126] S. Yean, B. S. Lee, C. K. Yeo, C. H. Vun, and H. L. Oh, "Smartphone orientation estimation algorithm combining kalman filter with gradient descent," IEEE Journal of Biomedical and Health Informatics, vol. PP, no. 99, pp. 1–1, 2017.

[127] A. Lapham and R. Bartlett, "The use of artificial intelligence in the analysis of sports performance: A review of applications in human gait analysis and future directions for sports biomechanics," Journal of Sports Sciences, vol. 13, no. 3, pp. 229–237, 1995.

[128] S. Dreiseitl and L. Ohno-Machado, "Logistic regression and artificial neural network classification models: a methodology review," Journal of biomedical informatics, vol. 35, no. 5, pp. 352–359, 2002.

[129] C. Svarer, Neural networks for signal processing. Elektronisk Institut, Danmarks Tekniske Højskole, 1994.

[130] D. Kingma and J. Ba, "Adam: A method for stochastic optimization," arXiv preprint arXiv:1412.6980, 2014.

[131] X. T. B.V. (2013) Mti user manual. https://www.xsens.com/wp-content/uploads/2013/11/MTi-usermanual1.pdf.

[132] R. Nussbaum, C. Kelly, E. Quinby, A. Mac, B. Parmanto, and B. E. Dicianno, "A systematic review of mobile health applications in rehabilitation," Archives of physical medicine and rehabilitation, 2018.

[133] O. Health. Knee decide - education and engagement. https://itunes.apple.com/us/app/knee-decide-education-engagement/id405607817?mt=8.

[134] Winzig. Pain therapy - physical therapy exercise videos. https://itunes.apple.com/us/app/pain-therapy-physical-therapy/id523530592?mt=8.

[135] Pt pal. http://www.ptpal.com/.

[136] Q. A. LLC. Pt timer: Stretch and exercise. https://itunes.apple.com/us/app/pt-timer-stretch-exercise/id410605817?mt=8.

[137] CoachMyVideo.com. Cmv: Slow frame-frame video analysis coachmyvideo. https://appadvice.com/app/cmv-slow-frame-frame-video-analysis-coachmyvideo/499915119.

[138] Goniometer. https://itunes.apple.com/us/app/goniometer/id406942245.

[139] S. L. Lim, S. Yean, B. S. Lee, and Y. C. Kiat, "Rehabpartner: Motion tracking assistant using a novel complementary feedback filter," in 2018 15th IEEE Annual Consumer Communications & Networking Conference (CCNC). IEEE, 2018, pp. 1–6.

[140] O. D. Lara, M. A. Labrador et al., "A survey on human activity recognition using wearable sensors." IEEE Communications Surveys and Tutorials, vol. 15, no. 3, pp. 1192–1209, 2013.

[141] scikitlearn. Selectkbest. http://scikitlearn.org/stable/modules/generated/sklearn.featureselection.SelectKBest.html.

[142] ——. Extratree classifier. https://scikit-learn.org/stable/modules/generated/sklearn.tree.ExtraTreeClassifier.html.

[143] J.-Y. Yang, J.-S. Wang, and Y.-P. Chen, "Using acceleration measurements for activity recognition: An effective learning algorithm for constructing neural classifiers," Pattern recognition letters, vol. 29, no. 16, pp. 2213–2220, 2008.

[144] R. Takeda, S. Tadano, A. Natorigawa, M. Todoh, and S. Yoshinari, "Gait posture estimation using wearable acceleration and gyro sensors," Journal of biomechanics, vol. 42, no. 15, pp. 2486–2494, 2009.

[145] A. Avci, S. Bosch, M. Marin-Perianu, R. Marin-Perianu, and P. Havinga, "Activity recognition using inertial sensing for healthcare, wellbeing and sports applications: A survey," in Architecture of computing systems (ARCS), 2010 23rd international conference on. VDE, 2010, pp. 1–10.

[146] M. Mubashir, L. Shao, and L. Seed, "A survey on fall detection: Principles and approaches," Neurocomputing, vol. 100, pp. 144–152, 2013.

[147] scikitlearn. Random forest classifier. https://scikit-learn.org/stable/modules/generated/sklearn.ensemble.RandomForestClassifier.html.

[148] A. Subasi, M. Radhwan, R. Kurdi, and K. Khateeb, "Iot based mobile healthcare system for human activity recognition," in Learning and Technology Conference (L&T), 2018 15th. IEEE, 2018, pp. 29–34.

[149] Z. Bankó, L. Dobos, and J. Abonyi, "Dynamic principal component analysis in multivariate time-series segmentation," Conservation, Information, Evolution-towards a sustainable engineering and economy, vol. 1, no. 1, pp. 11–24, 2011.

[150] L. Sun, D. Zhang, B. Li, B. Guo, and S. Li, "Activity recognition on an accelerometer embedded mobile phone with varying positions and orientations," in International conference on ubiquitous intelligence and computing. Springer, 2010, pp. 548–562.

[151] T. Watanabe and H. Saito, "Tests of wireless wearable sensor system in joint angle measurement of lower limbs," in 2011 Annual International Conference of the IEEE Engineering in Medicine and Biology Society. IEEE, 2011, pp. 5469–5472.

[152] M. Tada, "Wireless sensor and display modules for on-site motion measurement and intervention," in the 19th System Integration Symposium, 2018, Conference Proceedings, pp. 418–422.

[153] H. Toda, M. Tada, T. Maruyama, and Y. Kurita, "Effect of contraction parameters on swing support during walking using wireless pneumatic artificial muscle driver: A preliminary study," in SICE Annual Conference 2019. IEEE, 2019, Conference Proceedings, pp. 727–732.

Author's Publications

Journals

- **Seanglidet Yean**, Bu Sung Lee, Chai Kiat Yeo, Chan Hua Vun, and Hong Lye Oh, "Smartphone Orientation Estimation Algorithm combining Kalman Filter with Gradient Descent ", IEEE Journal of Biomedical and Health Informatics, vo. 22(5), 2017, pp. 1421-1433.
- **Seanglidet Yean**, Bu Sung Lee, and Chai Kiat Yeo, "Lower-limb Rehabilitation at Home: A Survey on Exercise Assessment and Initial Study on Exercise State Identification toward Biofeedback ", International Journal of Interdisciplinary Telecommunications and Networking (IJITN), 2019.
- **Seanglidet Yean**, Bu Sung Lee, and Chai Kiat Yeo, "Feature Engineering and Pattern Recognition for Rehab Exercise Segmentation ", submitted to Sensors, 2019.

Conferences

- **Seanglidet Yean**, Bu Sung Lee, Chai Kiat Yeo, and Chan Hua Vun, "Algorithm for 3D orientation estimation based on Kalman Filter and Gradient Descent ", 7th IEEE Information Technology, Electronics and Mobile Communication Conference (IEMCON), New York, USA, 2016, pp. 1-6.
- Shao Loong Lim, **Seanglidet Yean**, Bu Sung Lee, and Chai Kiat Yeo, "RehabPartner: Motion Tracking Assistant Using a Novel Complementary Feedback Filter ", in IEEE Consumer Communications & Networking Conference (CCNC), Las Vegas, USA, 2018.
- **Seanglidet Yean**, Bu Sung Lee, Chai Kiat Yeo, and Zhaomin Chen, "Automated Oscillation Detection and Correction of Fused Wearable Sensor Signals using Machine Learning ", 16th IEEE Wireless Telecommunications Symposium (WTS), Phoenix, USA, 2018.
- **Seanglidet Yean**, Mitsunori Tada, Haruki Toda, Bu Sung Lee, and Yuichi Kurita, "Adaptive Automatic Controller for Swing Assist by Pneumatic Artificial Muscle ", accepted to 2020 IEEE Sensors Applications Symposium (SAS), Kuala Lumpur, Malaysia, 2020.